UNIVERSITEIT VAN PRETORIA
UNIVERSITY OF PRETORIA
YUNIBESITHI YA PRETORIA

Amphotericin B as a mycolic acid specific targeting agent in tuberculosis

Yolandy Benadie

Submitted in partial fulfillment of the requirements for the Master of Science

in the

Department of Biochemistry
Faculty of Natural and Agricultural Sciences
University of Pretoria
Pretoria

December 2006

Acknowledgements

I would humbly like to thank the following individuals and organizations for their support towards my completion of my MSc. degree.

Most importantly, **our Creator and King**, for the guidance and support in the good and trying times and never leaving my side.

Prof. J.A. Verschoor my promoter, for his door always being open whether it is science related or not. For all the interesting discussions, valuable input, positive criticism and for guiding me in the writing of my dissertation.

Dr. L.A. Colett my promoter in chemistry, for assisting me in my chemistry work and helping me when my reactions failed, for being so patient and willing to help when I struggled to understand, as well as the excellent help and contribution in the writing of my dissertation - without your help it would not have been successful.

Very special thanks to **Mrs. Sandra van Wyngaardt**, for going out of your way to help me in the lab even in the late hours of the night especially the BACTEC experiments and most of all being my second mother.

The BIA group, for all the valuable suggestions and help in my work and always making me feel welcome.

A special thanks to **Dr. Gianna Toschi** for her excellent ideas and being a good friend. I would also like to thank **Mr. Eric Palmer** for his technical assistance with the NMR analyses.

The **NRF** for financial support and the **MRC** for the use of their facilities.

My family and friends, for their moral support and always trying to understand. Special thanks to my **mother** and **father** for the sacrifices they made for me to be able to study at a tertiary institution. My twin sister and room mate for 25 years **Xelia**, for

always being there and for just being you. Thank you to **Marshant** for being such a good brother. Lastly, I would want to especially thank **Corné**, words can not express the gratitude I have and how deeply I appreciate all that you have done, my true guardian angel.

Table of contents

List of abbreviations

ACP	acyl carrier protein
AG	arabinogalactan
AmB	amphotericin B
AmB DII	AmB derivative II
AU	absorbance units
BCG	Bacille Calmette-Guerin
B. napus	*Brassica napus*
CM	cytoplasmic membrane
CPC	cetylpyridinium chloride
$dddH_2O$	double distilled deionized water
DMSO-d_6	deuterated dimethyl sulfoxide
DMSO	dimethyl sulfoxide
E. coli	*Escherichia.coli*
EnvM	enoyl-reductases
Et_3N	triethyl amine
FA	fatty acid
FAS	fatty acid synthetase
FDA	United States Food and Drug Administration
GC-MS	gas-chromatography mass-spectrometry
GL	glycolipids
HIV	human immune deficiency virus
HPLC	High Performance Liquid Chromatography
3β/17β-HSD	3β/17β- hydroxysteroid dehydrogenase
3αHSD	3-α hydroxysteroid dehydrogenase
17β-HSD1	17β- hydroxysteroid dehydrogenase
7α HSDH	7 α-hydroxysteroid dehydrogenase
IFN-γ	interferon-gamma
INH	isoniazid
INH-TPA	isonicotinic acid p-formylbenzylidenehydrazide
KatG	catalase peroxidase
LDH	lactate dehydrogenase

LDL	low density lipoproteins
MA / MY	mycolic acids
M. bovis	*Mycobacterium bovis*
MBSA	maleylated bovine serum albumin
MDR-TB	multidrug-resistant TB
MeOH	methanol
MIC	minimum inhibitory concentration
M. smegmatis	*Mycobacterium smegmatis*
M. tb	*Mycobacterium tuberculosis*
$NaBH_4$	sodium borohydride
NADH	β-nicotinamide adenine dinucleotide
NAT	arylamine N-acetyltransferase
PG	peptidoglycan
RP	reverse phase
RT	room temperature
SCAD	short chain alcohol dehydrogenases
SDR	short chain dehydrogenases/reductases
TACO	tryptophane aspartate containing coat protein
TA/TU	teichoic acid/ teichuronic acid
TB	tuberculosis
TLC	thin layer chromatography
TNF-α	tumour necrosis factor alpha
TPA	terephthalaldehyde
WHO	World Health Organization

List of figures

Summary

The serious threat of tuberculosis, especially XDR-TB, is a reality in Southern Africa particularly in individuals with HIV/AIDS. Therefore the importance of development of new or improved anti-TB treatment must now be emphasized more than ever. In this study, a model was created to target isoniazid (toxophore) specifically to a cholesterol rich environment where mycobacteria reside in macrophages, by making use of a sterol binding drug, Amphotericin B (haptophore). Isoniazid was covalently linked to Amphotericin B via a Schiff base to a linker molecule, terephthalaldehyde. Although this molecule showed a loss of biological activity, a discovery was made by serendipity that could have great impact in understanding how *Mycobacterium tuberculosis* enters and survives in the host macrophage. During the testing of the compound, it was discovered that Amphotericin B bound to mycolic acids at least as well as it binds to cholesterol, its natural ligand. This could provide proof of the structural similarity between mycolic acids and cholesterol but many more controls need to be investigated. As cholesterol was previously shown in literature to be critical for entry and survival of *Mycobacterium tuberculosis* in macrophages, the indication of a structural mimicry between the cell wall mycolic acids and cholesterol and the attraction of these two chemical entities to one another seems to be highly relevant. This characteristic can now be further explored to improve the understanding of the process of entry and survival of *Mycobacterium tuberculosis* in the macrophage host.

Opsomming

Die ernstige bedreiging van tuberkulose, veral XDR-TB is ‘n realiteit in Suidelike Afrika veral vir diegene met MIV/VIGS. Daarom is dit noodsaaklik dat daar klem gelê moet word op die noodsaaklikheid van ontwikkeling van nuwe of verbeterde anti-TB middels. Tydens hierdie studie was ‘n model ontwerp om isoniazid (toksofoor) spesifiek na ‘n cholesterol ryke omgewing te teiken waar die mikobakterieë in makrofages voorkom deur gebruik te maak van ‘n sterol-bindende molekule naamlik Amphotericin B (haptofoor). Isoniazid is kovalent gebind aan Amphotericin B deur middel van ‘n Schiff basis met ‘n verbindingsmolekule tereftalaldehied. Al was die nuwe molekule nie biologiese aktief nie, was ‘n nuwe ontdekking gemaak wat ‘n impak kan hê op die begrip van hoe *Mycobacterium tuberculosis* bakterieë die gasheermakrofage binnedring en oorleef. Gedurende die toetsing van die nuut gesintetiseerde molekule is die ontdekking gemaak dat Amphotericin B ook aan mikoolsure bind net soos dit aan cholesterol, die natuurlike ligand, bind. Die bevinding kan dui op ‘n strukturele ooreenkoms tussen mikoolsure en cholesterol. In die literatuur is dit al voorheen bewys dat cholesterol noodsaaklik is vir die toegang en oorlewing van die *Mycobacterium tuberculosis* bakterieë in die makrofage. Die indikasie van ‘n strukturele ooreenkoms tussen die selwand-mikoolsure en cholesterol en die onderlinge aantrekking van hierdie twee chemiese entiteite blyk hoogs relevant te wees. Die eienskap kan nou verder ondersoek word om die proses van toegang en oorlewing van *Mycobacterium tuberculosis* in die makrofaag-gasheer te verstaan.

Chapter 1: General introduction

1.1 Introduction

Tuberculosis (TB) is a bacterial disease caused by *Mycobacterium tuberculosis* (*M. tb*). It is a multifaceted pathogen capable of causing both an acute disease and an asymptomatic latent infection. The bacteria primarily infect the lungs and are transmitted by inhalation of droplet nuclei containing the bacteria. Patients with pulmonary or laryngeal tuberculosis generate these nuclei when they talk, sneeze or cough and can infect other people in this manner. Only 10% of immunocompetent people infected with *M. tb* develop active disease in their lifetime - the other 90% do not become ill and cannot transmit the organism. However, in some groups such as infants or the immunocompromised, e.g. those with human immune deficiency virus (HIV) or persons suffering from malnutrition, the proportion that develops clinical TB is much higher.

TB kills approximately 2 million people each year. The global epidemic is growing and becoming more dangerous. The breakdown in health services, the spread of HIV/AIDS and the emergence of multidrug-resistant TB (MDR-TB) are contributing to the worsening impact of this disease. In 1993, the concern about the modern TB epidemic was so great, that the World Health Organization (WHO) took the unprecedented step to declare tuberculosis a global emergency. It is estimated that between 2002 and 2020, approximately 1000 million people will be newly infected, over 150 million people will get sick, and 36 million people will die of TB - if control is not further strengthened [1].

A particularly dangerous form of drug-resistant TB is MDR-TB, which could be defined as the disease due to a bacillus resistant to at least Isoniazid (INH) and Rifampin, the two most powerful anti-TB drugs currently available. Apart from MDR-TB, another problem in tuberculosis is the persistence of the bacteria despite

prolonged chemotherapy. A period of six to twelve months is required to cure the acute disease or to eliminate latent infection. Phenotypic adaption or tolerance might explain the unusually long treatment required. One possibility is that actively growing bacteria adapt to the administration of anti-microbial drugs by moving into a dormant state (latent state). The micro-environment containing dormant bacteria might change over time causing the bacteria to resume growth, at which stage they are vulnerable to the standard drugs if they did not become resistant [2, 3]. Relapses usually occur within six months of the end of treatment, and in most cases are due to poor patient compliance. The risk that the bacteria will now be drug resistant increases dramatically with these relapses. If a new TB treatment is going to replace the already existing therapy then it should at least shorten the duration of treatment or reduce the number of dosages to be taken. Furthermore the new drug should improve the treatment of MDR-TB or provide effective treatment against latent TB infection [4].

Unfortunately statistics from the United States food and drug administration (FDA) database indicated that the approval of new antimycobacterial agents decreased over the past 20 years (1998-2002 vs. 1983-1987) by 56% [5]. The re-examination and re-evaluation of existing drugs and the detailed clarification of the mechanism of action of antimycobacterial compounds must therefore be emphasized in current research. Due to the high costs and extensive research needed before a new or improved drug could enter the market this drug should show (at very early stages of the development) strong activity *in vitro* and *in vivo*, low toxicity and good bioavailability [6]. Much research has been focused on developing an improved second generation INH drug.

1.2 Isoniazid and its mechanism of action

Isoniazid has remained the most valuable first-line drug in the treatment of tuberculosis since its discovery in 1952. Currently chemotherapy for TB treatment consists of two months therapy with INH, Rifampin, Pyrazinamide and ethambutol (Fig. 1.1). To eliminate persistent bacilli another 4 months of treatment with Rifampin and INH are applied. In order to improve INH's effectiveness, the mechanism of action of its target should first be well defined.

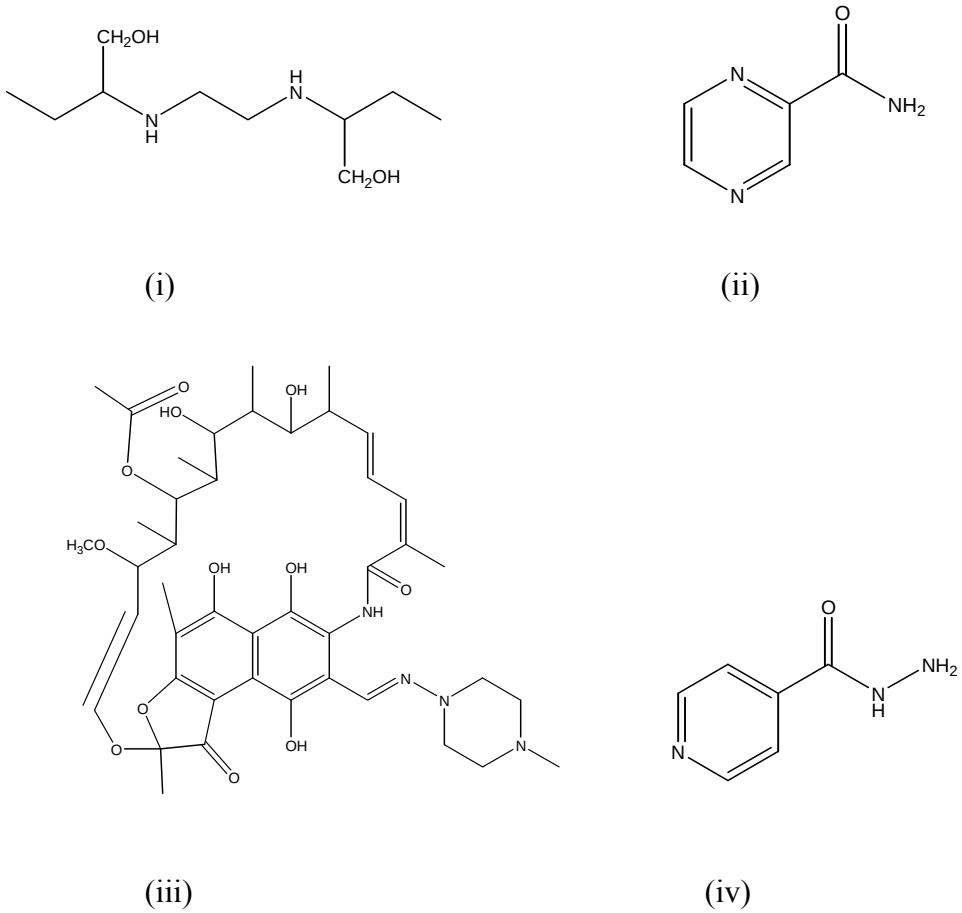

Fig. 1.1 Chemical structures of (i) ethambutol, (ii) pyrazinamide, (iii) Rifampin , (iv) isoniazid [4]

1.2.1 INH mechanism of uptake

The cell wall has an important function in bacterial growth and for the survival of bacteria in hostile environments. The cell wall helps to control the cell shape, protect against high internal osmotic pressure, aids in adhesion to surfaces and other cells and also functions in the export of cellular products. The penetration of toxic molecules differs between the Gram-positive, Gram-negative bacteria and mycobacteria. Gram-positive bacteria have a more permeable cell wall than Gram-negative and mycobacteria do. High lipid content in mycobacterial cell walls is assumed to act as a major barrier against the penetration of antimicrobial agents (Fig. 1.2).

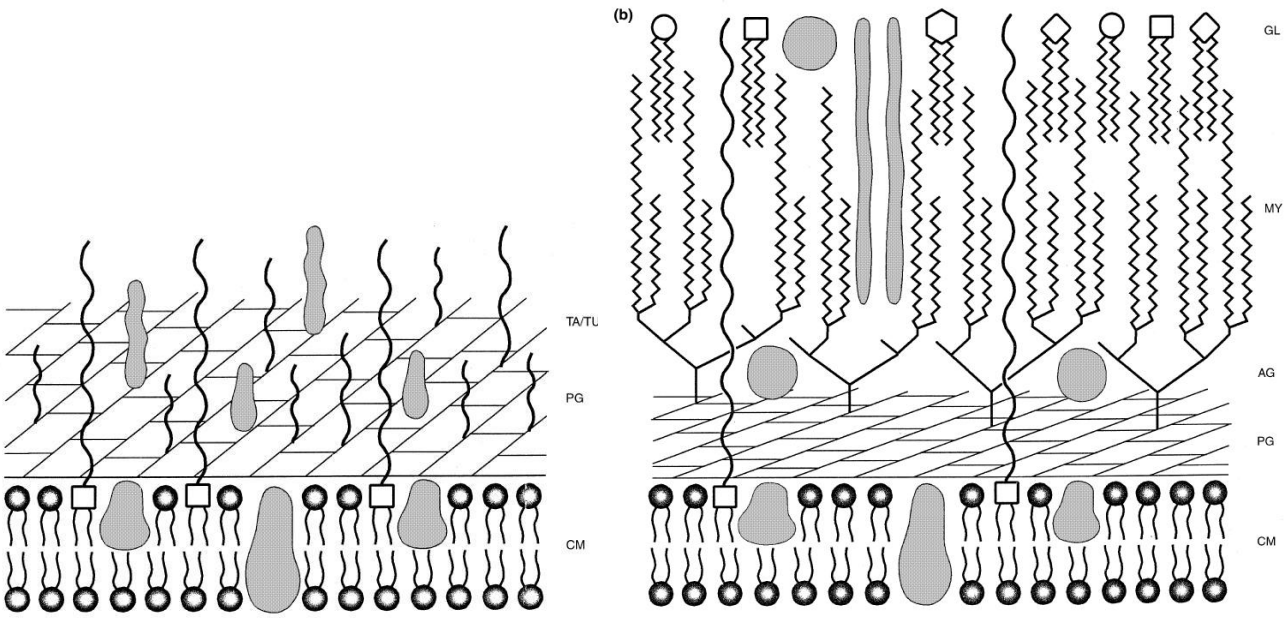

Fig. 1.2 Schematic representation of a Gram-positive cell wall (left) and mycobacterial cell wall (right) TA/TU: teichoic acid/ teichuronic acid, PG: peptidoglycan, CM: cytoplasmic membrane, GL: glycolipids, MY: mycolic acids, AG: arabinogalactan, the shaded areas represent different proteins present in the membranes[7].

In mycobacteria, hydrophobic antibiotics such as fluoroquinolones and Rifampin may diffuse through the cell membrane; whereas hydrophilic antibiotics and nutrients are believed not to diffuse through the membrane, but to use porin channels [7]. For the small, water soluble INH molecule, it was shown by radio-active labelling experiments, that INH enters the mycobacterial cell via passive diffusion [8]. This transport was shown not to be energy-dependent nor make use of facilitated diffusion [8].

The mycobacterial cell envelope has a unique lipophilic nature comprising of high molecular weight lipids. Briefly, the outer surface comprises of mycolic acids (Fig. 1.3), which are long chain 2-alkyl 3-hydroxyl fatty acids comprising typically of 70-90 carbon atoms. Some of the other molecules also present in the membrane are glycolipids based on trehalose and lipopolysaccharides such as lipoarabinomannan. Apart from lipids there are also waxes such as phtiocerol dimycocerosate [7, 9]. After

inactivation of antigen 85C - one of three mycolyltransferases that plays a role in the final assembly of cell envelope components - 40% fewer mycolates were transferred to the cell wall. After measuring the uptake of INH into the cell it was discovered that the transport of INH was not affected by the decrease in mycolate content of the cell wall. Thus the inability of the mycolic acid layer to affect the transport of the INH could be either due to the diffusion of INH through a porin or by the intrinsic high diffusion rate of INH through the membranes [10].

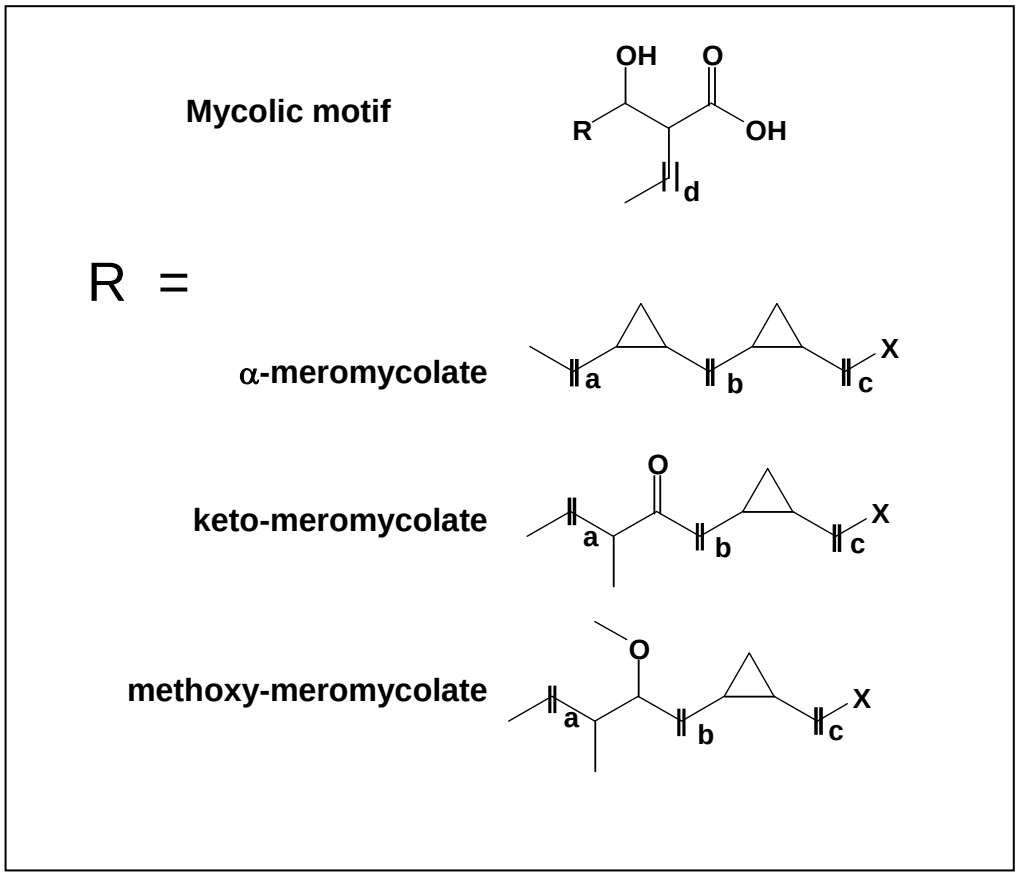

Fig. 1.3 Generalised structures of MA from M. tb.

1.2.2 Activation of INH by Catalase peroxidase (KatG)

INH is a prodrug and its anti-tuberculosis function requires *in vivo* activation by the catalase peroxidase (KatG) enzyme, a haem containing catalase peroxidase. Isonicotinoyl-NAD, derived from INH and NAD^+, inhibits cell wall synthesis of *M.*

tb. The product binds to the NADH binding site of InhA, an enoyl carrier protein reductase [11] and possibly KasA, a β-ketoacyl carrier protein synthase. INH resistance is frequently associated with mutations in the katG gene but also less frequently in inhA, oxyR and kasA genes [12]. KatG is involved in the detoxification of peroxides from endogenous or exogenous sources. InhA and KasA are enzymes that are involved in the elongation cycle of fatty acid biosynthesis. OxyR (a regulatory protein) functions as an oxidative stress sensor and activates gene transcription of genes involved in detoxification, such as katG and ahpC.

KatG was found to be a culture filtrate protein [13]. When *M. tb* cultures grow *in vitro,* it causes the accumulation of a set of different proteins termed the culture filtrate proteins. The formation of these proteins depend on reaction conditions such as the incubation time, temperature and shaking. Some of these proteins were shown to be immunologically active. For example the high molecular weight fractions of the culture filtrates reacted with sera from the TB patients. By making use of liquid chromatography and mass spectrometry it was discovered that the KatG enzyme was associated with the culture filtrate proteins [13]. Some enzymes that were also detected in the culture filtrate were: alcohol dehydrogenase, glutamine synthetase and superoxide dismutase [14].

KatG typically protects the Mycobacterium against oxygen radicals produced by the macrophage. Activated murine macrophages can generate a variety of oxygen and nitrogen derived radicals that possess anti-microbial activities. Biological agents such as interferon-gamma (IFN-γ) and tumour necrosis factor alpha (TNF-α) could trigger the formation of oxygen and nitrogen based particles. Because KatG was also found extracellularly, this enzyme could possibly resist the toxic oxygen intermediates produced by the host phagocytes [14]. A highly active oxidant, peroxynitrite anion ($ONOO^-$) formed by O_2^- and NO, could be generated by activated macrophages. *M. tb* was shown to be resistant to $ONOO^-$ while non-pathogenic mycobacteria were susceptible to $ONOO^-$ [15]. It was previously shown that KatG in *M. tb* clearly exhibits efficient peroxynitritase activity that removes ONOOH. The persistence of *M. tb* inside the macrophages may also be due to the ability of KatG to detoxify $ONOO^-$, preventing oxidative damage to the bacterium [16].

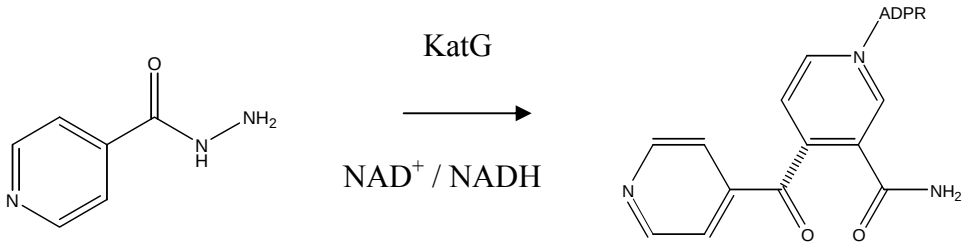

INH

INH-NAD adduct

Fig. 1.4 Formation of Isonicotinoyl-NAD by KatG [17].

Fig. 1.4 indicates the formation of the Isonicotinoyl-NAD adduct by a KatG enzyme. INH can be activated by *M. tb* catalase peroxidase with a peroxidase compound or a superoxide dependent oxyferrous pathway. The peroxidase pathway uses peroxide as the oxidant while the superoxide pathway uses molecular oxygen and produces superoxide and an oxyferrous intermediate at the catalase peroxidase site [18].

KatG enzyme purified from *Mycobacterium smegmatis* catalyses the peroxidation of Mn^{2+} to Mn^{3+} [19]. Mn^{2+} oxidation by *M. tb* has also been reported. It was shown that the oxidation of INH for its activation could be performed non-enzymically by Mn^{3+}, which can in turn be generated by low level manganese peroxidase [16]. Mn^{3+} mediated activation of INH is slow; whereas KatG activation is fast. Some authors investigated the importance of Mn^{3+} for INH activation by KatG and experimentally showed that Mn^{3+} was not essential [20]. This means that the oxidation of INH by catalase peroxidase is the favoured mechanism of activation in *M. tb*, rather than the manganese dependent superoxide mechanism [16, 21, 22]. This supports the view that activation of INH in *M. tb* differs from that of *M. smegmatis*, which shows a Mn^{3+} dependent activation of INH [19].

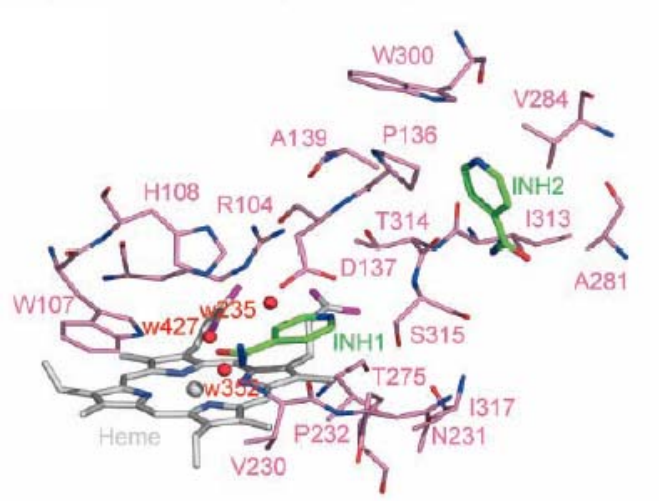

Fig. 1.5 Two potential binding sites for INH (green) in M. tb catalase peroxidase [23]. Protein carbon atoms are depicted in pink, oxygen atoms are in red, nitrogen atoms are in blue, haem carbon atoms are in gray, oxygen atoms are in magenta, and nitrogen atoms are in slate. Water molecules are labeled with red w's.

As discussed earlier the role of the KatG enzyme is to protect the bacteria from toxic molecules, such as hydroperoxides or hydroxy radicals present in the aerobic environment. This KatG enzyme is classified as a class I peroxidase and is a bifunctional haem-dependent enzyme. Activation of INH *in vitro* yields acid, amide and aldehyde products. The amide product is formed by the cleavage of the C-N bond, forming an acyl radical that could react with NADH or NAD^+ [23-25].

After crystallization of the *M. tb* catalase peroxidase, it was predicted *in silico* that the binding site for INH in the *M. tb* catalase peroxidase will be near the δ-meso edge of the haem rather than the surface loop as predicted [24] for *Burkholderia pseudomallei* catalase peroxidase, which shares 65% identity with *M. tb* catalase peroxidase [23] (see Fig. 1.5). The position of *INH1* (Fig. 1.5) was based upon the super-positioning of the *M. tb* catalase peroxidase crystal structure onto a horseradish peroxidase-INH complex derived from nuclear magnetic resonance (NMR) studies [25].

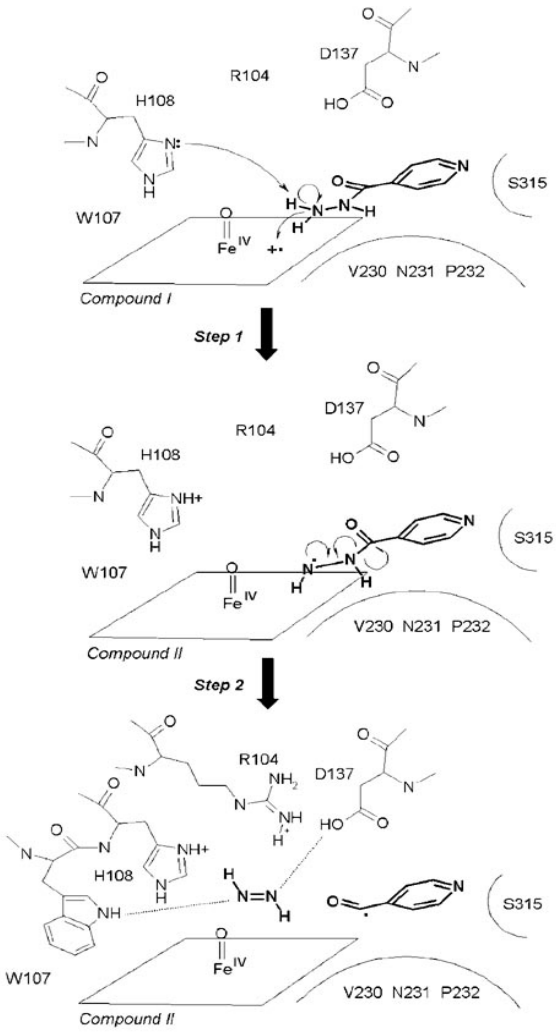

Fig. 1.6 KatG enzyme residues potentially involved in production of isonicotinoyl radical. Possible interactions are shown with dotted lines. The haem porphyrin is represented by a rhombus [25].

A possible reaction mechanism of INH binding to catalase peroxidase in the haem cavity (*INH1*, Fig. 1.6) is shown in Fig. 1.6 [25]. In the first step, compound I is formed after KatG-Fe^{III} reacts with a peroxide to give Fe^{IV}=O and the heam is then reduced by INH in a single electron transfer to the haem. A proton from the hydrazide is lost and could be accepted by His-108. In the second step, the C-N bond of the hydrazide is cleaved forming diazene. The resultant acyl radical could remain near the δ-meso edge of the haem or could diffuse from the active site. The diazene reaction intermediate could be stabilized in the active site by interacting with Trp-107, Asp-137. Transforming the diazene to hydrazine and then ammonia may involve the deprotonation of the His-108, Asp-137 side chains, although given its location, Arg-

104 could also act as a proton donor for the transformation of diazene to ammonia [25]. If INH binds inside the haem pocket, substitution of Ser-315 with Thr of katG (S315T) mutant could reduce the accessibility to the KatG haem pocket by steric hindrance in the access channel [15, 24].

Independent catalase, peroxidase, oxidase, hydrazinolysis and synthase activities exist in the KatG enzyme. KatG catalyzes the reaction of NADH to form NAD^+. Although the binding site of NADH has not yet been identified, the investigation of the interaction of the KatG enzyme and NADH indicated that the NAD^+ /NADH binding site was separate from the INH binding site, due to the finding that INH doesn't inhibit NADH oxidation, whereas NAD^+ doesn't inhibit hydrazinolysis. It was also indicated that KatG catalyses the formation of isonicotinoyl –NAD from NAD^+ and INH [26].

1.3 InhA mechanism

INH targets *M. tb* virulence genes involved in mycolic acid synthesis. Virulence genes are generally defined as genes that are necessary for the survival of the pathogen in a host and are involved in pathogenesis but are not necessary for growth of the pathogen in culture medium. Genes induced during infection are possibly significant for the survival and growth of the pathogen. Several such genes identified in *M. tb* were involved in fatty acid (FA) metabolism [27].

Some pathogenic mycobacteria such as *M. tb* synthesize α-, keto- and methoxy-mycolic acids (see Fig. 1.3), whereas attenuated *Mycobacterium bovis (M bovis)* Bacille Calmette-Guerin (BCG) strains sometimes produce α- and keto-mycolic acids only. *M. tb* with an inactivated hma gene did not synthesize oxygenated mycolic acids, exhibited decreased cell wall permeability and were of attenuated virulence in mice. The methyl transferase coded by hma (formerly known as cmaA or mma4) methylates a double bond in α-mycolic acids, which can be hydrated to form hydroxyl-mycolic acids. Because the hma KO strain of *M. tb* was attenuated in mice, one can deduce that oxygenated MA could be important for the pathogenicity of the bacteria [28].

A few types of fatty acid synthetases (FAS) occur in nature. The Type I synthetases occurring mainly in animal and yeast cells are high molecular mass proteins covalently bound to an acyl carrier protein (ACP) and are multifunctional. The Type II FA synthetases occurring in plants and bacteria are monofunctional. Mycobacteria contain both Types I and II FAS. The InhA protein was shown to be part of the FAS-II system as FA synthesis was inhibited by inhibitors of InhA such as INH, hexadecanoyl-coA and octadecanoyl-coA [29].

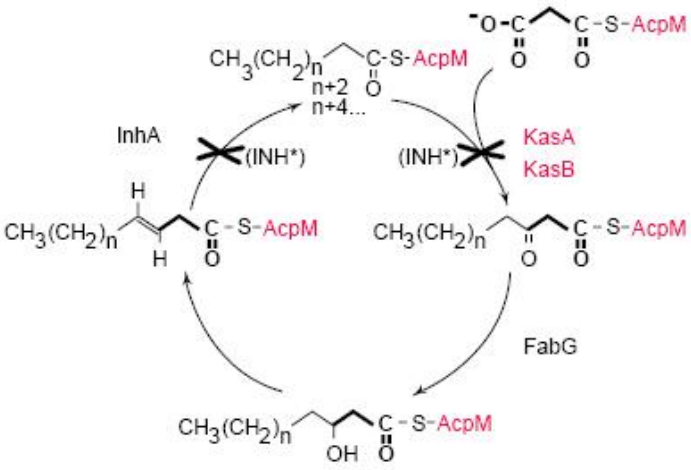

Fig. 1.7 The FAS-II pathway of M. tb Enzymes inhibited by INH [30]

The role of FAS I is to perform *de novo* synthesis of FA from acetate to make acyl chains up to 24 carbons in length. FAS-II has an elongation function and is unable to perform *de novo* synthesis from acetate units. FA synthesis occurs through cycles of condensation, carbonyl reduction, dehydration and enoate reduction. The saturated FA produced during one cycle is used as a substrate for the next cycle until the required chain length is obtained. Fig. 1.7 indicates a mechanism for the FAS-II system. The first step in the elongation is catalysed by KasA and KasB enzymes. The growing chain, which is attached to cysteine at the active site, couples to malonate. This malonate is attached to a serine residue of an ACP. In the second step the β-ketone formed from the condensation is reduced to a secondary alcohol by the NADPH dependent ketoacyl reductase FabG. For the third step the alcohol is dehydrated by the hydroxyacyl reductase to form α,β-unsaturated enoyl ACP. The final reaction of this

elongation is the reduction of the unsaturated enoyl ACP to a saturated hydrocarbon chain by the enoyl reductase using NADH as cofactor [31].

INH blocks a type II FAS complex required for the extension of the meromycolate chain in MA synthesis. Considering results of different studies, it can be concluded that INH targets three FAS-II complex proteins. It first binds to NADH and attaches to the active site of InhA, and then forms a covalent complex between β-ketoacyl ACP synthase (KasA) and acyl carrier protein (AcpM) [11, 32]. By making use of microarray analyses and the *M. tb* genome [33] INH treatment was shown to induce the AcpM, kasA, FabG and fbpC (ag85) genes. Dominantly produced exported proteins and protective antigens of *M. tb* called antigen 85 (ag85) complex (fbpC) [34], esterifies mycolates to specific carbohydrates, a terminal step of mycolate maturation. FbpC is up-regulated by a feedback mechanism that senses the depletion of mature mycolates.

InhA is an enoyl ACP reductase that catalyzes the β-nicotinamide adenine dinucleotide (NADH) specific reduction of 2-trans enoyl acyl carrier protein (Fig. 1.7). Strains with InhA missense gene mutations showed INH resistance in *M. smegmatis, M. bovis* and *M. tb*. InhA protein can use nicotinamide or flavin nucleotides as substrate or cofactors. Resistance against INH could be due to missense mutations in the coding region of InhA or mutations that cause the overexpression of InhA. Crystal structure determinations of InhA showed the enzyme had a “chair-like” conformation composed of seven β-strands and eight α-helices. The crystal structure of InhA complexed with NAD^+ and a C16 fatty acyl substrate showed that the substrate bound in a general U-shape conformation [35]. It was revealed that the location for the fatty acyl substrate binding product was adjacent to the bound NADH [36]. The overall fold of the InhA enzyme is highly reminiscent of a “Rossmann” fold involving parallel β-strands surrounded by α-helices [37].

Kinetic and structural studies showed that activated INH-NAD binds in the NADH binding site of InhA [38]. In addition X-ray crystallography and mass spectrometry showed that the activated, covalent complex of INH and NADH is bound within the active site of InhA. It was also shown that mutants of InhA have a decreased affinity for NADH and would thus preferentially bind acyl ACP substrates before isonicotinic

acyl-NADH, allowing normal catalysis to proceed resulting in INH resistant *M. tb* [35].

The INH-NAD adduct was isolated and purified and the affinity towards the wild-type and drug resistant mutants of InhA was investigated by means of enzyme kinetic studies. It was observed that the INH-NAD adduct was a slow, tight-binding, reversible inhibitor that interacts rapidly with the enzyme to form an initial complex that slowly converts to a more stable inhibited complex. The experiments have also shown that the adduct binding to the mutants was just as stable as that of the wild type strain but the conversion to the more stable complex was slower due to the weaker interaction of INH-NAD with the enzyme in the initial complex [17].

Some articles suggest that INH has a different primary target in *M. tb* than in *M. smegmatis*. Examination of protein profiles of *M. tb*, in response to INH treatment indicated that INH formed a covalent cross-link between ACP and KasA by means of a covalent bridge of both to INH [32, 39]. In another study thermal inactivation of the InhA gene or INH treatment in *M. smegmatis,* indicated morphological changes to the cell wall leading to cell lysis [40]. Characterisation of InhA mutations together with KatG mutations in relation to lipid metabolism of INH-resistant isolates could perhaps solve the difference in opinion that research groups have about the different main targets in *M. tb* and *M smegmatis* [41].

Thus, to conclude the above discussion INH must be activated by the KatG enzyme which resides either in the cytosol or possibly on the outside of the bacillus. Whether INH enters the bacillus before or after activation by the catalase is not known. The activated INH must then move towards the cell wall on the inside of the bacillus in order to inhibit the enzymes of FAS II, whether it is KasA, InhA or both.

1.4 InhA and cholesterol

The intrinsic drug resistance of mycobacteria has been attributed at least in part to the low permeability of the cell wall. The influx of small hydrophilic agents is likely to occur through porin channels. Lipophilic agents may cross the cell wall through its

lipid domains. By making use of differential scanning calorimetry it was shown that mycolic acids produce a bilayer structure of exceptionally low fluidity and low permeability. A more fluid cell wall allows for a more rapid accumulation of agents, than less fluid walls [42].

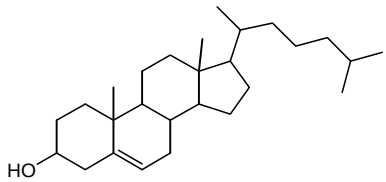

Fig. 1.8 General structure of cholesterol

Cholesterol (Fig. 1.8) is the predominant sterol in all mammalian cells. It is a vital constituent of cell membranes and the precursor of steroid hormones and bile acids. Transport proteins could be affected by the cholesterol content of the membrane. For example, an increase in the amount of cholesterol inhibits ATPases and activates most other transport proteins [43]. Cholesterol could do this indirectly by changing the membrane fluidity or directly by interacting with the transport proteins. When the genome of *M. tb* was investigated, homologies towards yeast sterol biosynthetic enzymes as well as homology towards the sterol 14α-demethylase biosynthetic enzyme was observed. By making use of gas chromatography-mass spectrometry (GC-MS) it was found that cholesterol was a minor constituent in *M. smegmatis*. The results confirmed the presence of a sterol biosynthetic pathway within the bacteria that could lead to new opportunities for chemotherapy [44].

3β/17β-Hydroxysteroid dehydrogenase (3β/17β-HSD) from the bacterium *Comamonas testosteroni* is able to degrade steroids. Hydroxysteroid dehydrogenases belong to the aldo-keto reductases or the short chain dehydrogenases/reductases (SDR) family. 3β/17β-HSD contains the catalytic triad Tyrosine, Lysine and Serine similar to those found in SDR enzymes [45]. InhA is a member of the SDR family of enzymes. The main characteristic of this family is a polypeptide backbone topology in which each subunit consists of a domain containing a Rossmann fold supporting an NADH binding site. Within the InhA several α helices and β strands extend beyond the NADH binding site creating a substrate binding site. Structural studies also indicated that InhA prefers fatty acid substrates of C16 or greater [41]. FAS-II system

enoyl-ACP reductases and several steroid dehyrogenases may also be part of the SDR family. The 7-α-hydroxysteroid dehydrogenase (7α-HSDH) catalyzes NAD^+ dependent dehydrogenation of bile acids. *M. tb* InhA and *Escherichia coli* (*E. coli)* 7α-HSDH show a 22% amino acid sequence identity. Superposition of their crystal structures indicated that their backbone topology was similar (Fig. 1.9). The bile acid substrate binds to *E. coli* 7α-HSDH in nearly the same location as the C16 fatty acyl substrate binds to InhA [35].

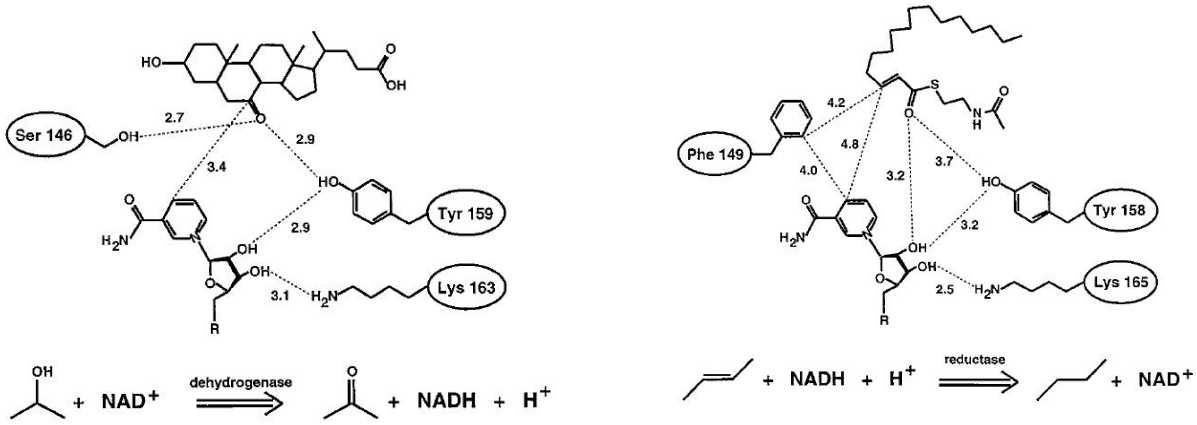

Fig. 1.9 Schematic representaion of the E. coli *7α-HSD (left) in complex with a bile acid and NADH product. The dashed lines indicate hydrogen bonds and the numeric values the distances in angstrom. InhA (right) in complex with a C16 fatty acyl sybstrate and NAD^+ [35].*

Fig. 1.9 shows differences between these two enzymes. The catalytic triad of *E. coli* 7α HSD is Ser^{146}- Tyr^{159}- Lys^{163} whereas for InhA is Phe^{149}-Tyr^{158}-Lys^{165}. Tyrosine interacting with the acyl substrate and Lysine interacting with NAD^+ is consistent in the SDR family [35].

As mentioned previously, the SDR family binds NAD(P)(H) in a modified "Rossmann" fold motif for steroid reductions or oxidation reactions. The "classical Rossmann" fold is defined for proteins resembling human lactate dehydrogenase (LDH). 17β- hydroxysteroid dehydrogenase (17BHSD1) is part of the SDR superfamily. Estrogen is reduced by the NADPH dependent 17β-HSD1 into a more potent estrogen involved in hormone sensitive breast cancer. Derivatives of Gossypol,

a polyphenolic binaphthyl derived from cottonseed were shown to inhibit 17β-HSD1 as derived from enzymatic assays. The compounds competitively inhibited NAD in the co-factor site. Docking studies suggested that the gossypol inhibitors interact primarily in the nicotinamide-binding region [46].

SDR proteins have low sequence identities to one another but their 3-dimensional structures have similar folding patterns typical of a "Rossmann" fold. A catalytic tetrad of Asn-Ser-Tyr-Lys was established [46]. SDR enzymes could form possible targets for drugs. The most conserved active site residue in the family is tyrosine. Three different sites in the SDR can be assigned, namely the coenzyme binding region with a typical Rossmann-fold, the active site and sections proximal to the substrate binding region. Of the critical amino acids in the active site, tyrosine acts as the catalytic base, serine stabilizes the substrate and lysine interacts with the nicotinamide ribose. Some SDR targets have been identified for the development of antibiotics such as β-ACP reductases and enoyl-ACP reductases (*E. coli, M. tb*) [47]. From the similarities between the enoyl-reductase and SDR enzyme families and their structurally related binding sites, it could be concluded that similar substrate structures might bind to the binding sites of these enzymes, for example a cholesterol type of molecule might bind to the binding site of *M. tb* InhA.

1.5 INH inactivation by acetylation

Different plasma levels of INH are detected in individuals that received the same dose of the drug. The reason is that INH is inactivated by acetylation in the liver to different degrees in different individuals. Acetyl-coA is the acetyl donor for INH acetylation [48].

Reaction:
INH + acetyl coenzymeA → Acetyl-INH + coenzyme A

Arylamine N-acetyltransferase (NAT) plays an important role in the pathways for detoxification or activating substrates when the enzymes are exposed to homo- and heterocyclic arylamine and hydrazine xenobiotics. INH acetylation occurs via NAT-2.

Some of the side effects from INH are related to a genetic polymorphism that impairs the drug's elimination. A reduction in the N-acetylation rate causes these impairments [49]. Individuals with fast INH acetylation have too low concentrations of the drug in their plasma. This can also lead to the drug not reaching the minimal concentration needed for inactivation of the target [50].

It was previously thought that acetyl-coA binds to the NAT enzyme before INH does, but nuclear magnetic resonance (NMR) studies showed that INH doesn't need acetyl-coA to bind the enzyme. It is therefore suggested that INH binds to NAT first which promotes acetyl-coA hydrolysis resulting in acetylation [51].

Serum concentrations of INH are influenced by enzymic acetylation by NAT-2. NAT is also present in mycobacterial pathogens. It was shown previously that NAT from *M. tb* could acetylate INH and therefore become more resistant towards INH's activity. It was shown that by protecting the hydrazine moiety of INH as a Schiff base, the de-activating process of NAT-2 acetylation was blocked both *in vitro* and *in vivo*. For Rifampin and Ethambutol resistant organisms a minimum inhibitory concentration (MIC), for the INH derivative molecule, of 0.05 mg/ml was achieved but that lesser activity was detected for INH resistant organisms (MIC >0.75 mg/ml). When N-acetylation of INH was prevented by chemical modification, the drug could display strong activity, low toxicity and excellent bioavailability [6].

1.6 Cholesterol in the uptake of Mycobacteria into macrophages

Mycobacteria can grow on a variety of carbohydrates and hydrocarbons *in vitro* with glycerol being one of the preferred carbon sources. In a study to test whether cholesterol could be used as a sole carbon source it was shown that when culturing *M. tb* in the presence of lecitin-cholesterol liposomes, lecitin was used as the carbon source [52]. Coulorimetric determinations, TLC and HPLC analyses illustrated that fast-growing non-pathogenic bacteria were able to grow on cholesterol as sole carbon source; whereas slow growing pathogenic bacteria did not. The pathogenic bacteria were able to accumulate the cholesterol. This could indicate that cholesterol may play a role in mycobacterial infection [53].

Normally the function of macrophages is to engulf micro-organisms to transport them in phagosomes to lysosomes for degradation. Pathogenic mycobacteria, such as *M. tb,* can survive within macrophage phagosomes, circumventing the host's defence mechanisms. In contrast to live *M. tb,* dead mycobacteria are readily transported to lysosomes where they are destroyed [54].

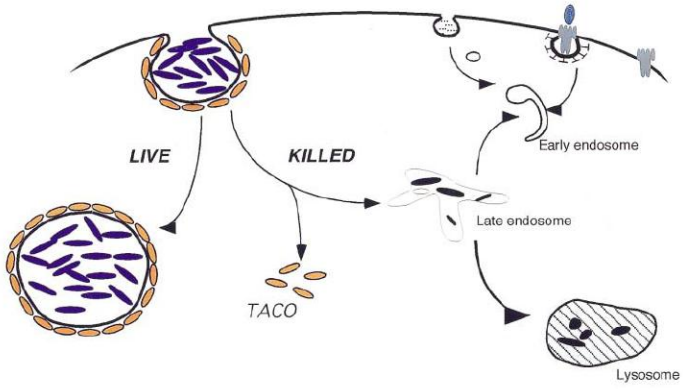

Fig. 1.10 Defense mechanisms of the mycobacteria, evading the macrophage host. Phagocytosis of mycobacteria (blue) into the macrophages triggers the recruitment of TACO (yellow) around the emerging phagosome. The TACO coat must be removed in order for the dead mycobacteria in the phagosome to be delivered to the lysosome where the contents of the phagosome are degraded. Living mycobacteria are able to retain TACO at the phagosomal membrane, preventing the delivery to the lysosome so that the bacteria can survive within the phagosome [54].

A coat protein (Fig. 1.10) termed TACO (tryptophane aspartate containing coat protein) that was retained at the cytoplasmic face of the phagosomes carrying the viable mycobacteria was discovered by Ferrari *et al*., 1999 [55]. TACO is expressed in cells of the lymphoid/myeloid lineage and is not an integral protein but is bound to the phagosomal membrane via a steroid moiety, cholesterol. Therefore, TACO associates with the phagosomal membrane in a cholesterol dependent manner. Killing the mycobacteria with chemotherapy caused a release of the TACO protein resulting in lysosome fusion. In addition, macrophages that lacked TACO (example in Kupffer cells) destroyed mycobacteria after being taken up, suggesting that TACO is involved in the intracellular survival of mycobacteria [55]. It was speculated that TACO, which

is a coat protein of the plasma membrane and phagosome, could mimic the plasma membrane thereby avoiding lysosomal delivery [56]. Infection of macrophages with mycobacteria coincided with the accumulation of cholesterol at the entry site of the mycobacteria and attracted TACO to the phagosome membranes in a cholesterol dependent way [57].

Mycobacteria enter the macrophage by means of a variety of surface receptors resulting in the delivery of the bacteria to the phagosome. It was found that cholesterol accumulated at the site of entry of the mycobacteria, compared to uninfected macrophages where cholesterol was distributed at the plasma membrane and intracellular stores. Depletion of cholesterol from the macrophages made the macrophages incapable of internalising the mycobacteria, indicating a cholesterol dependence for the entry of mycobacteria into the macrophages [57].

A possible structural relationship between mycolic acids (MA) and cholesterol was indicated by our group. By means of biosensor studies it was detected that MA attracted cholesterol. Antigenic cross-reactivity between MA and cholesterol was also observed [58]. These observations could indicate a structural relationship (mimicry) between these two molecules [59].

1.7 Rerouting possibilities

For effective chemotherapy of intracellular pathogens such as *M. tb*, it is necessary to maintain high concentration levels of drugs in the blood. The challenge is to develop systems capable of delivering the drugs to intracellular sites of infection at relatively low levels in the blood. INH is still the most widely used drug in tuberculosis treatment. INH is a small, water soluble molecule and gets quite rapidly metabolised leading to less effective treatment. Thus, changing the route that INH follows and possibly targetting it towards cholesterol, might enhance INH's activity and lower the required dosages. This may be achieved by chemical derivatisation of INH.

1.8 Isoniazid (INH) derivatives

1.8.1 Existing INH-derivatives

A chemical modification of an existing TB drug must show strong mycobactericidal activity *in vitro* and *in vivo* with low toxicity and good bioavailability. Many INH-derivatives have been described in the literature [60-62], some of them with improved MIC values against *M. tb.* A few of these derivatives will be briefly mentioned. By computer automated structure evaluation and *in vitro* testing, 136 INH-derivatives were analysed. Most of the INH-derivatives were N-monosubstituted. One type consisted of alkyl-substituted derivatives, whereas the others included N-hydroxyalkyl substituted derivatives. Some of these drugs had better minimum inhibitory concentration (MIC) values than INH and others not [63].

It has been shown that para-substituted isonicotinic acid benzylidene hydrazides retained a degree of activity against *M. tb* and were less toxic than INH alone [64]. An example of an N-monosubstituted drug is N-isonicotinoyl-N-(salicylidene) hydrazine (Fig. 1.11) [65] which retained activity against *M. tb*. Another derivative was a lipophilic schiff base, N2-cyclohexylidenyl isonicotinc acid hydrazide that was shown to block acetylation of INH (Fig. 1.11) [6]. The authors concluded that in order to improve the activity of INH, derivatisation should be directed towards increasing the lipophilicity of the compound, thereby slowing and prolonging the release of INH [64, 66, 67].

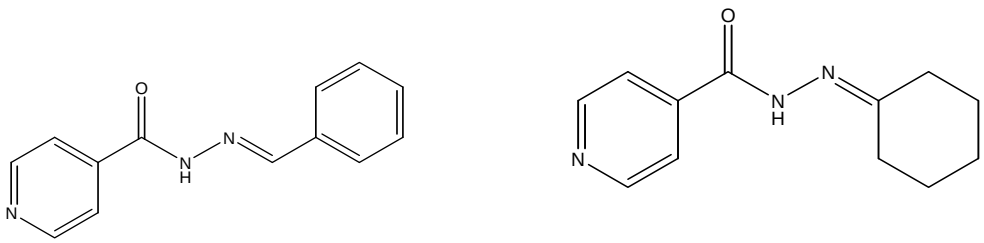

Fig. 1.11 Examples of INH-derivatives. N-isonicotinoyl-N-(salicylidene) hydrazine (left), N2-cyclohexylidenyl isonicotinc acid hydrazide (right).

An alternative approach to the synthesis of INH derivatives is to use carriers to deliver drugs to their target sites. For example, nebulized solid lipid based particles were used to incorporate drugs including INH. The results in animals indicated that the bioavailability and dose frequency was improved for INH [68]. Although good results were obtained with these nanoparticles, there is now a dispute amongst scientists about the safety of nanoparticles as drug carriers.

Mycobacteria enter macrophages by various receptors such as complement, mannose and scavenger receptors. Selective receptor blockade during phagocytosis indicated that class A scavenger receptors account for a significant fraction of *M. tb* macrophage interactions. Receptor blockade did not alter the uptake and survival of the *M. tb* in the human macrophage [69, 70]. Targeted delivery was investigated aiming at scavenger receptor mediated endocytosis of macromolecular drug conjugates in macrophages. p-Aminosalicylic acid (antitubercular agent) was conjugated to maleylated bovine serum albumin (MBSA). This combination was taken up by scavenger receptors on *M. tb* infected murine macrophages. The protein was degraded by lysosomes, leading to the release of the drug. The conjugated drug was nearly 100-fold more effective than the free drug. Thus by targeting the drug to the specific site of infection the efficacy of the drug could be improved [71].

1.8.2 INH - AmB linkage possibility

A way to increase the lipophilicity of INH, in order to increase its efficiency, is to link it to a hydrophobic molecule. The covalent linkage of an antifungal agent, Amphotericin B (AmB) to INH may fulfil this property while simultaneously targeting the drug to the host macrophages. AmB follows the route of low density lipoproteins (LDL) within the human body. It was shown that LDL type of molecules were taken up from circulation by macrophages through scavenger receptors [72]; therefore AmB could be taken up by similar receptors on macrophages as *M. tb.* If AmB is linked to INH it could be that AmB will change the trajectory of INH towards its target, thereby improving the efficacy of INH by increasing the lipophilicity and directing its uptake in macrophages via the lipoprotein route.

1.9 Amphotericin B structure and function

Amphotericin B (AmB, Fig. 1.12) is an amphipathic fermentation product produced by the South American soil Gram-positive bacterium *Streptomyces nodosus*.

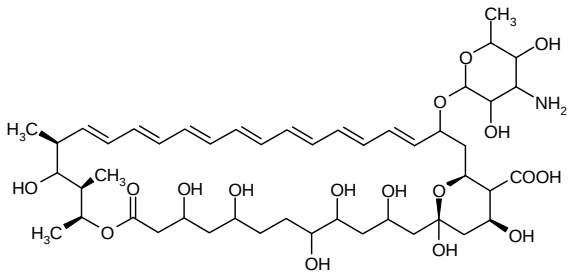

Fig. 1.12 Structure of the antibiotic AmB [73].

AmB is the treatment of choice for a variety of mycoses and is also used for the treatment of fungal infections in HIV positive patients. It is generally thought that the activity of this drug results from the interaction with ergosterol, the main sterol in fungal membranes (see Appendix E). However, AmB also interacts with cholesterol, the major sterol in mammalian membranes [73, 74]. AmB has a broad anti-fungal spectrum and little resistance has been observed against this drug. Unfortunately the therapy with AmB is limited due to its negligible solubility in aqueous solutions and poor solubility in most organic solvents. Therefore formulations with water soluble molecules such as arabinogalactan [75, 76] and deoxycholate as well as lipid based delivery systems are used for the administration into patients. Toxicity is mainly to the kidneys, central nervous system and liver, together with several other side effects also limiting the administration of this drug [77].

AmB interacts with components of the cell membrane and forms ion channels. These ion channels disrupt membrane functions by allowing free flow of cations through the channel that leads to cell death. The selective toxicity of AmB is mainly due to its greater affinity towards ergosterol. The main difference between channels formed in fungal and mammalian cells, is that the AmB in the ergosterol containing membrane create larger channel pore sizes than in cholesterol containing membranes and that the intermolecular hydrogen bonds are more specific between AmB and ergosterol [73].

A schematic representation of the interaction between AmB and the phospholipid bilayer is shown in Fig. 1.13 [78]. Each cylindrical shaped channel consists of eight AmB molecules non-covalently associated with eight sterol molecules.

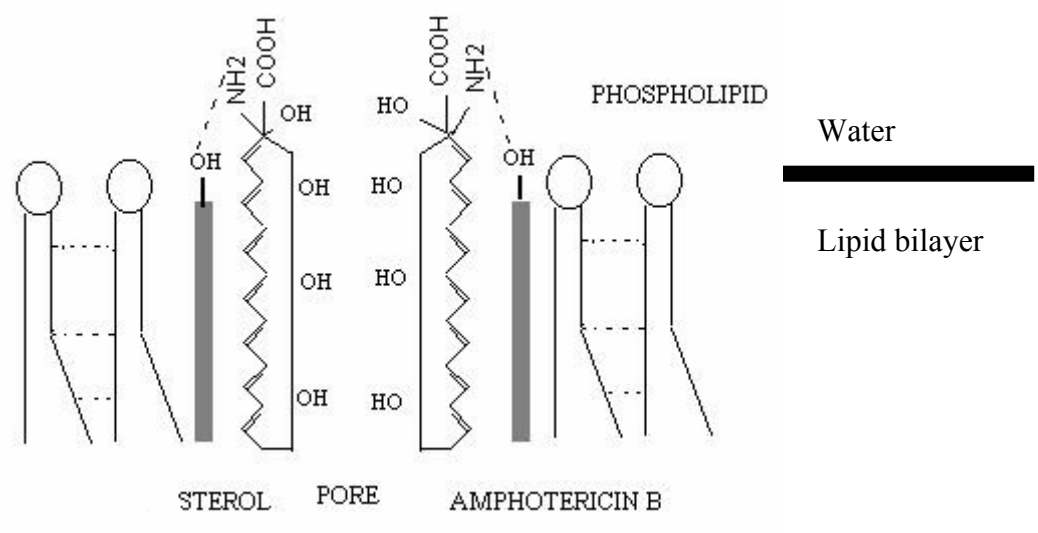

Fig. 1.13 Schematic representation of an AmB-sterol pore. The dotted lines between the hydrocarbon chains of the phospholipids represent short range London and van der Waals forces. The dashed lines represent hydrogen bonds formed between AmB and the sterol. Cartoon integrated from literature [74, 78].

Mycobacterium smegmatis showed sensitivity towards several azole compounds such as econazole and ketoconazole, but was not sensitive towards AmB, thus AmB should not have a toxic effect on *M. tb*. If linked to INH it is expected to act only as a haptophore for the INH toxophore [79, 80].

1.9.1 AmB and its receptors

Free molecules of AmB or formulations of AmB can associate with serum lipoproteins [81, 82]. One of the reasons for the toxicity of AmB may be due to the binding to low density lipoproteins (LDL) and also the internalisation of AmB through LDL receptors on the plasma membrane of the cell [81, 83]. It was also shown in Chinese hamster ovary cells that AmB was internalised by endocytosis in the presence of serum after binding to the plasma membrane. LDL receptors were thought to play a role in the uptake of the AmB. It was observed that at high

concentrations of AmB, endosome-lysosome fusion was blocked. AmB may therefore play a role in disordering the endosomal plasma membrane or have an effect on the Na^+/K^+ ATPase and in doing so have an effect on the endosomal pH. This result may cause an inhibition of endosomal maturation and fusion with the lysosome [82].

Previous reports showed that formulations of AmB could be internalised by macrophages. It was said that these macrophages could then also act as reservoirs for AmB. The drug could then either be released from the macrophages as monomeric AmB or directly kill parasites inside the macrophages. Tumour necrosis factor α (TNF–α) was also stimulated by AmB in the macrophages [81, 83]. It must be noted however that if AmB inhibits endosome-lysosome fusion, then AmB must be transported to phagolysosomes containing parasites by mechanisms other than fusion.

Microbial products are recognised by Toll-like receptors (TLRs) in immune cells and stimulate inflammatory cytokine release. AmB, as a microbial product, also stimulates immune cells to produce inflammatory cytokines such as TNF-α via TLR-2 and CD14. AmB could also modify and bind to the cholesterol and glycolipid-rich microdomains termed lipid rafts. CD14 is an integral lipid raft protein and TLR-2 and TLR-4 possibly associate with lipid rafting during activation. Sau K. and co-workers believed that the ability of AmB to create more ordered lipid structures in the cell membrane could assist in the interaction between AmB and TLRs that also associate with the lipid moieties. This mechanism may explain the acute inflammatory toxicity elicited by AmB [84].

1.9.2 The interaction of AmB and Human Immunodeficiency Virus (HIV)

AmB and its derivatives were shown to have anti-HIV properties. The mechanism is uncertain, but it could be that AmB associates with the HIV membranes because of the 2.5 times higher cholesterol: lipid ratio in the HIV membranes of the virions compared to that of their host [81, 85].

In more recent studies it was shown that AmB could reactivate latent HIV-1 infection in macrophages, but not directly in the T-cells. AmB's induction of TNF-α secretion

could contribute, but need not be essential to HIV-1 reactivation. Therefore elimination of cells harbouring previously latent HIV-1 infection could be assisted by the application of appropriate HIV-1 immunotoxins, including AmB. Because AmB could also produce proinflammatory cytokines and interfere with activation of macrophages, care should be taken in management of HIV-1 infection with combinations of chemotherapy [86, 87].

1.10 Aim of the project

This project will seek to improve INH (toxophore) by lipophilic modification through derivatisation of the hydrazine moiety and in that way also decrease potential acetylation. By conjugation to AmB (haptophore) the aim is to reroute INH and to create high drug concentrations around its target without exposing the body to similar high concentrations. The determination of the product's mycobactericidal and cholesterol binding properties will also be determined. This project is to serve as a model for rerouted and targeted delivery of anti-TB drugs.

Chapter 2: Synthesis and purification of a cholesterol targeting mycobactericidal drug

2.1 Introduction

The synthesis of INH derivatives to improve the therapeutic profile is not a new concept; it goes back as far as 1954 [65]. Antibacterial resistance to current drugs such as INH could be counteracted by designing new derivatives that could improve or re-establish the drug's effectiveness. For example, one derivative had 4 times improved the MIC of INH (Fig. 2.1.i) [60]. Resistance of *M. tb* to administered drugs is usually acquired by alteration of the drug target through mutation or by titration of the drug through overproduction of the target; this was also observed for INH in *M. tb* [41]. Pumping drugs out of the cell by means of ABC type multidrug transporters are also a form of resistance that the *M. tb* elicits against drug treatment [88]. Another process that decreases the potency of INH is enzymatic acetylation by NAT enzyme present in humans and also in *M. tb* [6, 89]. This acetylation causes a decrease in the drug's effectiveness due to lowered serum drug concentrations and consequently an increase of potential resistance to the drug.

Analysis of the structure of INH highlights a few chemical groups that could readily be derivatised. The primary amine (NH_2) which has a lone pair of electrons present and is a nucleophile, could react with an electrophile or could act as a base to form a salt. More specifically a few types of links that could be made to the amine are hydrazones (Schiff base or an imine) or hydrazides. Alkyl substitutions from the reduction of hydrazones are also feasible.

The amide nitrogen (O=C-NH) should be less reactive than the primary amine and therefore modification to this group would only be after the reaction or protection of the primary amine.

The pyridine present in the INH structure should have a low reactivity towards electrophilic aromatic substitutions but could undergo nucleophilic aromatic

substitutions more easily. From a biological perspective, however, chemical modification to the pyridine ring might not be advantageous. It is thought that the pyridine ring plays an important role in the toxicity of the INH as described in chapter 1.

Chemical modification of the hydrazine group (NH_2) of INH with a functional group that blocks acetylation has the potential to increase the effectiveness of the drug. Such an example of a Schiff base is illustrated in Fig. 2.1 (ii), a compound that was more active against *M. tb* than the parent INH [6]. Good activity of numerous hydrazones and hydrazides of INH against tubercular, fungal and bacterial infections was observed. An example in which both nitrogen groups were modified to effect improved activity is shown in Fig. 2.1 (iii). Several related derivatives were made by first preparing the hydrazide/hydrazone and then reacting the amide [62].Comparing the MIC values of the derivatives it seems as if only modification to the primary amine lowers the MIC values and not modification to both nitrogen groups [6, 60, 62, 67]. Modification of the hydrazine group of INH seems to be the trend most research groups follow. In an effort to correlate chemical structure with biological activity, the structures of 136 previously synthesized and *in vitro* tested hydrazide substituted INH derivatives were analyzed *in silico* with a software programme named MULTICASE. Using the molecular structures and corresponding experimental biological activities the MULTICASE calculates different chain lengths and number of atoms for each molecule in the database. These values are then subjected to a binomial distribution based statistical analyses and the molecules are rated as active or inactive. The programme's main objective was to find structural moieties that discriminate active compounds from inactive ones. The success was dependent on the hypothesis that a relationship exists between activity and structure. Overall it appeared that the compounds which had the best activity were hydrazones or N-alkyl substituted hydrazides. The final conclusion for the computer generated predictions (combined with *in vitro* studies) was that in order to improve activity and to, slow the release of INH and avoid negative hepatic effects due to large doses of INH, attempts should be directed towards increasing the lipophilicity [63].

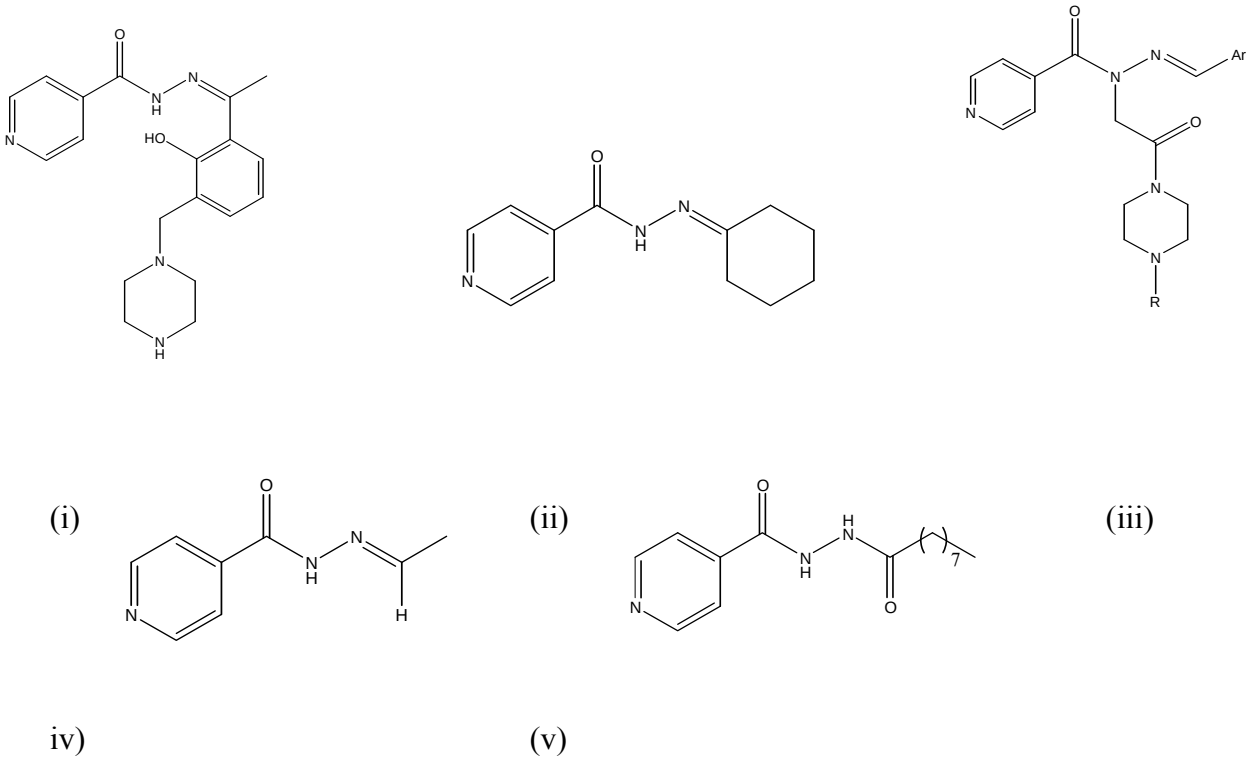

Fig. 2.1 Chemical structures of INH derivatives from previous studies: (i) [60], (ii) [6], (iii) [62], (iv)[67], (v) [66].

A great number of lipophilic INH analogues have been synthesized and tested over the last few years by Maccari R. and her colleagues, with several of these analogues having positive *in vitro* antimycobacterial properties. The authors indicated that upon increasing the lipophilicity of an INH derivative by forming the hydrazide (Fig. 2.1 iv) it increases the uptake and potency within cells [67]. In another study, the hydrophobicity of INH was increased by addition of a C-9 chain to the primary amine of the INH molecule. When the growth cycle and the morphological changes (wrinkling at the cell surface) of *M. tb* were studied on exposure to the drugs [Fig. 2.1 (v)], it was observed that the INH-C9 had a lower MIC value than the parent INH molecule. The authors suggested that due to the hydrophobic nature of the *M. tb* cell wall, increased lipophilicity should at least facilitate diffusion through the biomembranes. It was also noted that the bacteria were most susceptible to INH and its derivative during the initial stages of the growth cycle. The conclusion was made that a hydrophobic attachment improved the penetration of the drug into the bacteria [66, 90].

Chemical modification of a molecule need not only be used to enhance a drug's activity. Modification to enhance drug delivery is another field of study to improve the efficiency of the drug. The present challenge in therapy is to develop systems capable of delivering or targeting drugs at the intracellular sites of infection while maintaining low concentrations in the blood to prevent toxic side effects.

Receptor mediated drug delivery could be 100 times more effective than the free drug itself. This was shown for p-aminosalicylic acid, an anti-tuberculosis drug, when it was conjugated to maleylated bovine serum albumin. The conjugate is thought to bind to scavenger receptors present on the macrophages and was therefore taken up by endocytosis. The results showed that the conjugated drug effectively eliminated the mycobacteria that resided in the infected macrophages [71].

Initially liposomes and lipid emulsions were developed as carriers for therapeutic drugs particularly those that were not water soluble. Current research is aimed at developing solid lipid nanoparticles as a new form of therapeutic drug carrier [91]. The nanoparticles have the advantage that they can be used for controlled drug delivery that could enhance the bioavailability of the drugs. Three frontline antitubercular drugs; Rifampin, INH and pyrazinamide have been incorporated into the solid lipid nanoparticles. The results showed that the three drugs could be detected in the lungs, liver and spleen up to 7 days after administration, whereas the free drugs were cleared from the organs within 48 hours. With this type of carrier the dosage frequency could be reduced to 7 instead of 46 times [68]. Although this type of drug delivery holds potential, care should be taken when prolonging the half-life of the compounds, because it could increase their toxicity towards the patients. In addition, the route that nanoparticles follow within the body is still ill-defined and should be researched further to rule out new potential toxic side effects of existing drugs in nanoencapsulated carriers, eg. when nanoparticles cross the blood brain barrier to enter an area that was not accessible to drugs delivered in traditional ways.

Because INH is such a small water soluble molecule it is readily metabolised before reaching its target, so that unless particularly high doses are administered, it reaches its target at too low a concentration to have a lethal effect on the bacteria. From the literature it was suggested that in order to improve the activity of INH, the drug

should be made more lipophilic, enhance the specificity towards its target or reduce the propensity for acetylation [6, 63, 66, 67].

The investigation of a covalent linkage of an antifungal agent, Amphotericin B (AmB) to INH is described in this chapter. Linking AmB to INH could increase the lipophilicity of INH, because AmB is a very large hydrophobic molecule (M = 924.1 $g.mol^{-1}$). AmB is a polyene macrolide with well-defined cholesterol binding properties and could indirectly target INH more specifically to the cholesterol containing macrophages in which the *M. tb* reside, as discussed in chapter 1. Using a Schiff base to link AmB to INH could reduce the potential acetylation of INH that decreases its mycobactericidal effect. Thus in this project we aimed to target INH to the site of infection by lipophilic modification in a way that also decreases potential acetylation.

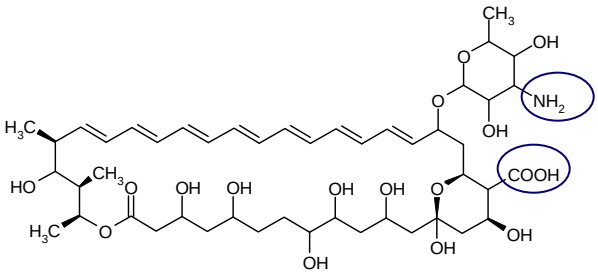

Fig. 2.2 Structure of the antibiotic AmB, the "polar head" is indicated with blue circles [73].

As previously discussed in detail in Chapter 1, AmB (Fig. 2.2) is a polyene macrolide used for treating fungal infections. The conjugated double bonds of AmB interact with the sterol molecules in the membrane by means of non-specific van der Waals forces. The "polar head" of AmB that consists of the amino group of the sugar and the carboxyl group forms hydrogen bonds with the hydroxyl group of the sterols [74, 78, 92].

Free molecules of AmB or formulations of AmB can associate with serum lipoproteins and could also be internalized by macrophages [81, 82]. One of the reasons for the toxicity of AmB may be due to its binding to LDL and also the internalisation of AmB through LDL receptors on the plasma membrane of the cell

[81, 83]. Since it has been shown that AmB binds to LDL receptors, it is assumed that AmB will be taken up by similar receptors as are responsible for the uptake of the *M. tb* pathogen. If INH were linked to the AmB it would reroute INH directly to its target by means of this hydrophobic pathway, hence the choice of AmB as the haptophore.

The following observations could be made on the potential for chemical modification of AmB: the polyene and hydroxyl groups would not be suitable for selective modification; alterations to the glycosidic link or the lactone ester would destroy the structure of AmB; the amine, acting as a nucleophile, could form an imine (Schiff base) or an amine bond; the carboxylic acid could undergo nucleophilic acyl substitutions, for example forming an amide (peptide bond). Chemical modification usually takes place at the amino and/or the carboxyl group of the molecule (Fig. 2.2). For example AmB was conjugated to oxidized arabinogalactan via Schiff base formation [75, 76]. Upon analyses of both of the INH and AmB molecules it was suggested that formation of an imine or amide bond would be the most practical in terms of ease of synthesis and purification. In our study we linked the amino group of AmB to the hydrazine group of INH with a linker molecule terephthalaldehyde (TPA). In this chapter the synthesis and the obstacles encountered during the synthesis of this conjugate will be discussed.

2.2 Hypothesis

If *Mycobacterium tuberculosis* could be envisioned as a cholesterol coated bacillus, drugs used in TB chemotherapy may be improved by linking them to a cholesterol targeting compound which will direct the drug towards the bacteria.

2.3 Aims of the study

To link AmB (haptophore) to INH (toxophore) by means of covalent bond (Schiff base) using terephthalaldehyde as linker molecule.

2.4 Materials

2.4.1 List of specific reagents used:

Acetonitrile	Riedel-de Haen, Seelze, Germany (HPLC grade)
Acetic acid (glacial)	Merck, Darmstadt, Germany (pro analysi)
Amphotericin B (AmB)	Sigma-Aldrich, Steinheim, Germany (isolated from *Streptomyces* to 80% purity, identified by HPLC)
Deuterated dimethyl sulfoxide (DMSO-d_6)	Aldrich, Steinheim, Germany/ Merck, Darmstadt, Germany
Dimethyl sulfoxide (DMSO)	Labchem, Edenvale, RSA
Ethanol	BDH, Gauteng, RSA (Analytical grade)
Ethyl acetate	Saarchem, Gauteng, RSA
Filters for HPLC solvents	Magna nylon filter 0.45µm, Osmonics, USA
Isoniazid (INH)	Sigma Aldrich, Steinheim, Germany (99% purity)
Methanol	Saarchem, Gauteng, RSA
Methanol	Sigma Aldrich Chromasolv, Steinheim, Germany (for HPLC)
Poly (styrene-co-divinyl-benzene) aminomethylated	Aldrich, Steinheim, Germany
Silica gel	Merck, Darmstadt, Germany
Silica gel plate	ALUGRAM SIL G/UV, layer: 0.2mm silica gel 60 with fluorescent indicator UV_{254}, Düren, Germany
Sodium borohydride	Aldrich, Steinheim, Germany
Sodium Chloride	Merck, Darmstadt, Germany
Sodium deoxycholate	Merck, Darmstadt, Germany
Terephthalaldehyde	Fluka, Sigma Aldrich, Steinheim, Germany
Triethyl amine	Acros organics, New Jersey, USA

2.5 Methods

^{1}H, ^{13}C and COSY Nuclear Magnetic Resonance (NMR) were recorded on a Bruker advance DRX-500 spectrometer or Bruker AC-300 spectrometer with chemical shifts in ppm. Analytical thin layer chromatography (TLC) was performed on Alugram SIL G/UV, layer: 0.2 mm silica gel 60 with fluorescent indicator UV_{254} plates. The plates were viewed under Ultraviolet light (254 nm and 366 nm). Flash column chromatography was performed using Merck silica gel. FT-IR was obtained with a Perkin Elmer BX-1. FT-IR Spectrum Software vs. 5.1 with a MIR source and a LiT aO3 detector (internal) resolution 2.00 cm^{-1} instrument. Optical rotations were measured on a Perkin Elmer model 341 polarimeter. For product purification a Waters High Performance Liquid Chromatography (HPLC) system was used with a Waters 610 fluid unit, Waters 600 controller and a Waters 996 Photodiode Array detector. A Waters C-18 reverse phase column (150 x 4.6 mm) was used for optimization of methods and a Phenomenex Luna C-18 reverse phase column (250 x 10 mm, 10 µ) was used to collect the product.

Safety note:

Due to the toxicity of the chemicals used during the synthesis, especially Amphotericin B, gloves were worn at all times and all the reactions were done in a fume cupboard. When Amphotericin B was used in the reaction, all flasks were covered in foil and kept at room temperature (RT) or below.

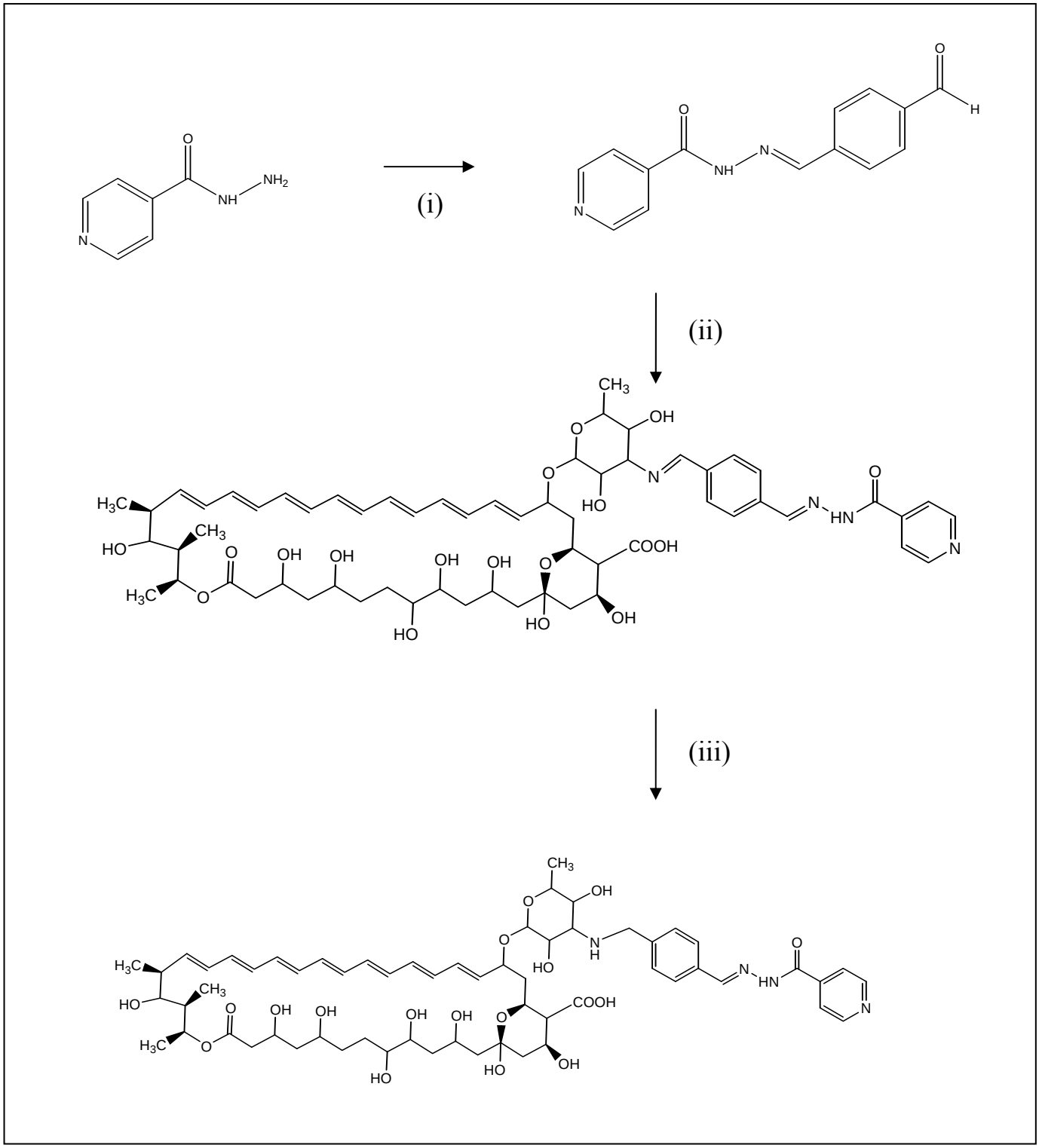

Fig. 2.3 Schematic representation of the main steps involved in the synthesis of Amphotericin B derivative.

Reagents: (i) TPA, ethanol; (ii) AmB, DMSO; (iii) $NaBH_4$, DMSO.

2.5.1 Synthesis of isonicotinic acid p-formylbenzylidenehydrazide (INH-TPA)

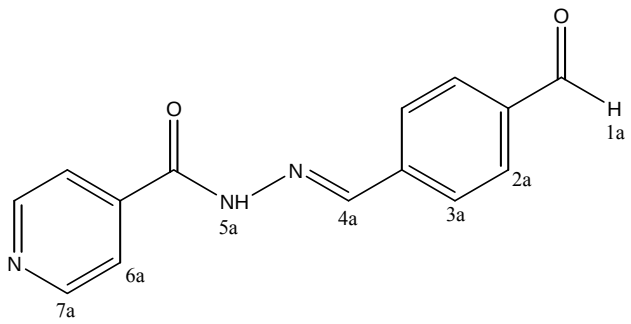

Fig. 2.4 H-numbering for INH-TPA.

INH (0.5 g, 3.65 mmol) was added in portions over an hour to a solution of (0.49 g, 3.65 mmol) terephthalaldehyde (TPA) in ethanol (50 ml) and stirred at room temperature (RT) overnight. Product formation was followed by TLC and the reaction was stopped when no more INH was observed (~ 24 hours). The fine off-white precipitate that had formed was removed by filtration and the mother liquor was retained. The solvent was removed under reduced pressure. The residue (0.15 g) was purified by flash column chromatography on silica gel eluting with a mobile phase of ethyl acetate: methanol: ethanol (v/v) (90: 9: 1). The ethanol contained 1% triethyl amine. From the column a pure INH-TPA (Fig. 2.4) derivative (0.12 g, 14 % yield) was obtained as a light yellow solid.

Molecular weight 253.2599 $g.mol^{-1}$. R_f 0.57 (ethyl acetate: methanol: ethanol with 1% Et_3N (v/v) (90: 9: 1); Mp. 219-220ºC; IR ν_{max} 3465, 3197 (NH), 1698 (CHO) cm^{-1}. ^1H NMR (300 MHz, $(CD_3)_2$ SO) δ 12.25 (1H, s, 5a), 10.06 (1H, s, 1a), 8.80 (2H, d, J = 5.4 Hz, 7a), 8.55 (1H, s, 4a), 8.01 (2H, d, J = 9 Hz, 2a), 7.97 (2H, d, J = 9 Hz, 3a), 7.84 (2H, d, J = 5.4 Hz, 6a); ^{13}C NMR (300 MHz, $(CD_3)_2$ SO) δ 193.1, 162.3, 150.7, 148, 140.7, 139.9, 137.4, 130.3, 128.1, 121.9 ppm, see Appendix F; HR-MS (EI) calculated for $C_{14}H_{10}O_2N_3$ $[M^+]$ 253.08513 $g.mol^{-1}$ found 253.08389 $g.mol^{-1}$, m/z (EI) 122 (74), 106 (100), 79 (10), 78 (47), 51 (22).

2.5.2 Synthesis of an Amphotericin B derivative

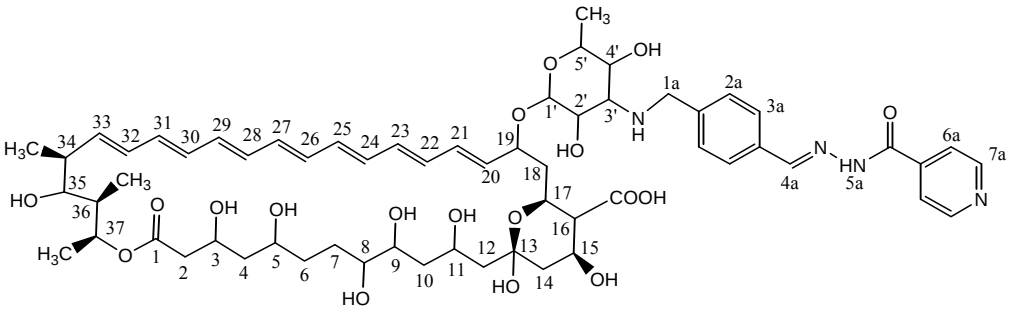

Fig. 2.5 H-numbering of AmB derivative II

In a typical synthesis, INH-TPA (0.01g, 0.04 mmol) was combined with AmB (0.043 g, 0.05 mmol) in 2 ml dimethyl sulfoxide (DMSO). The dark yellow reaction mixture was covered in foil and stirred at RT for an hour. The AmB-Derivative I that formed was reduced *in situ* with $NaBH_4$ (0.001 g, 0.04 mmol) and the reaction stirred overnight at RT [75, 76]. AmB-Derivative II (0.03 g, 18 % yield) a dark yellow solid, shown in Fig. 2.5 was purified by reverse phase (RP) HPLC at RT to separate the product from any unreacted or degraded materials. Elution was carried out with a gradient (see Appendix A) of methanol: H_2O from 20 % to 100 % methanol [93, 94]. The column eluent was monitored at 300 and 407 nm.

Molecular weight 1159.35 $g.mol^{-1}$, melting point not determined due to decomposition at about 40 °C, $\alpha\ ^{20}_{D}$ +328 (*c* 2.0, DMF), IR ν_{max} 3391, (NH, OH 's), 1564 (double bonds) cm^{-1}. ^1H NMR (500 MHz, $(CD_3)_2$ SO) δ 12.06 (1H, s, H-5a), 8.79 (2H, d, J = 3.3 Hz, H-7a), 8.46 (1H, s, H-4a), 7.83 (2H, d, J = 4.4 Hz, H-6a), 7.51 (2H, d, J = 7.9 Hz, H-3a), 7.7 (2H, d, J = 7.9 Hz, H-2a), 6.45-6.07 (m, 12H, olefinic), 5.95 (1H, dd, J = 13, 5.3 Hz, H-20), 5.43 (1H, dd, J = 11.3, 12 Hz, H-33), 5.21 (1H, m, H-37), 4.48 (1H, broad - s, H-1′), 4.4 (1H, m, H-19), 4.24 (1H, m, H-11), 4.23 (1H, t, H-17), 4.06 (1H, m, H-3), 3.99 (1H, dt, H-15), 3.89 and 3.67 (2H, s, H-1a), 3.73 (1H, d, H-2′), 3.54 -3.46 (HOD plus 3H), 3.2 (1H, m, H-5′), 3.09 (2H, m, H-4′, H-35), 2.82 (1H, m, H-3′), 2.28 (1H, s, H-34), 2.16 (3H, m, H-2, H-18), 1.88-1.05 (14H, m, CH_2, CH), 1.87 (1H,t, J = 6.7 Hz, H-16), 1.16 (3H, d, J = 5.5 Hz, CH_3), 1.11

(3H, d, J = 5.6 Hz, CH_3), 1.04 (3H, d, J = 5.6 Hz, CH_3), 0.91 (3H, d, J = 6.5 Hz, CH_3), ^{13}C NMR (300 MHz, $(CD_3)_2$ SO) δ 174.4, 170.6, 161.54, 150.3, 149.1, 143.6, 140.51, 133.9, 136.8, 133.7-128.5, 131.9, 127.2, 121.5, 97.2, 77.1, 73.8, 74.5, 74.4 69.8, 73.6, 69.4, 68.8, 66.2, 65.4, 65.2, 63, 57.1, 44.7, 49.5 - 44.3, 42.3, 42, 35.1, 29, 18.5, 12.1 ppm, see Appendix F.

2.6 Results

2.6.1 Synthesis of isonicotinic acid p-formylbenzylidenehydrazide (INH-TPA)

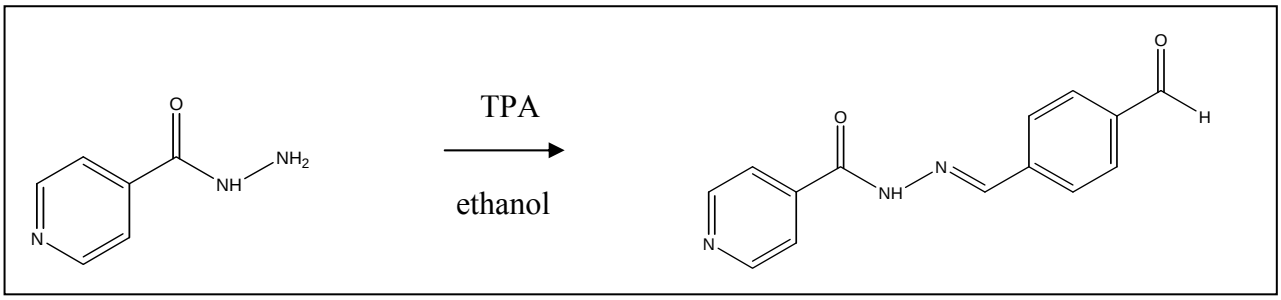

Fig. 2.6 Schematic representation of the formation of INH-TPA.

The synthesis of isonicotinic acid p-formylbenzylidenehydrazide (INH-TPA) by formation of an imine bond from the terminal NH_2 of INH to a C=O of TPA, is the first step in the synthesis of AmB derivative II (Fig. 2.3 i and Fig. 2.6). The synthesis of INH-TPA was originally reported in a patent published in 1952 [64]. The description of experimental details for the synthesis was very vague and initial attempts to repeat the synthesis were unsuccessful. The major product isolated from the reaction of INH and TPA in ethanol followed by recrystallisation from acetic acid was the INH-TPA-INH derivative (Fig. 2.7). The ^{1}H NMR spectrum of this product showed only 5 proton resonances indicative of a highly symmetrical compound and a conspicuous lack of a corresponding aldehyde proton. The INH-TPA-INH product was clearly not pure and a second imine peak at 8.55 ppm, integrating for (0.2) relative to the imine at 8.49 ppm (integrating for 1) was observed. Since there was a corresponding aldehyde resonance at 10.06 ppm (intergrating for 0.2) and appropriate aromatic resonances, it was apparent that the desired compound INH-TPA made up only 20 % of the isolated crystals.

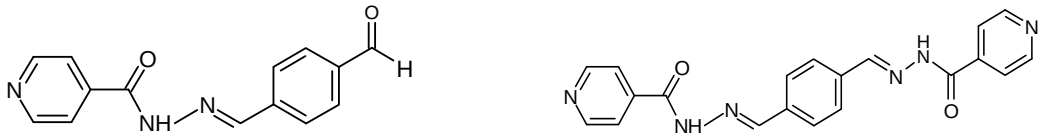

Fig. 2.7 Structure of the INH-TPA (left) and the INH-TPA-INH (right).

In an attempt to improve the method for increased formation of INH-TPA and reduced formation of INH-TPA-INH, the ratio of INH to TPA was increased from 1:1 to 1:10, but surprisingly the INH-TPA-INH adduct remained the major product. It was decided to use the ratio of 1:1 rather than the 1:10 because increasing the ratio increased the difficulty of purification but did not increase the yield.

INH-TPA and INH-TPA-INH can be distinguished from each other by means of TLC. Thus the reaction could be monitored via TLC and stopped when all the INH had reacted (~ 24hours). An example of a TLC plate is illustrated in Fig. 2.8. The TLC indicated the two products obtained together with unreacted starting material. Upon individual NMR analyses of the precipitate that formed and the mother liquor, it was confirmed that the precipitate consisted predominantly out of TPA linked to two INH molecules via an imine bond whereas the INH-TPA stayed soluble in the solvent together with unreacted TPA.

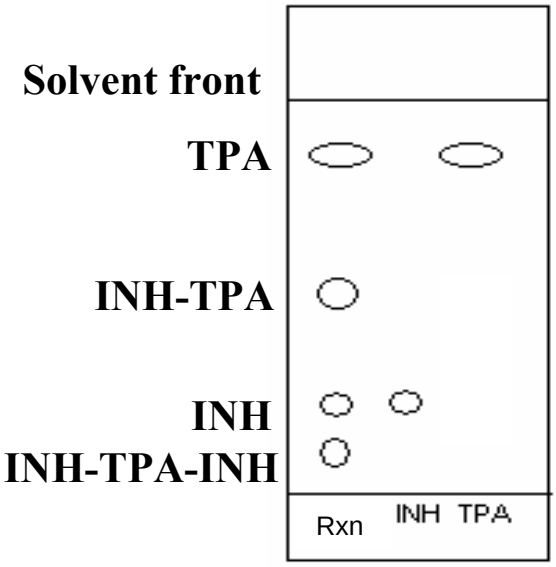

Fig. 2.8 TLC analysis of the formation of INH-TPA. Mobile phase consisted of ethyl acetate: methanol: ethanol with 1% Et_3N (v/v) (90: 9: 1). The plate was visualized at 254 nm and 366 nm. Rxn, represents the crude reaction mixture before filtration while INH and TPA represent pure commercial samples as standards.

Table 2.1: Colour observations and R_f values of the TLC results of Fig. 2.7:

Description	At 254 nm	At 366 nm	R_f = Sample migration /solvent migration
1. TPA	purple	None	0.95
2. INH-TPA	purple	Brown	0.57
3. INH	purple	None	0.32
4. INH-TPA-INH	purple	Yellow	0.19

The relative ratios of INH-TPA and INH-TPA-INH in the solid product precipitate and the supernatant indicated by TLC analysis suggested that the INH-TPA was much more soluble than the INH-TPA-INH. In order to obtain a pure sample of INH-TPA, the solid byproduct that formed during the reaction was removed by filtration of the crude reaction mixture. TLC analysis of the mother liquor showed that the majority, but not all of the unwanted byproducts had been removed. Concentration of the mother liquor gave solid product INH-TPA largely contaminated with unreacted TPA. Attempts to purify the INH-TPA from 10 % acetic acid in different alcohols (methanol, ethanol, isopropanol) were unsuccessful.

Since the INH-TPA, the byproduct and both starting compounds are well separated on TLC, it was likely that flash column chromatography could be used to obtain a pure sample of the desired compound. Following filtration to remove the majority of the INH-TPA-INH, the mother liquor was adsorbed onto silica gel for dry loading of the relatively insoluble material onto the column and the pure product INH-TPA was obtained in 14 % yield. Chromatography proved to be the best and fastest method to obtain pure INH-TPA as demonstrated by ^{1}H and ^{13}C NMR. Since enough material was obtained for future reactions with AmB, no attempts were made to increase the yield of the product.

The structure of the INH-TPA product was confirmed via NMR. ^{1}H NMR chemical shifts were assigned by comparing the NMR spectra of the starting materials to that of the formed product, measuring coupling constants and integrals, using two dimensional NMR techniques and making use of tabulated chemical shift values for organic functional groups (Fig. 2.9).

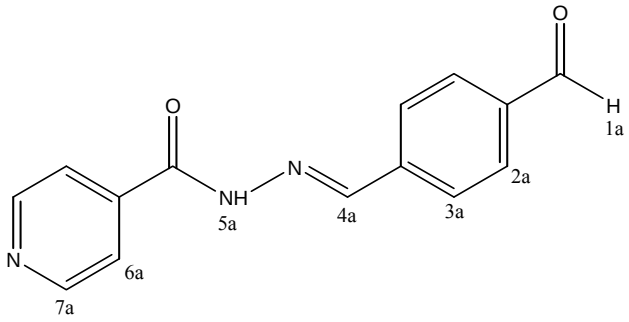

Fig. 2.9 H-numbering for INH-TPA

Protons 2a and 3a couple to each other with a vicinal coupling constant of 9 Hz and protons 6a and 7a couple with a vicinal coupling constant of 5.4 Hz. The peak integration was used to determine the ratio between the protons present, for example the aldehyde peak at 10.06 ppm representing one proton had an integration of one, whereas proton 7a at 8.8 ppm which represents two protons because of the symmetry of the pyridine ring that integrates for 2. The measured integral ratio was very close to the theoretical integral ratio for all proton resonances indicating high product purity with no contaminants contributing to the integration of any of the peaks.

For the IR interpretation, there were distinct peaks in the 3000-3500 cm^{-1} region that could be assigned to N-H stretching. Also bands in the 1600-1700 cm^{-1} region could possibly be assigned to an aldehyde. Another analytical confirmation of the product was the mass spectrometry results that indicated the obtained mass of 253.08389 $g.mol^{-1}$ an error of 1.2 mmu. which is within the allowable error of 5 mmu. for the molecule $C_{14}H_{10}O_2N_3$ with calculated mass of 253.08513 $g.mol^{-1}$.

2.6.2 Synthesis of Amphotericin B derivative

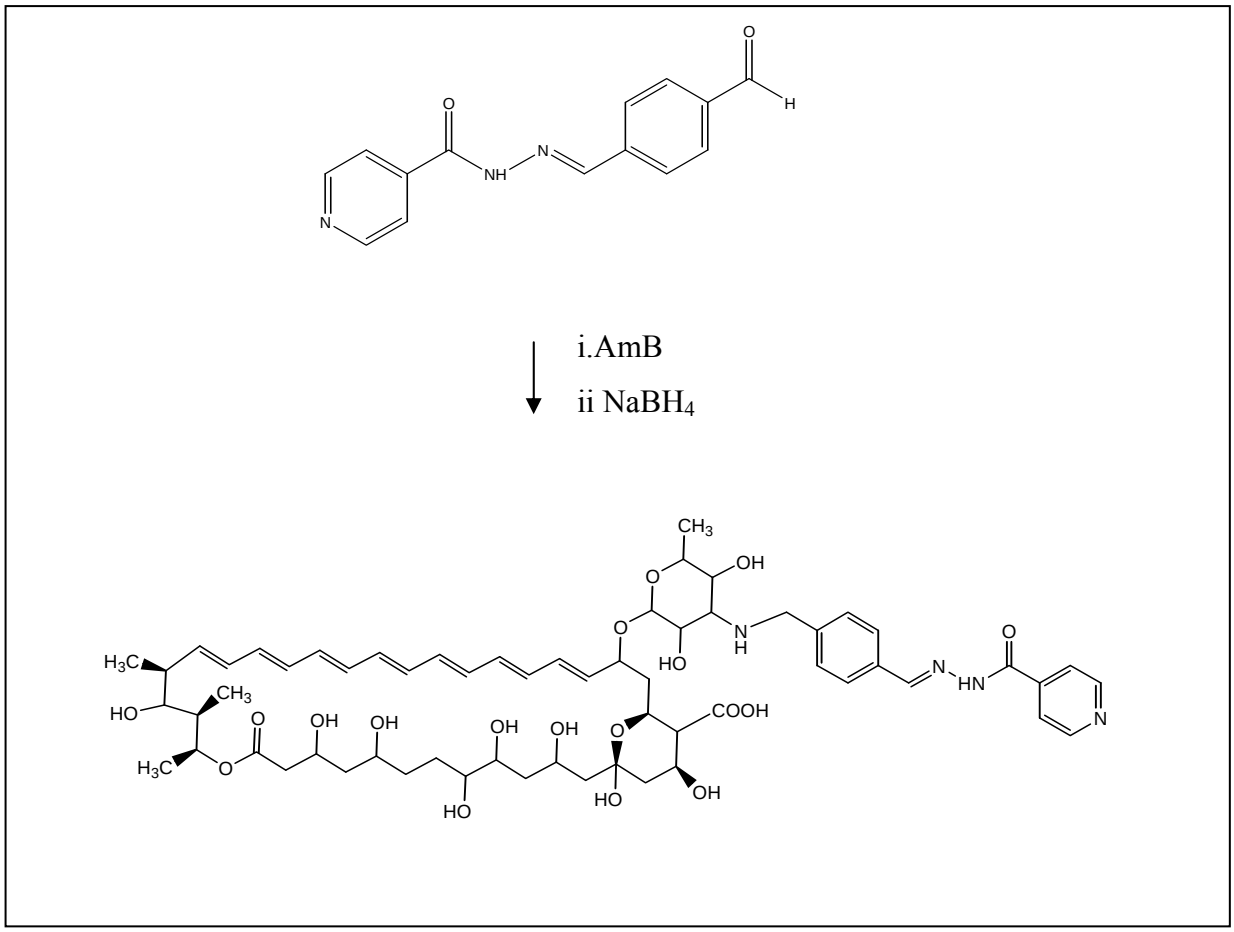

Fig. 2.10 Schematic representation of the formation of AmB-Derivative II.

The method described in 2.2 represents the coupling of AmB (Fig. 2.3.ii, Fig. 2.10), which would serve as the hydrophobic haptophore, to the already modified INH. The method of Ehrenfreund-Kleinman *et al.* and Falk. *et al.* was used [75, 76] in which AmB was linked to arabinogalactan by imine bond formation in borate buffer. The imine that formed was reduced with $NaBH_4$ to form an amine. Initially unpurified INH-TPA and AmB were combined together in borate buffer (pH 11), but the INH-TPA compound was not soluble in the aqueous buffer. Since AmB is not very soluble in aqueous solutions or in most organic solvents it was decided that the reaction should be performed in DMSO. The Schiff base formation between AmB and purified INH-TPA was fast and from careful integration of proton resonance of the AmB and INH-TPA components in the ^{1}H NMR spectrum it was determined that a 1:1 mixture

of the two compounds gave 95 % of the desired AmB derivative I. Using the measured integrals, the starting mass of each component and mathematical conversion to molar ratios, it could be deduced that the commercial AmB was only 80 % pure.

After reactions between AmB and INH-TPA, there was always a bit of INH-TPA left in the reaction mixture, even after adding excess AmB, possibly due to the continuous breakdown of AmB in solution (as confirmed with RP-HPLC, Fig. 2.11). This was determined by the aldehyde peak observed in the NMR results at 10 ppm. Thus the AmB derivative I formed had to be purified from the unreacted and broken down products. As an alternative, exploratory experiments with an aldehyde activated scavenger resin (aminomethylated polystyrene-co-divinyl-benzene) was used to remove unreacted INH-TPA from the product, but was not pursued further due to the resin binding more strongly to the INH-TPA than the AmB did. In this way, the Schiff base formation between INH-TPA and AmB was reversed.

The AmB derivative I was being prepared for the use as a drug in an aqueous environment. Since the formation of the Schiff base is an equilibrium reaction with water as a byproduct and the reaction took place at neutral pH, it was likely that the derivative would hydrolyse upon addition of water. This possibility was first tested by addition of D_2O to an NMR sample of AmB derivative I in DMSO-d_6. ^1H NMR analyses showed immediate complete disappearance of an imine proton signal and appearance of RCHO, however the ^1H NMR spectrum was difficult to interpret conclusively because the addition of D_2O caused a major distortion in the conformation and packing of AmB. Further confirmation of the rapid imine hydrolyses came from the RP-HPLC analyses of the derivative which showed the complete absence of any product with both the AmB and the INH-TPA chromophores (Fig. 2.12).

A few possibilities were investigated in order to increase the stability of the Schiff base. Addition of a borate buffer improved the solubility of AmB, but not the bond stability [75, 76].

It is possible that selective reduction of the Schiff bases of AmB-Derivative I could retard (or prevent) the dissociation of the INH toxophore. The reduction was achieved

in DMSO using a 1 molar equivalent of $NaBH_4$ to AmB-Derivative I and the reaction was followed by ^1H NMR. Reductions were also carried out with $NaBH_4$ in the presence of borate buffer according to the method of Ehrenfreund-Kleinman *et al.* and Falk. *et al* [75, 76] or in chemically dry methanol, but without success.

Following reduction of AmB derivative I; the ^1H NMR spectrum showed a loss of only one of the two imine proton resonances (at 8.38 ppm AmB-TPA and 8.46 ppm INH-TPA), leaving a product with a single imine proton resonating at 8.46 ppm. A comparison of chemical shift of the imine proton in the product with those of the substrate suggests that it is the imine link to the AmB that has been reduced. In addition it has already been noted that the imine link to the INH is very stable due to conjugation both to the benzene and the amide pyridine systems and is therefore likely to be unreactive to mild reducing agents such as $NaBH_4$. The chemical stability of this imine towards reduction by $NaBH_4$ was further demonstrated in that reduction of INH-TPA with up to 10 equivalents of $NaBH_4$ reduced only the aldehyde functional group and not the imine that showed a characteristic resonance at 8.46 ppm in the ^1H NMR spectrum of the product.

Gradient RP-HPLC on a C18 column was used to purify the reduced AmB derivative II from the unreacted or fragmented products. As previously mentioned and the RP-HPLC profile shown in Fig. 2.11, AmB continuously degrades in solution. Initially an eluent of acetonitrile: water (3:7) pH 5, was used according to Eldem *et al*., [93] but no defined peaks could be observed for AmB. The method of Cleary *et al* in a patent published in 2004 [94] used methanol: water (7:3). The eluent gave a much better definition of peaks.

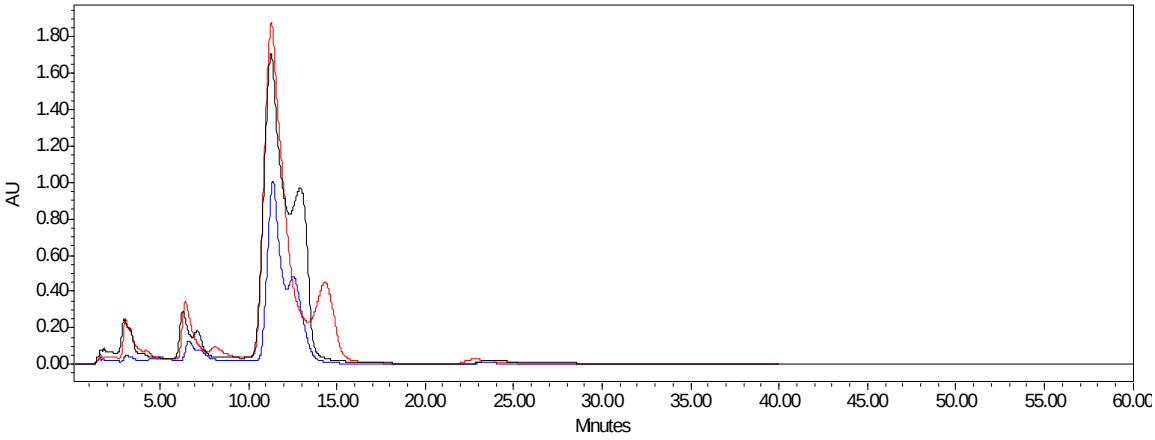

Fig. 2.11 RP-HPLC on an analytical C18 column of an overlay of AmB samples measured at 407 nm. Isocratic flow of methanol: water (7:3). Red = AmB prepared on day of injection, black = AmB 5 days in solution, blue = AmB 2 weeks in solution (AU = absorbance units).

The isocratic flow was changed to a gradient flow of methanol: water from 20 % to 100 % methanol in order to increase the separation of the peaks over 51 minutes on a C18 preparative column. Following optimization on an analytical column, the protocol was transferred and adjusted for the preparative column for the purification of 5 mg crude product per injection. All the samples were separated and collected on the preparative column.

Analytical RP-HPLC on a C18 column and a gradient flow of methanol: water from 20 % to 100 % methanol was used for AmB derivative I (Fig. 2.12). It was demonstrated that the sample dissociated when it came in contact with the aqueous environment The AmB with an absorbance maximum at 407 nm was observed between 35-40 min. but the INH-TPA part of the molecule with an absorbance at 300 nm was not observed in the 35-40 min. region, indicating the dissociation of the AmB derivative I into AmB and INH-TPA.

AmB derivative II (Fig. 2.13) was purified on the C-18 preparative column with a gradient flow of methanol: water from 20 % to 100 % methanol. The sample was prepared one day before use and ~ 5 mg injected manually into the column without prior filtration. Fractions that were collected: 9.7-12.7 min., 12.7-19 min., 19-36 min., 36-40 min. and 40-50 min.

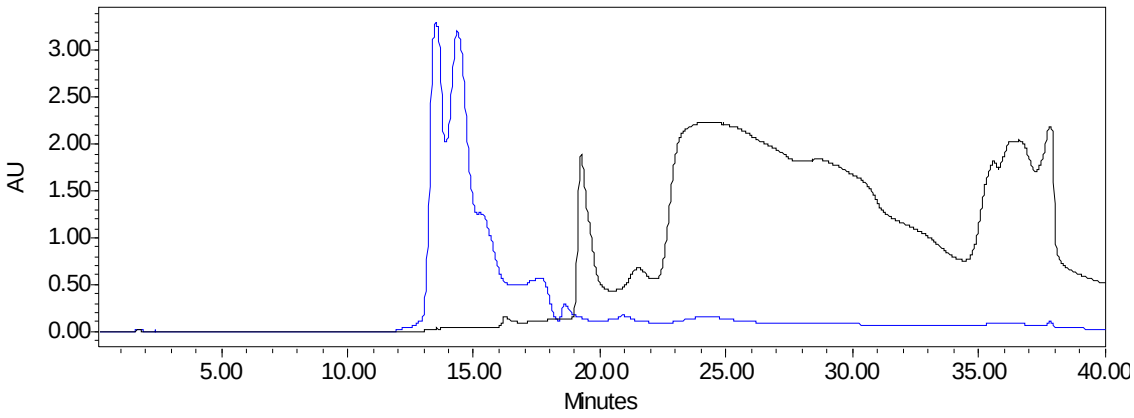

Fig. 2.12 RP-HPLC of AmB derivative I. The blue graph represents the absorption at 300 nm (for INH-TPA) and the black graph represents absorption at 407 nm (for AmB).

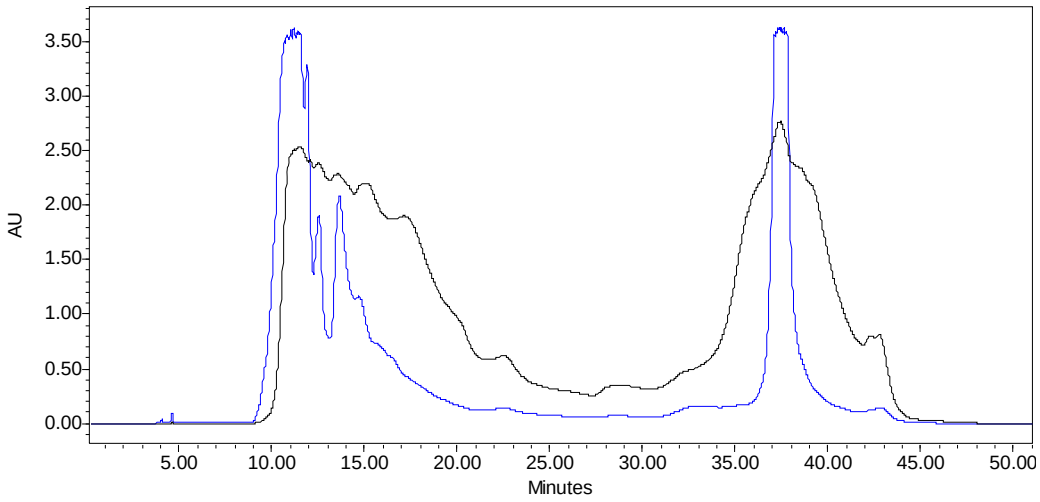

Fig. 2.13 Typical RP-HPLC profile of the purification of AmB DII. The blue graph represents absorption at 300 nm and the black graph at 407 nm over time.

When the samples eluted from the column they were pooled, the methanol reduced under vacuum and then frozen at -20ºC. The fraction between 36-40 minutes was

confirmed to be AmB derivative II (Fig. 2.13) via NMR analysis. The AmB part of the molecule has a maximum absorption at 407 nm whereas the INH derivative part of the molecule has a maximum absorption at 300 nm. Thus an overlay of the two absorbancies was used as an indication when the product eluted from the column. The product was frozen and then lyophilized and stored as a powder at -20ºC until further use. RP-HPLC analyses also showed that AmB Derivative II was stable in solution for a minimum of 6 days. In contrast, the AmB derivative I (Fig. 2.12) as mentioned earlier, dissociates upon contact with an aqueous environment.

NMR analyses of the purified product compared to the unreduced product were performed to confirm product formation. For peak assignment of the AmB part of the molecule the reference of Nicolaou *et al*., [95] was used. The data indicated that the Schiff base between AmB and INH-TPA (8.34 ppm) was not observed any more although the Schiff base between INH and TPA was still observed. A new CH_2-NH bond was now observed instead at 3.89 and 3.67 ppm (possibly the diastereotropic H's of the CH_2) as confirmed by COSY analysis. The peak on the NMR data of the H-3´ on the sugar ring of AmB also shifted more upfield (from 3.25 to 2.82 ppm) after the reduction. Thus only the Schiff base on the AmB side of the molecule was reduced.

Because the 2-dimensional spectra could not be completely obtained due to instrumental problems, only derived comments can be made on the ^{13}C NMR spectrums obtained. The aldehyde peak of the INH-TPA (193.1 ppm) was no longer observed in the AmB derivative I and II spectrums. A new CH=N peak was observed at 149.6 ppm. Reduction to form AmB derivative II caused this peak to shift more upfield to 73.1 ppm. The 3' carbon on the sugar ring of AmB also changed in ppm value with the coupling to INH-TPA and the reduction reactions (from 56.2 ppm to 70.6 ppm and then 63 ppm).

IR analyses were also performed, but because of the large amount of hydroxyls present at 3391 cm^{-1}, it masked any observable NH peaks to confirm the INH-TPA presence.

2.7 Discussion

The aim to synthesize a new formulation of INH, which is more lipophilic and thus more specific towards its target, was achieved by linking AmB and INH with TPA. The desired product INH-TPA was obtained in low yield (14 %) as the majority of the INH reacted with the TPA to form the byproduct INH-TPA-INH. The mechanism for the formation first of INH-TPA, then INH-TPA-INH is illustrated in Fig. 2.14. Formation of the imine (Schiff base), started with a nucleophilic addition of the hydrazine amine to the carbonyl group of the aldehyde. Proton transfer between the nitrogen and the oxygen formed an amino alcohol and subsequently an iminium ion is formed through loss of water. The nitrogen lost a proton and a neutral imine was formed.

The initially formed INH-TPA had a reactive aldehyde group that could be attacked by another INH-amine to form a second imine by the same mechanistic process. This is an equilibrium process that presumably favours the formation of the highly conjugated (every non H atom is sp^2 hybridized) and therefore stable product (INH-TPA) in the anhydrous polar solvent ethanol. This same equilibrium process favoured formation of the second imine link to give INH-TPA-INH as the byproduct that was sparingly soluble and precipitated out of the reaction solution. The driving force of the precipitation appears to be so strong that even adding a large excess of the TPA did not shift the equilibrium to favour the formation of the INH-TPA product. Since such a small amount of AmB derivative II was needed for biological studies the product obtained from the reaction of 0.5 g each of INH and TPA was sufficient for the remainder of the synthesis and the reaction was not further optimized. The mechanism (Fig. 2.14) also applies for the Schiff base formation between AmB and INH-TPA.

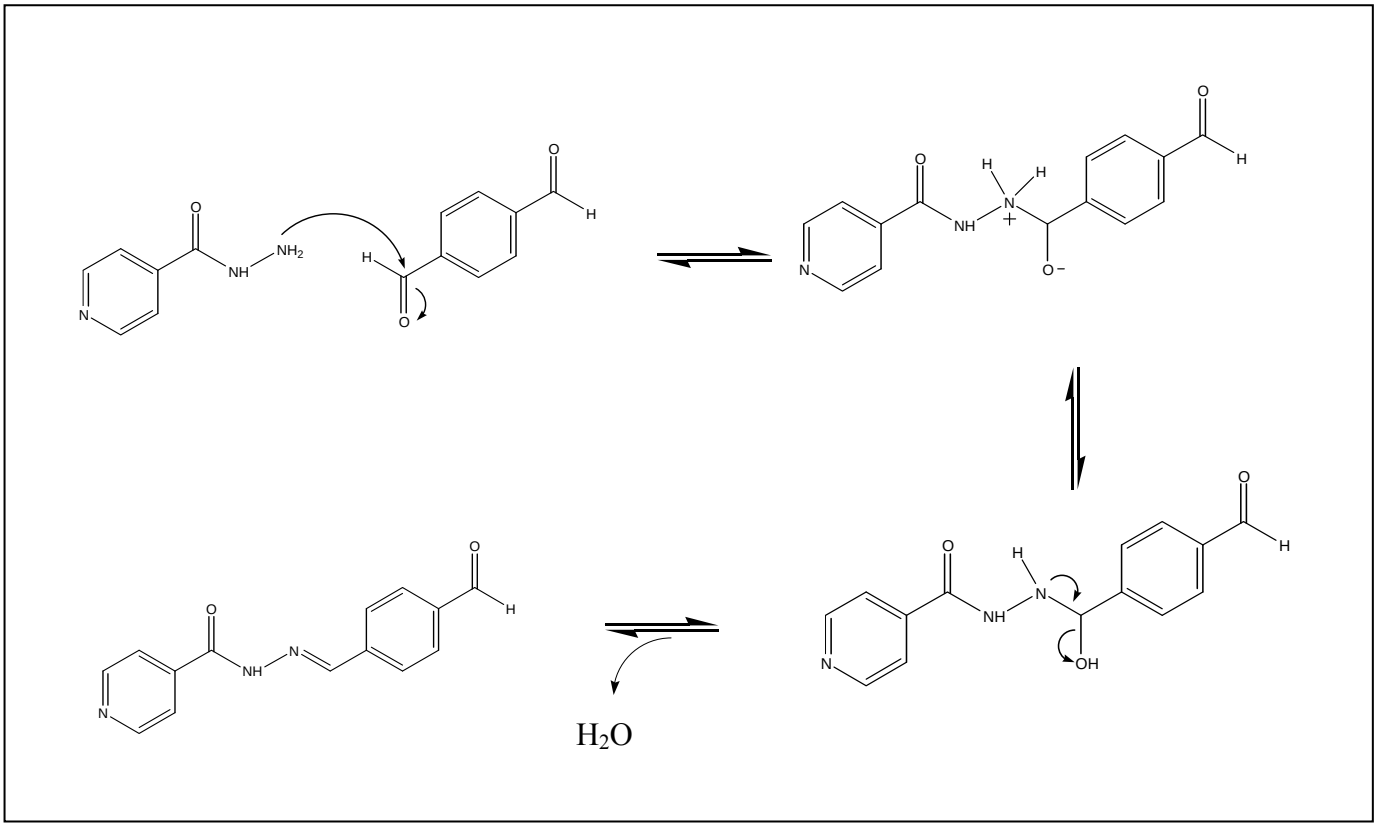

Fig. 2.14 Proposed mechanism for the formation of a Schiff base of INH-TPA [96].

The coupling of AmB to INH-TPA occurred spontaneously in DMSO. The choice of reaction solvent was dictated by the solubility of AmB which shows negligible solubility in aqueous solutions and poor solubility in most organic solvents. Upon further investigation it was observed that the imine bond between AmB and INH-TPA was hydrolysed in aqueous environments.

In an attempt to improve the stability of this AmB derivative, salts and buffers were used to increase the solubility of the derivative in an aqueous environment. The deoxycholate salt of AmB is the favored treatment for fungal infections and is used to increase the solubility of AmB in aqueous environments forming micelle dispersions [81]. The results indicated that deoxycholate improved the solubility, but not bond stability of the molecule. borate buffer, pH 11 was shown to enhance Schiff base formation for AmB derivatives more than phosphate or carbonate buffers, possibly due to the boric acid that forms complexes with AmB diols to increase solubility and minimize aggregate formation [75], but the buffer didn't prevent bond dissociation. Stability of Schiff bases are also influenced by the environment which they reside in.

For example, detergents such as SDS and Triton X-100 and solvents such as chloroform, 2-propanol or methanol: water mixtures allows for the breakdown of the imine bond.

Stability of a Schiff base can be increased by reduction to imine, since the C-N bond in amines is very strong and is not susceptible to hydrolysis [97]. Imines can be efficiently reduced to amines by several reducing agents [97-101] such as $NaBH_4$ and $NaBH_3CN$. In literature, the amino group of AmB was conjugated to the dialdehyde of arabinogalactan through an imine bond. Reduction of the imine to a more stable amine was accomplished by $NaBH_4$ [75, 76]. We predicted that selective reduction of the second imine bond in conjugation would be much slower to hydrolyse and could therefore retard (or prevent) the dissociation of the toxophore. It would be preferable if the linker molecule (TPA) could dissociate from INH (toxophore) rather than from AmB (haptophore).

When INH-TPA was reduced with $NaBH_4$, NMR analysis showed that the aldehyde of the TPA was reduced to an alcohol and the Schiff base between the INH and TPA was not reduced, confirming the resistance to reduction (with $NaBH_4$).

Reduction of AmB derivative I with $NaBH_4$ was selective for imine to give AmB derivative II as proven by NMR spectra. RP-HPLC graphs showed that the derivative was stable in aqueous environments. The stability is needed, because a biological system is an aqueous environment where the drug must be able to reach its target intact. Only then can it dissociate to elicit the toxic effect of INH.

AmB is a light sensitive molecule that degrades easily at mild temperatures (40ºC and higher). It also has an amphipathic nature due to the rigid lipophilic chain of seven conjugated double bonds on the one side and the hydroxyl groups at the opposite side of the macrolide ring. These characteristics of the molecule make it a very challenging reactant to use during synthetic procedures and might contribute to the low yield obtained. Even when using new commercial AmB there is always some degraded product present. This was one of the reasons why RP-HPLC [93, 94] was used to purify the end product, not only to remove unreacted substrates, but also to remove degraded AmB products. Highly purified AmB was also shown to be less toxic to

cells than the mixture of products, possibly due to the removal of some endotoxins [94]. Different mobile phases were tested to enhance separation of products. Isocratic elution with acetonitrile: H_2O at pH 5 [93] that was used for AmB determination in human plasma in literature did not show sufficient peak separation. Gradient elution with methanol: H_2O showed to have sufficient peak separation to collect the product of interest. Here, an AmB derivative was successfully synthesized and characterized by modification of the amino group on the sugar ring of the AmB molecule.

Our aim to create a model to target INH specifically to a cholesterol rich [57] macrophage environment adds a new contribution to the numerous INH derivatives that have been synthesized in the past to increase the efficacy of the parent drug. The AmB-INH derivative is meant to target the body areas in which the mycobacteria reside by making use of a sterol binding drug such as AmB as haptophore. In the next chapter the outcome of the *in vitro* studies as well as the binding properties of the Amphotericin B derivative II will be discussed.

Chapter 3: Characterisation of the synthesized AmB derivative II.

3.1 Introduction

In vitro susceptibility testing of a novel, chemically synthesized drug is required to determine if it has any potential for treatment of a specific disease. Here, the concept of an existing anti-TB drug, INH, covalently linked to a targeting compound, AmB is tested. AmB with sterol binding properties was chosen as the haptophore, to act as a carrier for INH the toxophore, in order to increase the effectiveness of the latter. After successful synthesis of the AmB derivative II as described in chapter 2, this drug was tested against the tuberculosis mycobacterium in bacteriological cell culture. The reason why AmB was chosen as the haptophore was for its specific sterol binding properties that serves as a model for specific drug targeting. The cholesterol-binding property of AmB following covalent modification was also assessed.

Experimental efforts in the past were focused on the synthesis of AmB derivatives that would increase the affinity towards ergosterol and in that way lower the toxicity to human cells that contain cholesterol as the weaker ligand. For this study, the focus was not to improve the activity of AmB towards fungal cells, but to exploit the cholesterol binding properties of AmB after covalent modification, to guide INH to macrophages, preferably those already infected with *M. tb*.

AmB has two prominent fragments in its structure. The one fragment is the macrolide ring with a hydrophobic side consisting of seven conjugated double bonds and a hydrophilic side with polar substituents, mostly hydroxyl groups. The other fragment is a mycosamine sugar moiety. This residue is linked to the macrolide ring with a β-glycoside bond and can rotate freely [102].

AmB promotes formation of pores in the cell membrane by interacting with sterols or lipids in the membrane. Formation of AmB channels in sterol-free membranes have

been observed [102-104]. Possible interactions could be antibiotic/sterols, antibiotic/phospholipids or antibiotic/sterols/phospholipids. Since AmB is an amphipathic molecule and the sterols are mainly hydrophobic with one hydroxyl group, interactions between the two molecules could be either hydrophobic or polar.

AmB could form hydrogen bonds with itself (intramolecular interactions) or with other polar groups of another AmB or sterols and lipids (intermolecular interactions) [102]. The polar head of AmB consists of the amino group on the sugar ring and the carboxyl group. The hydrophilic interaction takes place between the polar head group of the polyene and the hydroxyl groups of the sterol (Fig. 1.14), which is necessary for channel formation [73, 74]. Hydrophobic interactions between AmB and sterols could also take place but is speculated not to be of primary importance [74]. Modification to the carboxyl group (amides, esters etc.) or amino group (N-alkylation, aminoacylation etc.) could change the hydrophobic and electrostatic interactions between the molecules and in that way decrease or increase the affinity between AmB and the sterols present in the membrane [74, 76, 102]. The mechanism of action of binding differs between AmB and various sterol types [103].

AmB has an effect on the hydrophobic core of ergosterol containing membranes, which indicates that AmB penetrates into the membrane to form a pore that causes cell leakage. This was previously thought to be the general mechanism for all membrane sterols interacting with AmB [73, 74, 92, 102]. It was recently discovered with liposomal studies [105] that, in an aqueous environment, AmB binds preferentially to the polar head group region of the lipid membrane through electrostatic interactions. AmB then restricts molecular motion at the hydrophilic region of the surface and increases fluidization at the hydrophobic core that could decrease the penetration barrier for small molecules. This effect was stronger for cholesterol containing membranes than membranes containing ergosterol.

For the purpose of this study we wanted to measure the cholesterol binding capacity of the modified AmB derivative. The instrument used was a resonant mirror biosensor, which is an analytical device that measures the accumulation of mass on a sensitized surface in real time. Important advantages that this technique has above

others, is that no labeling is required and that low affinity specific binding can be detected.

We also wanted to test the antibiotic efficacy of our AmB derivative II towards *M. tb.* The technique used was a radiometric cell culture system, BACTEC 460. *In vitro* drug susceptibility testing for *M. tb, M. avium* and related species is often time consuming due to the slow growth of the organisms, especially when the technique used relies on the development of colonies or turbidity testing. Conventional antimicrobial susceptibility testing for first line and second line anti-TB drugs, with solid media such as Löwenstein-Jensen or Middlebrook 7H10 agars require 3 or more weeks to be completed. A much more time saving technique that was employed is the radiometric BACTEC 460 system that takes between 4-8 days [106-109]. The BACTEC system is superior to the agar based techniques when concerns exist over compound stability during agar preparation or inactivation by agar medium components with extended periods of incubation. A drawback of the BACTEC system is that it is expensive, uses radio-isotopes and requires a high medium volume of 4ml.

The BACTEC 460 method is specific for mycobacterial growth [109]. The system detects the mycobacteria by means of their metabolism rather than visible growth. The bacteria are grown in a confined atmosphere in BACTEC vials containing an enriched Middlebrook 7H9 broth base with ^{14}C-labeled palmitic acid as a substrate. The BACTEC 460 quantitatively detects $^{14}CO_2$ gas produced by the bacteria as they metabolize the ^{14}C labeled substrate. The amount of $^{14}CO_2$ gas released by the mycobacteria is translated into a growth index (GI) that varies from 0-999. Mycobacterial growth can be monitored at very early stages, because very small quantities of $^{14}CO_2$ (g) can be measured by the apparatus [90].

A number of other mycobacterial drug susceptibility assays exist, eg. the non-radioactive technique, Microplate Alamar blue assay that detects cellular growth. The blue, non-fluorescent oxidized form of the Alamar blue dye is reduced by the bacteria to a pink fluorescent form. Growth could be measured by a fluorimeter or spectrophotometer. When the MIC values of known mycobacterial drugs were compared in the BACTEC and Alamar blue assay the values compared well with each other [107]. Similar techniques to the Alamar blue assay are the nitrate reductase and

the resazurin assays [110]. The nitrate reductase assay is based on the ability of *M. tb* to reduce nitrate to nitrite which is an indication of growth. The resazurin microtitre assay is done in a 96 well plate. The resazurin changes from the oxidized (blue) to the reduced (pink) state as a sign of growth. Although the Alamar Blue test is currently the more modern and widely accepted method of preference, we used the BACTEC system due to its availability and support by expert staff.

3.2 Hypothesis

A cholesterol binding pharmaceutical agent (Amphotericin B) can act as a haptophore for targeted delivery of a mycobactericidal toxophore (INH) in covalent linkage.

3.3 Aims of the study

Testing the ability of AmB and the AmB derivative II to associate with mycolic acids and cholesterol. Determining the mycobactericidal activity of AmB derivative II towards *M. tb*.

3.4 Materials

3.4.1 Consumables

Alcohol swabs	TYCO Health care (PTY) LTD, Midrand, RSA
Amber vials	Separations Pty Ltd, Randburg, RSA
BACTEC performance test kit	Becton Dickinson and Co., Maryland, USA
Cetylpyridinium chloride (CPC)	Sigma, St Louis, USA
Chloroform	Merck, Darmstadt, Germany
Cholesterol	Sigma Chemical Co., St Louis, USA
Dimethyl sulphoxide (DMSO)	Sigma Chemical Co., St Louis, USA, (for cell culture)
Ethanol	BDH, Gauteng, RSA, Analytical grade
Membrane filters:	
0.22 µm, hydrophilic	Sartorius AG, Goettingen, Germany
Phosphatidyl choline	Sigma Chemical Co., St Louis, USA, (99 % pure)
Potassium chloride	Merck, Darmstadt, Germany
Potassium dihydrogen phosphate (KH_2PO_4)	Merck, Darmstadt, Germany
Potassium hydroxide	Saarchem, Gauteng, RSA
Sodium azide	Sigma Chemical Co., St Louis, USA
Sodium chloride	Saarchem, Gauteng, RSA
di-Sodium hydrogen phosphate (Na_2HPO_4)	Merck, Darmstadt, Germany
1 ml syringe with integrated 29G needles	Anhui Kangola Medical Products, China
TB medium culture vials	Becton Dickinson International, Belgium
Tetrasodium salt (EDTA)	Merck, Darmstadt, Germany

3.4.2 Buffers

PBS-Azide EDTA buffer (PBS/AE): 8.0 g NaCl, 0.2 g KCl, 0.2 g KH_2PO_4 and 1.05 g Na_2HPO_4 per 1 ℓ double distilled, deionized water with 1 mM EDTA and 0.025 % (m/v) sodium azide, adjusted to pH 7.4

3.4.3 Instrumentation

For *in vitro* experiments the BACTEC 460 radiometric apparatus was used from Becton Dickinson, Johnston Laboratories, USA.

For the measurement of the binding properties an IAsys *plus* Resonant Mirror Biosensor from IAsys Affinity Sensors, Saxon Way, Bar Hill, Cambridge, UK was used.

For preparation of liposomes a Branson sonifier, model B30 (Branson Sonic Power Co., USA) was used.

3.5 Methods

3.5.1 Biosensor experiments

3.5.1.1 Preparation of liposomes with mycolic acid, synthetic protected α-mycolic acids or cholesterol

For the preparation of mycolic acid (MA), which was isolated from the cell wall of the virulent Erdman strain of *M. tuberculosis* as described by Goodrum *et al.* [111], or synthetic protected α-mycolic acid (acetylated on the β-hydroxyl position and methylated on the α-carboxylic group of the mycolic acid and was prepared by Al-Dulayymi *et al.* [112]) containing liposomes, phosphatidyl choline stock solution (90 µl, 100 mg/ml chloroform) was added to an amber glass vial containing either mycolic acid (1 mg) or synthetic protected α- mycolic acids (1 mg). The sample was mixed well until the mycolic acid was dissolved, then dried under a stream of N_2 gas at 85ºC. Saline (2 ml) was then added and the sample was heated on a heat block for 20 min. at 85ºC. The sample was then vortexed for 1 min., sonified (50 cycles, output 2 for 1 min.), aliquoted at 0.2 ml per vial, lyophilized and stored at -70ºC until use. For the preparation of cholesterol containing liposomes, phosphatidyl choline stock solution (60 µl, 100 mg/ml chloroform) was added to an amber glass vial containing cholesterol (30 µl, 100 mg/ml chloroform). The sample was mixed well, dried, suspended in 2 ml saline, sonified and stored as for the mycolic acid containing liposomes. The "empty" liposomes were prepared similarly, but containing phosphatidyl choline (90 µl) only. Before use, all liposomes were reconstituted with PBS/AE (2 ml). The liposomes were placed on a heatblock for 30 min. at 85ºC, vortexed for 2 min. and sonified (30 cycles, output 5 for 2 min.). Each day before use the liposomes were reheated for 10min. and re-sonified. The final liposome concentration was 500 µg lipid /ml.

3.5.1.2 Measuring the interactions between Amphotericin B derivative II and either mycolic acids, synthetic protected α-mycolic acids or cholesterol .

The IAsys affinity biosensor was set for data sampling every 0.4 seconds, temperature of 25ºC and a stirring rate of 75 % (60 % for the synthetic protected α-mycolic acids). Non-derivatised cuvettes were used for all the experiments. The cells of the cuvette were washed with PBS/AE prior to use. PBS/AE (60 µl) was pipetted into both cells of the cuvette to obtain a stable baseline, aspirated and 50 µl of CPC (0.02 mg/ml in PBS/AE) added for 10 min to the cells in order to activate the surface. The cells were then washed five times with PBS/AE (60 µl) and eventually filled with PBS/AE (25 µl) for 5 min. to obtain a stable baseline. Different liposomes (25 µl) were then added to the cells for immobilization to the surface for 10-15 min, washed seven times with PBS/AE (60 µl) and the content substituted with PBS/AE (25 µl) for 5 min. or until a stable baseline was obtained. AmB or AmB derivative II (1×10^{-4} M, 25 µl) was then added to the cells and the binding response towards the immobilized liposomes monitored in arc seconds. After 5 min. the cuvette was washed three times with PBS/AE (60 µl). For regeneration the cuvette was washed five times with ethanol (50 µl) and seven times with PBS/AE (70 µl) and then 5 times with 12.5 M KOH (50 µl). The final wash with PBS/AE (70 µl) was repeated ten times. The statistical significance between the values obtained for AmB immobilized on cholesterol liposomes and AmB immobilized on MA liposomes were calculated by making use of the student's t-test.

3.5.2 BACTEC 460 experiments

3.5.2.1 In *vitro* testing of the synthesized drugs on *Mycobacterium tuberculosis*

The *Mycobacterium tuberculosis* H37Rv strain was used for drug susceptibility testing by making use of the radiometric CO_2 (g) - release BACTEC 460 apparatus.

Frozen stock of *M. tb* H37Rv was thawed at room temperature. The clumps of bacteria were resuspended with a 29G needle to obtain a homogenous solution.

Dilutions of 10-fold and 100-fold were made with saline (0.9 %) and 0.1 ml aliquots of the diluted suspensions were injected into 4 ml 7H12 broth in BACTEC 12B vials. The vials containing the inocula were read in the BACTEC 460 apparatus after flushing with 5 % CO_2 (g) for aerobic culturing. The vials were incubated at 37ºC and read at the same time every day until a GI between 300-500 was obtained. These vials were used as the primary inoculum and after the GI reached 300-500, 0.1 ml aliquots of the bacterial suspensions from the BACTEC vials were injected into drug containing vials.

The compounds that were tested included INH, AmB, TPA, INH-TPA and AmB derivative II. All the compounds were tested at final concentrations of 2.19 x 10^{-6} M, 2.19 x 10^{-7} M and 2.19 x 10^{-8} M, such that the final volume consisted of 4 ml medium, 0.1 ml *M. tb* H37Rv and 0.1 ml drug. These concentrations cover the Minimum Inhibitory Concentration (MIC) for INH of 2.19 x 10^{-7} M and one order of magnitude of concentration higher and lower [90]. The synthesized compounds must at least be as effective as pure INH alone in order to be considered as an improvement on the parent drug. All the solutions for the test compounds were prepared on the day of use. The stock solutions of the drugs were prepared in DMSO and double distilled deionized water (dddH_2O) in a 1:1 ratio. Subsequent dilutions were made in saline (0.9 %) and filter sterilized with a 0.22 µm filter. For the susceptibility tests 0.1 ml of the dilutions were injected with a 1 ml insulin syringe into the BACTEC 12B vials already containing the 4 ml growth medium. The bacteria were added last, just before the vials were read and flushed with 5 % CO_2 (g). Each concentration was tested in triplicate. The experiment was done twice.

For the controls, drug free vials consisted of 0.1 ml of the 10-fold diluted bacterial inocula. DMSO instead of a drug was also tested at the concentrations used in the drug solutions to compensate for any possible toxic effect the DMSO may have on the bacteria. Negative control vials contained saline without any bacteria or drugs to monitor if any contamination occurred. All the vials were read daily until the GI of the bacterial control reached 999.

3.6 Results

3.6.1 Biosensor experiments

3.6.1.1 Measuring the interactions between Amphotericin B derivative II and either mycolic acids, synthetic protected α-mycolic acids or cholesterol.

The ability of AmB and AmB derivative II (AmB DII) to associate with cholesterol liposomes was investigated by means of the IAsys affinity biosensor. Fig. 3.1 gives a typical graph that was obtained when the interactions were measured on the biosensor (values shown in Appendix B). An experiment was designed to test whether the AmB DII retained its ability to bind to cholesterol as the parent AmB could, and simultaneously to disprove that the compound could bind to mycolic acids (MA) before the latter was allowed to attract cholesterol to it.

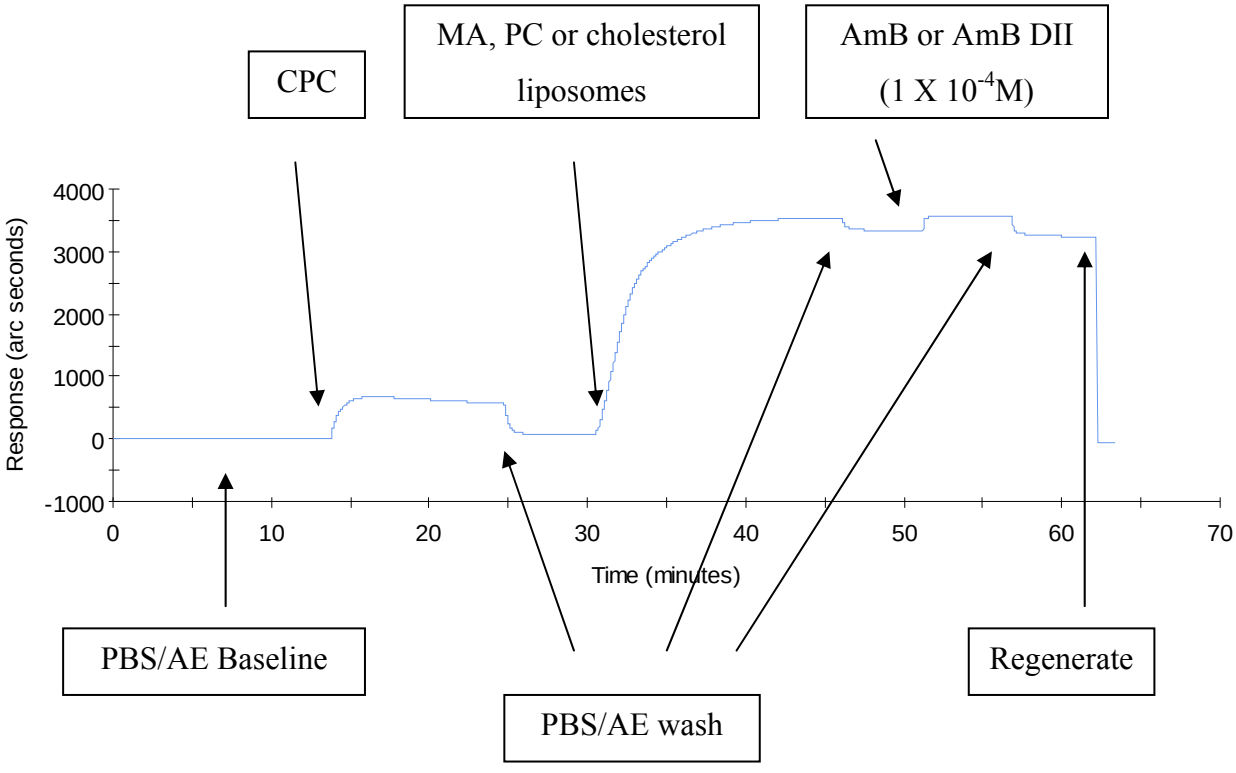

Fig. 3.1 Representative sensorgram relating the sequence of events to the signal profile in arc seconds over time of a typical biosensor experiment to determine the binding of soluble AmB or AmB DII to either MA, synthetic protected α-MA or cholesterol containing liposome coats.

(A)

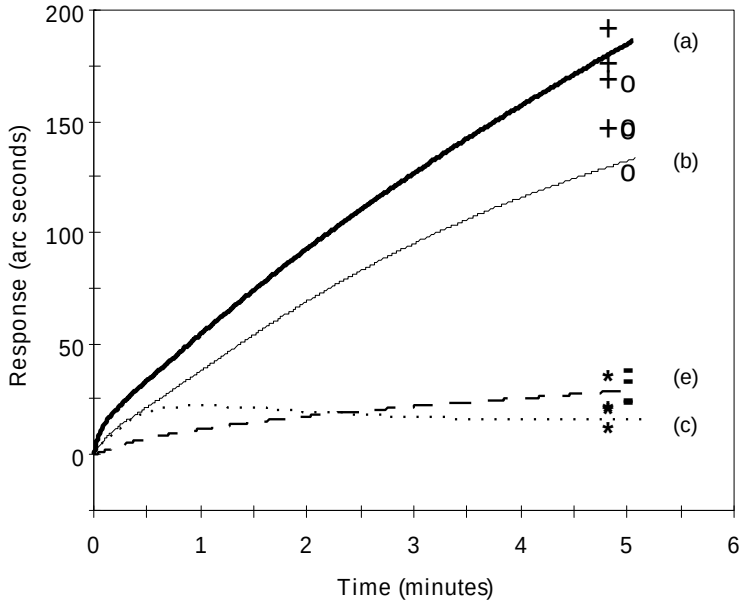

(B)

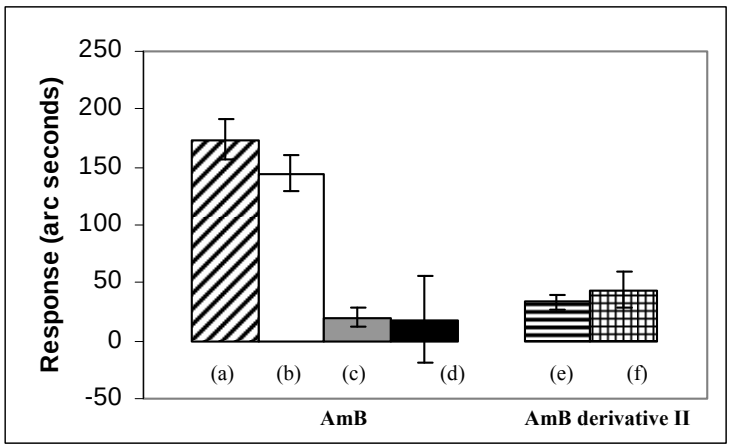

Fig. 3.2

*Binding curves (Fig. 3.2 A) and binding capacity (Fig. 3.2 B) of AmB on immobilized (a) mycolic acids, thick line, +, hatched bar; (b) cholesterol, thin line, o, white bar; (c) synthetic protected α-MA, dotted line, *, grey bar or (d) PC liposomes, black bar.*

Binding curves (Fig. 3.2 A) and binding capacity (Fig. 3.2 B) of AmB derivative II on immobilized (e) cholesterol liposomes, dashed line, -, horizontal stripes bar or (f) mycolic acids liposomes, grid bar. -. n = 5 for each set. Immobilization of liposomes were monitored to achieve binding of at least 2000 arc seconds before contacting with AmB or AmB derivative II.

Amphotericin B was shown to associate with immobilized cholesterol in real time, but when the AmB derivative II was tested, the association was much less than that of the pure AmB alone as illustrated in Fig. 3.2. These results indicate that the modification to the amino group of the AmB molecule destroyed the latter's ability to bind to cholesterol. Remarkably, AmB did bind to immobilized (Fig. 3.2) mycolic acids, an activity that could similarly be destroyed by covalent linkage of AmB to INH. When the values obtained for AmB binding to cholesterol or mycolic acids where analyzed by the student's t-test, there was a statistical significant difference between these two groups. AmB did bind more strongly to MA than cholesterol. The determination of how AmB interacts with α, keto and methoxy MA is still underway. It could be that these different subgroups will have a different affinity due to their different structural arrangements as suggested in literature. Keto- MA could form arrangements similar to that of cholesterol by forming conformations of four long chains packed in parallel producing a W-shape [113]. These different conformations of MA may depend on interactions of hydrogen bonding between the hydroxyl and carboxyl groups.

AmB bound well to cholesterol and MA, but it bound very little to both the synthetic protected α-MA (it is not yet sure how this synthetic MA corresponds to natural MA) and PC (Fig. 3.2 B). The PC liposomes were not very stable upon immobilization onto the cuvette surface which was evident from the large standard deviation observed.

All these results imply that the covalent linkage of AmB to INH destroyed the former's ability to bind to cholesterol, but at the same time provided a way to demonstrate the specificity of interaction between AmB and cholesterol. The AmB derivative II is a good negative control to exclude the possibility that the interaction between AmB and cholesterol was due to non-specific interaction. Because no specific interaction was observed between AmB and synthetic protected α-MA, the interaction observed between AmB and MA can therefore be classified as specific, strongly suggesting a structural mimicry between cholesterol and at least a part of MA.

3.6.2 BACTEC 460 experiments

3.6.2.1 Determination of the mycobactericidal activity of AmB derivative II to *Mycobacterium tuberculosis*

To investigate the mycobactericidal activity of the synthesized AmB derivative II and INH-TPA compounds, they were compared to the parent INH molecule in the BACTEC 460 system. The *M. tb* H37Rv strain was used in the radiometric experiments as described in the methods. The radiometric experiments for the various compounds were conducted at the same molar concentrations as the MIC of INH (0.03 µg/ml) reported in literature [90] and at 10 x and 1/10 x molar concentrations thereof. The calculations used and the GI values obtained are listed in the Appendix C and D.

The results in Fig. 3.3. indicated that the DMSO solvent that was used did not have a toxic effect on the bacteria. The lack of bacterial growth that was observed for the negative control indicated that no biological contamination occurred during the course of the experiment. TPA and AmB that were part of the building blocks of the modified INH were tested to exclude any possibility of their contribution to the toxicity towards *M. tb*. The results indicated that TPA and AmB had no effect at the concentrations tested. INH-TPA did show some inhibition at 10 x the MIC of INH but was far less efficient than the parent INH. AmB Derivative II only indicated slight inhibition at 10 x the MIC of INH. The activity of INH was also tested with the addition of AmB. At the MIC of INH the mixture did show some inhibitory effects compared to INH alone. It could be assumed that some spontaneous association between INH and AmB (salt formation) in the solution occurred. In that way AmB could limit the effect of INH. None of the test compounds were comparable to the parent INH at its MIC, indicating that the covalent linkage between INH and AmB destroyed the mycobactericidal effect of the former. No inhibitory effects were observed for the test compounds at 1/10 MIC of INH.

(A)

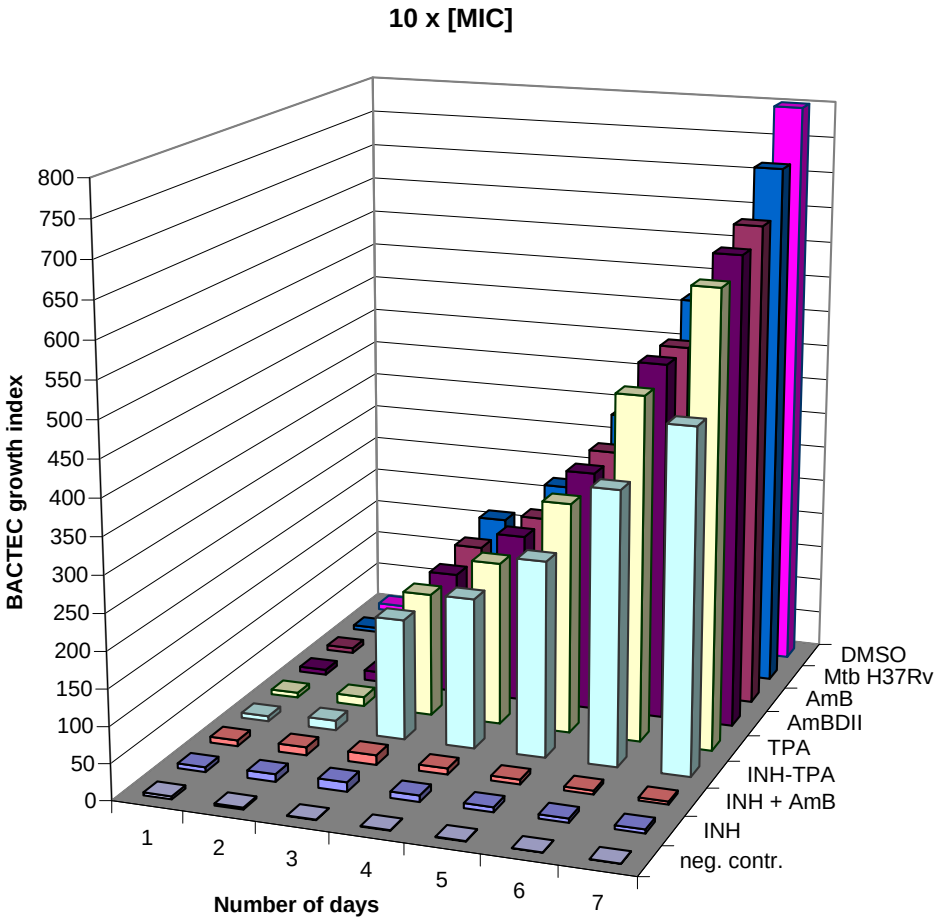
10 x [MIC]
BACTEC growth index
800
750
700
650
600
550
500
450
400
350
300
250
200
150
100
50
0
1
2
3
4
5
6
7
Number of days
DMSO
Mtb H37Rv
AmB
AmBDII
TPA
INH-TPA
INH + AmB
INH
neg. contr.

(B)

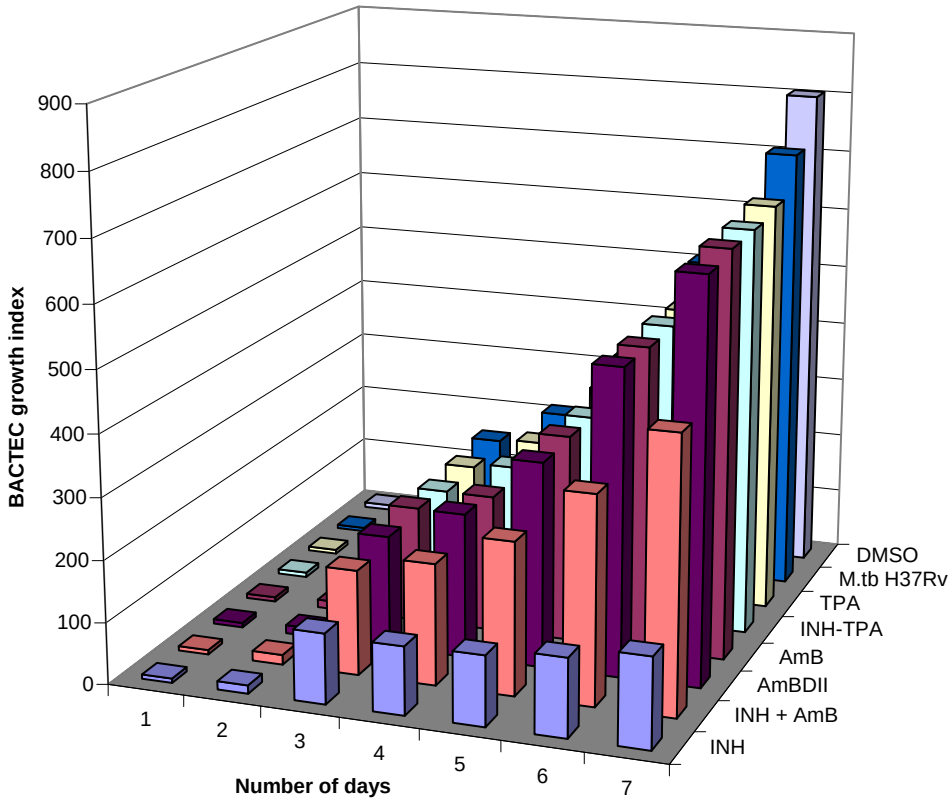
MIC of INH
BACTEC growth index
900
800
700
600
500
400
300
200
100
0
1
2
3
4
5
6
7
Number of days
DMSO
M.tb H37Rv
TPA
INH-TPA
AmB
AmBDII
INH + AmB
INH

(C)

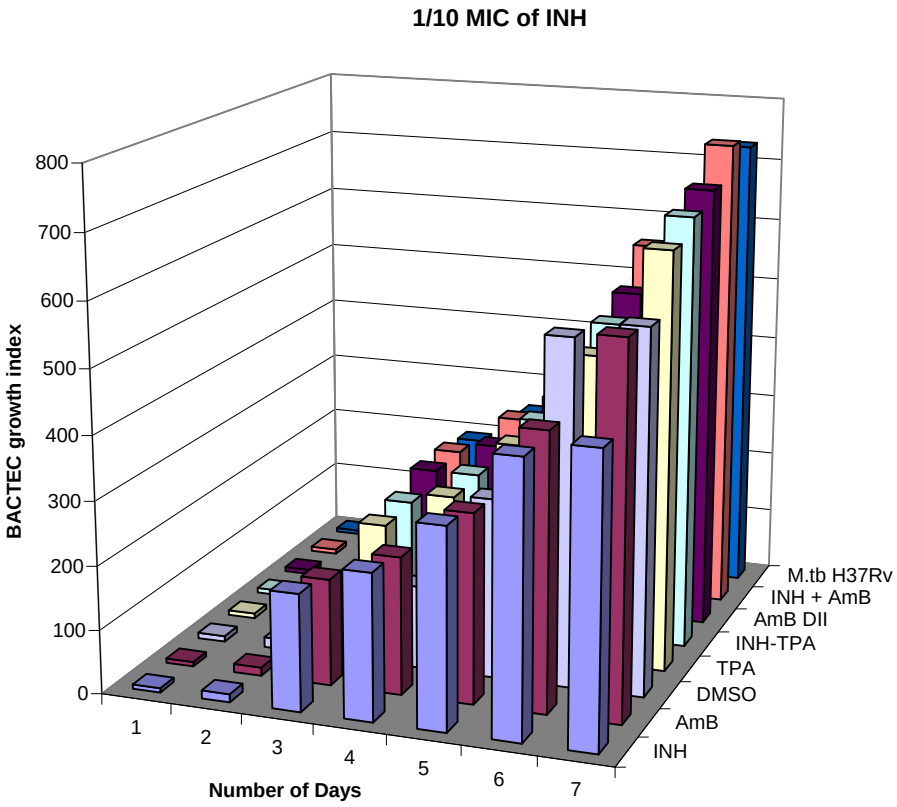

Fig. 3.3 BACTEC growth index of M. tb after treatment with various test compounds at (A) 10 times MIC (B) MIC and (C) 1/10 of MIC of INH. M. tb H37Rv represents untreated bacteria. The negative control (Neg.contr.) contained saline without any bacteria present. The results represent the average of two consecutive experiments done in triplicate.

3.7. Discussion

The ch olesterol binding capacity of the newly synthesized AmB derivative II molecule was compared to that of the parent molecule AmB by means of an evanescent field biosensor. The results confirmed that AmB, but not AmB derivative II bound to cholesterol containing liposomes immobilized on the cuvette surface. Upon covalent modification of the amino group of AmB the binding towards cholesterol was abrogated.

In solution, AmB forms a mixture of water soluble monomers and oligomers with insoluble aggregates [114]. AmB exists in monolayers at molar concentrations smaller

than 10^{-7}. At higher concentrations AmB exists in different aggregated states. AmB only interacts with cholesterol when AmB is in its aggregated state [115] thus in our experiments we tested a range of concentrations and decided to use the concentration of 1 x 10^{-4} M for AmB and AmB derivative II, to ensure that AmB will theoretically bind to cholesterol, which it did.

As mentioned before, the polar head of AmB is responsible for the ionophoric activity. Intermolecular hydrogen bonding takes place between the 3β-hydroxyl group of the sterol and the amino group of AmB [73, 74]. Chemical modification to the polar head of AmB influences the affinity AmB has towards sterols in a positive or negative way depending on the type of modification [74, 92, 102, 116]. The biosensor results indicated that the covalent bond formation between AmB and INH influenced the cholesterol binding capacity of AmB in a negative way. This is corroborated by a very recent report [105], demonstrating that for cholesterol-containing membranes the electrostatic interactions between the polar head group of AmB and the polar groups of the lipid membrane play the major role in binding. This information was not in the public domain when we designed our experimental approach. The chemical modification to the amino group of AmB can now be said to lead to the loss of binding activity between the modified AmB and cholesterol, as was observed in the experiments described and according to the latest literature on the topic.

Surprisingly the biosensor experiments demonstrated that AmB bound to MA as well as it did to cholesterol, while AmB derivative II bound neither. Earlier experimental observations made by other members of our research group led to the prediction of a structural mimicry between cholesterol and parts of MA. Briefly, cross-reactivity between cholesterol and antibodies to MA from tuberculosis patients was observed in an ELISA assay [58]. By means of biosensor studies it was shown that MA attracted cholesterol but that the methylester of MA was unable to do so (Deysel, M. *et al*. 2007, manuscript submitted), but as mentioned earlier the interactions between the hydroxyl and carboxyl groups might play an important role in the structural conformation of the molecule. Lastly cholesterol was shown to compete with INH for its enzyme targets in BACTEC 460 experiments [117]. These results and those presented here suggest a structural mimicry between cholesterol and a part of MA as postulated by our group already since 2000.

Because polar interactions between AmB and cholesterol are important for binding [105] it can also be expected that polar interactions are responsible for the interaction between MA and AmB. The major interaction could be between the polar head group of AmB and the polar groups of MA. This is confirmed by the observation made here that AmB did not bind to a synthetic, α-MA derivative [112] that is protected at the polar groups of the molecule (see Appendix E). This probably blocked the polar interactions between the MA derivative and AmB, but could also indirectly influence the conformation of the MA and therefore the hydrophobic interactions with AmB. The specific polar group that does interact with AmB cannot be deduced from these results. Further biosensor experiments with modified MA or specific subgroups (α-, keto- and methoxy-) MA might shed more light on the subject.

Cholesterol seems to play a large role in the infection and survival of mycobacteria in macrophages [54, 57] as discussed in chapter 1. It could be concluded that MA in the mycobacterial cell wall attracts cholesterol from the macrophage host cell membrane, by means of its structural mimicry to the ligand, to enable successful infection and survival within its host.

Literature suggests, that in order to improve the activity of INH, the drug should be made more lipophilic, the specificity towards its target should be enhanced or the propensity for its acetylation should be reduced [6, 63, 66, 67]. Theoretically, AmB should have concentrated INH to the cell wall of the bacteria due to its sterol binding properties and its ability to bind to MA as observed on the biosensor. Even though the AmB affinity towards MA was destroyed upon covalent modification we wanted to test whether INH could still have a toxic effect on the bacteria.

Determination of the mycobactericidal activity of the synthesized AmB derivative II to *Mycobacterium tuberculosis* was done by the BACTEC 460 method. The concentrations that were used were 10 times, 1/10 times and at the MIC of INH. INH was found to have lost its mycobactericidal activity when in covalent linkage with AmB in AmB DII, but retained some activity when covalently coupled to the TPA linker. The Schiff base bond that links INH to TPA could not be a reason for the decreased activity. Successful Schiff base type of modifications made to INH are

reported in literature to retain activity as discussed in chapter 2 [6, 60, 62, 67]. Research has demonstrated that AmB was not toxic to *M. smegmatis* [80]. This corroborated with the results that AmB did not inhibit the growth of *M. tb* H37Rv at the concentrations tested. In literature, it was reported that INH-TPA did have some degree of activity against the bacteria [64], but the AmB derivative II only had a slight toxic effect at 10 x the MIC of INH. Thus, the toxophore, INH, did not lose its activity due to covalent modification (INH-TPA did show activity against the bacteria) but possibly due to the bigger size of the AmB-INH derivative II.

Hydrophilic antibiotics and nutrients cross bacterial membranes via porin channels [7]. However, INH, which is a hydrophilic molecule, enters the mycobacterial cell wall through passive diffusion [8, 10]. INH is a prodrug that requires activation by the catalase peroxidase enzyme, KatG. Whether INH enters the bacteria in its activated form or as the prodrug is still a topic of investigation. The reason for this is that the catalase peroxidase enzyme has not only been found intracellularly, but also amongst culture filtrate proteins [13, 14]; thus it could be that INH becomes activated by KatG when still on the outside of the bacteria. INH binds in the haem cavity of the catalase peroxidase for activation [23-25]. It could be possible that the AmB does not dissociate from INH before reaching the enzyme due to the stability of the highly conjugated shiff base linkage and that due to its large size, it blocks access to the active site for INH activation.

Although the basic tenet of this chapter found no experimental support, meaning that a cholesterol targeting, mycobactericidal, covalently linked INH-AmB could not be found to work, a discovery was made by serendipity that could have great impact in understanding how *M. tb* enters and survives in the host macrophage. The observation that AmB directly interacts with MA, as it does to cholesterol, has not been demonstrated previously. As cholesterol was shown to be critical for entry and survival of *M. tb* in macrophages [57], the indication of a structural mimicry between the cell wall MA and cholesterol and the attraction of these two chemical entities to one another seem to be highly relevant. This characteristic could now be further explored to improve the understanding of the process of entry and survival of *M. tuberculosis* in the macrophage host.

Chapter 4: Conclusion

A current strategy in drug development for anti-TB drugs is to design systems capable of targeting the drug to the site of infection at relatively low drug concentrations in the blood to prevent systemic toxic side effects. There are different approaches that could be followed in order to focus the drug towards its target.

One approach that could be followed is chemical modification of an existing drug. For example to increase the lipophilicity of the drug to target the drug to hydrophobic sites of infection [6, 63, 66, 67]. Receptor mediated drug delivery could also be done, by linking a ligand to the drug where specific receptors, such as scavenger receptors, are targeted which are present at the site of infection [71].

Another approach apart from chemical modification directly to the drug, is modified carriers that deliver the drugs to their target sites. Although liposomes or lipid emulsions have been successfully used in the past as carriers for anti-TB drugs for treatment [91], current research is more focused on solid lipid nanoparticles as drug carriers [68]. Drugs are entrapped within the carrier system from where they are released over a period of time, thereby reducing the amounts and the frequency of drug required to be administered.

A unique opportunity for specific drug targeting was provided by the discovery of the structural relationship between cholesterol and mycolic acid by members of our research group. The first observation leading to this insight was cross-reactivity between cholesterol and MA by antibodies from tuberculosis patients, observed in an ELISA assay [58]. By means of biosensor studies it was subsequently shown that MA attracted cholesterol [59]. The structural specificity of this attraction was demonstrated by showing that the methylester of MA was unable to do so (Thanyani, T.S. unpublished). Evidence of a more circumstantial nature was found in that cholesterol was shown to hinder the effectivity of INH to eradicate *M. tb* in BACTEC 460 experiments [117]. That the enzyme target of INH, called InhA, is related to the steroid dehydrogenase family of enzymes suggested the possibility that the cholesterol

could compete with MA for binding to the substrate binding site of the enzyme, thereby lowering the efficiency of INH. Competitive inhibition between MA and cholesterol for binding to an enzyme's active site would further support the notion of a structural mimicry between MA and cholesterol. This could be further explored as a drug target for the future.

The aim of this study was to create a model to target INH specifically to a cholesterol rich [57] environment where mycobacteria reside in macrophages, by making use of a sterol binding drug such as AmB. Numerous INH derivatives (as described in chapter 1 and 2) have been synthesized in the past to increase the efficacy of the parent drug. The main reasons why we chose INH as our drug of choice, was because INH is inexpensive and still the most widely used anti-TB drug. The uncomplicated chemical structure of INH also simplifies modification to the molecule. The history of successful chemical derivatisations of INH to reduce toxicity to the host while maintaining mycobactericidal activity made it a good molecule with which to test our model.

When entering the host, bacteria are engulfed by phagocytes through multiple receptors on the macrophages which include complement, mannose, Fc and scavenger receptors [56, 69]. Mycobacteria are very specific in terms of their uptake and survival within the macrophages. Selective receptor blockade during phagocytosis indicated that class A scavenger receptors are essential for infection, while the complement, mannose and Fc receptors merely enhance the process. Scavenger receptors have been shown to bind low density lipoproteins as well as lipopolysaccharides of gram negative and lipoteichoic acids of gram positive bacteria [70, 118, 119]. The different receptors initiate various signal-transduction pathways that activate microbial killing mechanisms, but in *M. tb* infection this does not happen [69, 70].

AmB is a polyene macrolide with well defined cholesterol binding properties. Covalent linkage of AmB, which would serve as a hydrophobic haptophore, to INH, the toxophore, could increase its lipophilicity and indirectly target INH to cholesterol containing macrophages. The *in vivo* toxicity of AmB results partly from direct interactions with mammalian cells. AmB binds to human serum components, in

particular to lipoproteins and albumin or is engulfed by macrophages [81, 92]. AmB binds to LDL and is internalized through LDL receptors [81, 82]. Apart form LDL receptors, it was shown that LDL type of molecules were taken up from circulation by macrophages through scavenger receptors [70, 72, 118, 119]; therefore AmB could be taken up by similar receptors on macrophages as *M. tb* does. This created the opportunity to investigate AmB for a role to target the INH drug specifically to macrophages harbouring *M. tb*.

By designing new derivatives of a specific drug, the resistance elicited by the bacteria could be overcome. INH is a small water soluble molecule, which readily gets metabolized after absorption so that it does not reach its target at sufficient concentrations that are lethal to the bacteria. It was suggested from literature that the activity of INH can be improved by, modifying the drug in such a way as to increase its hydrophobicity, enhance the specificity towards its target or reduce the propensity of acetylation [6, 63, 66, 67]. Enzymic acetylation, that decreases the effectiveness of INH, can be inhibited by chemical modification of the hydrazine group [6, 89]. Increasing the hydrophobicity of the INH molecule could also increase effectiveness of the drug as was shown with lipophilic analogues of INH [66, 67]. Upon examination of the structure of INH, it was decided to derivatise the molecule at the primary amine (NH_2). Literature indicated that derivatising the INH at the primary amine could lead to improved activity compared to the parent INH molecule [6, 60, 66, 67, 101].

This study reports the technical achievement of covalently linking INH to AmB via Schiff base formation to a linker molecule, TPA. The chemical stability of the molecule was increased by reducing only the imine between AmB and INH-TPA to an amine, while the imine bond between INH and TPA resisted reduction. By carefully following the synthesis with NMR analyses, the structure and purity of the synthesized product was substantiated. Due to its structure and physical properties AmB, was a challenging molecule to work with during synthetic reactions hence the low yields obtained.

In vitro mycobactericidal activity of the synthesized AmB derivative II was tested with the radiometric BACTEC 460 system, to determine the effectiveness of the drug

against *M. tb* H37Rv. *In vitro* tests showed that in AmB DII the INH lost its toxic properties towards *M. tb,* possibly due to the inability of the AmB molecule to dissociate from the INH before reaching its target and the bulkiness of the derivative inhibiting/blocking binding.

In this study, the ability of AmB to bind to cholesterol after covalent modification was tested in a resonant mirror biosensor. The results indicated that unmodified AmB associated with cholesterol as well as with MA containing liposomes. The binding activity to both these molecules was abrogated upon covalent modification of the amino group of AmB. Chemical modification to the polar head of AmB influences the affinity of AmB towards sterols in a positive or negative way depending on the type of modification [74, 92, 102, 116]. The reason for the decreased binding could possibly be that the major interactions between AmB and cholesterol are the electrostatic interactions between the polar head group of AmB and the hydroxyl group of the lipid membrane [105]. It is assumed that AmB interacts in a similar way with MA than with cholesterol where the hydroxyl and carboxyl groups of MA could be involved in hydrogen bonded interactions. The polar groups of MA are therefore probably involved in the binding to the polar groups of AmB.

When PC (empty liposomes) and synthetic protected α-MA were used to substitute MA as binding controls in the coated liposome layer of the biosensor, little binding towards AmB was observed. This demonstrated the specificity of the interaction - it was not merely a hydrophobic association of AmB to either cholesterol or MA. AmB did not bind to synthetic protected α - MA [112] in which the polarity of the hydroxyl group and the carboxylic acid of the mycolic motif is reduced and appears to block the polar interactions with AmB. It is also possible that the protection of the polar groups could prevent the MA from assuming a configuration that would allow a structural fit for binding to AmB.

As mentioned before, the polar head of AmB is responsible for the ionophoric activity. Intermolecular hydrogen bonding takes place between the 3β hydroxyl group of the sterol and the amino group of AmB [73, 74]. The biosensor results indicated that our covalent bond formation to AmB with INH influenced the cholesterol binding capacity of AmB in a negative way. At the time of writing this dissertation, it was

shown [105] that for cholesterol-containing membranes the electrostatic interactions between the polar head group of AmB and the polar group of the lipid membrane plays the major role in binding. According to this new insight, the loss of binding activity between the modified AmB and cholesterol observed with the biosensor is due to chemical modification to the amino group of AmB. This result therefore strongly corroborates the conclusion made by Gabrielska *et al.* [105].

It has been reported before that cholesterol plays an important role in the entry and survival of *M. tb* in macrophages. The cholesterol content of macrophages has been shown to be much increased upon mycobacteria infection [52, 120]. Because cholesterol was required for the physical interaction of the mycobacteria with the plasma membrane, the membrane cholesterol could play a role in transmitting or coordinating the signals necessary for mycobacterial uptake into the macrophage [56]. Mycobacteria enter the host macrophage via cholesterol enriched domains in the plasma membrane. Inside the normal macrophage plasma membrane, tryptophane-aspartate rich coat proteins (TACO) associate with cholesterol. These are now transferred to coat the cholesterol rich phagosomes preventing the fusion of the infected phagosome with lysosomes [57, 121, 122], thereby ensuring the survival of the mycobacterial intruder. A necessary requirement for blocking maturation as observed by de Chastellier and her co-workers was that the phagosome membrane must be in close apposition with the entire mycobacterial surface [123]. That cholesterol played an important role in the interaction between the mycobacterial surface and the phagosome membrane, was demonstrated when cholesterol depletion in *M. avium* containing macrophages eliminated the close interaction between these two surfaces [124].

Previous work done by our group indirectly indicated a structural relationship between MA and cholesterol. Here, direct evidence is provided for a structural mimicry between MA and cholesterol, because both were shown to be specifically bound by AmB. This structural mimicry suggests that the close interaction that exists between the mycobacterial surface and the phagosomal membrane may serve the purpose that in the cell wall of the Mycobacterium MA integrates with the phagosome membrane to attract TACO proteins by assuming a cholesterol conformation.

The aim of this dissertation was to create AmB in covalent linkage to INH and use it to target mycolic acid – cholesterol complexes present on the cell wall of the mycobacteria in order to improve the delivery of INH to its target. The AmB-INH conjugate was successfully created, but with loss of biological activity. During the testing of the compound, it was discovered that AmB bound to MA at least as well as it binds to cholesterol, its natural ligand. This provided an indication of the structural similarity between MA and cholesterol. MA, however, is not a homogeneous chemical entity of the mycobacterial cell wall. There are literally hundreds of different structural MA types among the species of *Mycobacterium, Nocardia* and *Rhodococcus*. Because AmB binds directly to the MA cluster of *M. tb*, this molecule could be used as a tool to determine which subclasses of MA exhibit a cholesterol mimicry. This could largely enhance the understanding of the role of MA in the virulence and survival of mycobacteria in the mammalian host, as the critical role of cholesterol in this is well documented.

References

1. W.H.O., *World health organization, Fact Sheet No 104*. 2002: Geneva.
2. Dick, T., Dormant tubercle bacilli: the key to more effective TB chemotherapy? J Antimicrob Chemother, 2001. **47**(1): p. 117-118.
3. Parrish, N.M., Dick, J.D., Bishai, W.R., Mechanisms of latency in *Mycobacterium tuberculosis*. Trends Microbiol, 1998. **6**(3): p. 107-112.
4. Barry 3rd, C.E., New horizons in the treatment of tuberculosis. Biochem Pharmacol, 1997. **54**(11): p. 1165-1172.
5. Spellberg, B., Powers, J.H., Brass, E.P., Miller, L.G., Edwards, J.E., Trends in antimicrobial drug development: implications for the future. CID, 2004. **38**: p. 1279-1286.
6. Hearn, M.J., Cynamon, M. H., Design and synthesis of antituberculars: preparation and evaluation against *Mycobacterium tuberculosis* of an isoniazid Schiff base. J Antimicrob Chemother, 2004. **53**(2): p. 185-191.
7. Lambert, P.A., Cellular impermeability and uptake of biocides and antibiotics in Gram-positive bacteria and mycobacteria. J Appl Microbiol, 2002. **92**(Suppl): p. 46S-54S.
8. Bardou, F., Raynaud , C., Ramos, C., Laneelle, MA., Laneelle, G., , Mechanism of isoniazid uptake in *Mycobacterium tuberculosis*. Microbiology, 1998. **144**(9): p. 2539-2544.
9. Minnikin, D.E., Kremer, L., Dover, L.G., Besra, The methyl-branched fortifications of *Mycobacterium tuberculosis.* Chem Biol, 2002. **9**: p. 545-553.
10. Jackson, M., Raynaud, C., Laneelle, M.A., Guilhot, C., Laurent-Winter, C., Ensergueix, D., Gicquel, B., Daffe, M., Inactivation of the antigen 85C gene profoundly affects the mycolate content and alters the permeability of the *Mycobacterium tuberculosis* cell envelope. Mol Microbiol, 1999. **31**(5): p. 1573-1587.
11. Rozwarski, D.A., Grant, G.A., Barton, D.H., Jacobs , W.R Jr., Sacchettini, J.C . Modification of the NADH of the isoniazid target (InhA) from *Mycobacterium tuberculosis*. Science, 1998. **279**(5347): p. 98-102.
12. Herrera, L., Valverde, A., Saiz, P., Saez-Nieto, J.A., Portero, J.L., Jimenez, M.S., Molecular characterization of isoniazid-resistant *Mycobacterium tuberculosis* clinical strains isolated in the Philippines. Int J Antimicrob Agents, 2004. **23**(6): p. 572-576.
13. Sonnenberg, M.G., Belisle, J. T., Definition of *Mycobacterium tuberculosis* culture filtrate proteins by two-dimensional polyacrylamide gel electrophoresis, N-terminal amino acid sequencing, and electrospray mass spectrometry. Infect Immun, 1997. **65**(11): p. 4515-4524.
14. Raynaud, C., Etienne, G., Peyron, P., Lanéelle, M. A., Daffé, M., Extracellular enzyme activities potentially involved in the pathogenicity of *Mycobacterium tuberculosis*. Microbiology, 1998. **144**(Pt 2): p. 577-587.
15. Yu, K., Mitchell, C., Xing, Y., Magliozzo, R. S., Bloom, B. R., Chan, J., Toxicity of nitrogen oxides and related oxidants on mycobacteria: M. tuberculosis is resistant to peroxynitrite anion. Tuber Lung Dis, 1999. **79**(4): p. 191-198.
16. Wengenack, N.L., Jensen, M. P., Rusnak, F., Stern, M. K., *Mycobacterium tuberculosis* KatG is a peroxynitritase. Biochem Biophys Res Commun, 1999. **256**(3): p. 485-487.

17. Rawat, R., Whitty, A., Tonge, P.J., Takayama, K., The isoniazid-NAD adduct is a slow, tight-binding inhibitor of InhA, the *Mycobacterium tuberculosis* enoyl reductase: adduct affinity and drug resistance. Proc Natl Acad Sci U S A, 2003. **100**(24): p. 13881-13886.
18. Wengenack, N.L., Rusnak, F., Evidence for isoniazid-dependent free radical generation catalyzed by *Mycobacterium tuberculosis* KatG and the isoniazid-resistant mutant KatG(S315T). Biochemistry, 2001. **40**(30): p. 8990-8996.
19. Magliozzo, R.S., Marcinkeviciene, J. A., The role of Mn(II)-peroxidase activity of mycobacterial catalase-peroxidase in activation of the antibiotic isoniazid. J Biol Chem, 1997. **272**(14): p. 8867-8870.
20. Bodiguel, J., Nagy, J. M., Brown, K. A., Amart-Gregoire, B., Oxidation of isoniazid by manganese and *Mycobacterium tuberculosis* catalase-peroxidase yields a new mechanism of activation. J Am Chem Soc, 2001. **123**(16): p. 3832-3833.
21. Ghiladi, R.A., Cabelli, D. E., Ortiz de Montellano, P. R., Superoxide reactivity of KatG: insights into isoniazid resistance pathways in TB. J Am Chem Soc, 2004. **126**(15): p. 4772-4773.
22. Lei, B., Wei, C. J., Tu, S. C. , Action mechanism of antitubercular isoniazid. Activation by *Mycobacterium tuberculosis* KatG, isolation, and characterization of InhA inhibitor. J Biol Chem, 2000. **275**(4): p. 2520-2526.
23. Bertrand, T., Eady, N.A.J., Jones, J.N., Jesmin, Nagy, J.M., Jamart-Gregoire, B., Raven, E.L. and K. Brown, Crystal structure of *Mycobacterium tuberculosis* catalase-peroxidase. J Biol Chem, 2004. **279**(37): p. 38991-38999.
24. Carpena, X., Loprasert, S., Mongkolsuk, S., Switala, J., Loewen , P.C., Fita , I., Catalase-peroxidase KatG of *Burkholderia pseudomallei* at 1.7Å resolution. J Mol Biol, 2003. **327**(2): p. 475-489.
25. Pierattelli, R., Banci, L., Eady, N.A., Bodiguel, J., Jones, J.N., Moody, P.C., Raven, E.L., Jamart-Gregoire, B., Brown, K.A., Enzyme-catalyzed mechanism of isoniazid activation in class I and class III peroxidases. J Biol Chem, 2004. **279**(37): p. 39000-39009.
26. Singh, R., Wiseman, B., Deemagarn, T., Donald, L.J., Duckworth, H.W., Carpena, X., Fita, I., Loewen, P.C., Catalase-peroxidases (KatG) exhibit NADH oxidase activity. J Biol Chem, 2004. **279**(41): p. 43098-430106.
27. Dubnau, E., Fontan, P., Manganelli, R., Soares-Appel, S., Smith, I., *Mycobacterium tuberculosis* genes induced during infection of human macrophages. Infect Immun, 2002. **70**(6): p. 2787-2795.
28. Dubnau, E., Chan, J., Raynaud, C., Mohan, V. P., Lanéelle, M. A., Yu, K., Quemard, A., Smith, I., Daffé, M., Oxygenated mycolic acids are necessary for virulence of *Mycobacterium tuberculosis* in mice. Mol Microbiol, 2000. **36**(3): p. 630-637.
29. Marrakchi, H., Lanéelle, G., Quémard, A . InhA, a target of the antituberculous drug isoniazid, is involved in a mycobacterial fatty acid elongation system, FAS-II. Microbiology, 2000. **146**(2): p. 289-296.
30. Wilson, M., DeRisi, J., Kristensen, H.H., Imboden, P., Rane, S., Brown, P.O., Schoolnik, G.K., Exploring drug-induced alterations in gene expression in *Mycobacterium tuberculosis* by microarray hybridization. Proc Natl Acad Sci U S A, 1999. **96**(22): p. 12833-12838.

31. Barry 3rd, C.E., Lee, R.E., Mdluli, K ., Sampson, A.E., Schroeder, BG., Slayden, R.A., Yuan, Y . Mycolic acids: structure, biosynthesis and physiological functions. Prog Lipid Res, 1998. **37**(2-3): p. 143-179.
32. Mdluli, K., Slayden, RA., Zhu, Y., Ramaswamy, S., Pan, X., Mead, D., Crane, D.D., Musser, J.M., Barry 3rd ,C.E., Inhibition of a *Mycobacterium tuberculosis* beta-ketoacyl ACP synthase by isoniazid. Science, 1998. **280**(5369): p. 1607-1610.
33. Cole, S.T., Brosch, R., Parkhill, J., Garnier, T., Churcher, C., Harris, D., Gordon, S.V., Eiglmeier, K., Gas, S., Barry 3rd, C.E., Tekaia, F., Badcock, K., Basham, D., Brown, D., Chillingworth, T., Connor, R., Davies, R., Devlin, K., Feltwell, T., Gentles, S., Hamlin, N., Holroyd, S., Hornsby, T., Jagels, K., Barrell, BG., Deciphering the biology of *Mycobacterium tuberculosis* from the complete genome sequence. Nature, 1998. **393**(6685): p. 537-544.
34. Belisle, J.T., Vissa, V.D., Sievert, T., Takayama, K., Brennan, P.J., Besra, G.S., Role of the major antigen of *Mycobacterium tuberculosis* in cell wall biogenesis. Science, 1997. **276**(5317): p. 1420-1422.
35. Rozwarski, D.A., Vilcheze, C., Sugantino, M., Bittman, R., Sacchettini,J. C., Crystal structure of the *Mycobacterium tuberculosis* enoyl-ACP reductase, InhA, in complex with NAD+ and a C16 fatty acyl substrate. J Biol Chem, 1999. **274**(22): p. 15582-15589.
36. Quémard, A., Sacchettini, J. C., Dessen, A., Vilcheze, C., Bittman, R., Jacobs Jr, W. R. , Blanchard, J. S., Enzymatic characterization of the target for isoniazid in *Mycobacterium tuberculosis*. Biochemistry, 1995. **34**(26): p. 8235-8341.
37. Sacchettini, J.C., Blanchard, J. S., The structure and function of the isoniazid target in M. tuberculosis. Res Microbiol, 1996. **147**(1-2): p. 36-43.
38. Dessen, A., Quémard , A ., Blanchard, J.S., Jacobs, W.R Jr., Sacchettini, J.C., Crystal structure and function of the isoniazid target of *Mycobacterium tuberculosis*. Science, 1995. **267**(5204): p. 1638-1641.
39. Slayden, R.A., Barry 3rd,C.E., The genetics and biochemistry of isoniazid resistance in *Mycobacterium tuberculosis*. Microbes Infect, 2000. **2**(6): p. 659-669.
40. Vilcheze, C., Morbidoni, H. R., Weisbrod, T. R., Iwamoto, H., Kuo, M., Sacchettini, J. C., Jacobs Jr, W. R., Inactivation of the inhA-encoded fatty acid synthase II (FASII) enoyl-acyl carrier protein reductase induces accumulation of the FASI end products and cell lysis of *Mycobacterium smegmatis*. J Bacteriol, 2000. **182**(14): p. 4059-4067.
41. Rattan, A., Kalia, A., Ahmad, N., Multidrug-resistant *Mycobacterium tuberculosis*: molecular perspectives. Emerg Infect Dis, 1998. **4**(2): p. 195-209.
42. Liu, J., Barry 3rd ,C.E., Besra G.S., Nikaido, H., Mycolic acid structure determines the fluidity of the mycobacterial cell wall. J Biol Chem, 1996. **271**(47): p. 29545-29551.
43. Bastiaanse, E.M., Hold, K.M., Van der Laarse, A., The effect of membrane cholesterol content on ion transport processes in plasma membranes. Cardiovasc Res, 1997. **33**(2): p. 272-283.
44. Lamb, D.C., Kelly, D. E., Manning, N. J., Kelly, S. L., A sterol biosynthetic pathway in *Mycobacterium*. FEBS Lett, 1998. **437**(1-2): p. 142-144.
45. Benach, J., Filling, C., Oppermann, U. C., Roversi, P., Bricogne, G., Berndt, K. D., Jornvall, H., Ladenstein, R., Structure of bacterial 3β/17β-

hydroxysteroid dehydrogenase at 1.2 A resolution: a model for multiple steroid recognition. Biochemistry, 2002. **41**(50): p. 14659-14668.

46. Brown, W.M., Metzger, L.E., Barlow, J.P., Hunsaker, L.A., Deck, L.M., Royer, R.E., Vander Jagt, D.L., 17-beta-Hydroxysteroid dehydrogenase type 1: computational design of active site inhibitors targeted to the Rossmann fold. Chem Biol Interact, 2003. **143-144**: p. 481-491.
47. Oppermann, U., Filling, C., Hult, M., Shafqat, N., Wu, X., Lindh, M., Shafqat, J., Nordling, E., Kallberg, Y., Persson, B., Jornvall, H., Short-chain dehydrogenases/reductases (SDR): the 2002 update. Chem Biol Interact, 2003. **143-144**: p. 247-253.
48. Goedde, H.W., Schoepf, E., Fleischmann D., Studies on pharmacogenetics .I. The enzymatic acetylation of isonicotinic acid hydrazide (INH). Biochem Pharmacol, 1964. **13**: p. 1671-1675.
49. Grant, D.M., Hughes, N. C., Janezic, S. A., Goodfellow, G. H., Chen, H. J., Gaedigk, A., Yu, V. L., Grewal, R., Human acetyltransferase polymorphisms. Mutat Res, 1997. **376**(1-2): p. 61-70.
50. Augustynowicz-Kopec, E., Zwolska, Z., The type of isoniazid acetylation in tuberculosis patients treated at National Tuberculosis and Lung Diseases Research Institute. Acta Pol Pharm, 2002. **59**(6): p. 443-447.
51. Delgoda, R., Lian, L. Y., Sandy, J., Sim, E., NMR investigation of the catalytic mechanism of arylamine N-acetyltransferase from *Salmonella typhimurium*. Biochim Biophys Acta, 2003. **1620**(1-3): p. 8-14.
52. Kondo, E., Kanai, K., Accumulation of cholesterol esters in macrophages incubated with mycobacteria in vitro. Jpn J Med Sci Biol, 1976 (b). **29**(3): p. 123-137.
53. Av-Gay, Y., Sobouti, R., Cholesterol is accumulated by mycobacteria but its degradation is limited to non-pathogenic fast-growing mycobacteria. Can J Microbiol, 2000. **46**(9): p. 826-831.
54. Pieters, J., Evasion of host cell defense mechanisms by pathogenic bacteria. Curr Opin Immunol, 2001. **13**(1): p. 37-44.
55. Ferrari, G., Langen, H., Naito, M., Pieters, J., A coat protein on phagosomes involved in the intracellular survival of mycobacteria. Cell, 1999. **97**(4): p. 435-447.
56. Pieters, J., Gatfield, J., Hijacking the host: survival of pathogenic mycobacteria inside macrophages. Trends Microbiol, 2002. **10**(3): p. 142-146.
57. Gatfield, J.P., J., Essential role for cholesterol in entry of mycobacteria into macrophages. Science, 2000. **288**(5471): p. 1647-1650.
58. Vermaak, Y., Properties of anti-mycolic acid antibodies in human tuberculosis patients, in Faculty of Natural and Agricultural Sciences Department of Biochemistry. 2004, University of Pretoria: Pretoria.
59. Siko, D.G.R., Mycobacterial mycolic acids as immunoregulatory lipid antigens in the resistance to tuberculosis, in Faculty of Natural and Agricultural Sciences Department of Biochemistry. 2002, University of Pretoria: Pretoria.
60. Sriram, D., Yogeeswari, P., Madhu, K., Synthesis and in vitro and in vivo antimycobacterial activity of isonicotinoyl hydrazones. Bioorg Med Chem Lett, 2005. **15**: p. 4502-4505.
61. Copp, B.R., Christiansen, H.C., Franzblau, L., Franzblau, S.G., Identification of heteroarylenamines as a new class of antituberculosis lead molecules. Bioorg Med Chem Lett, 2005. **15**: p. 4097-4099.

62. Sinha, N., Jain, S., Tilekar, A., Upadhayaya, R.S., Kishore, N., Jana, G.H., Arora, S.K., Synthesis of isonicotinic acid N-arylidene-N-[2-oxo-2-(4-aryl-piperazin-1-yl)-ethyl]-hydrazides as antituberculosis agents Bioorg Med Chem Lett, 2005. **15**: p. 1573-1576.
63. Klopman, G., Fercu, D., Jacob, J., Computer-aided study of the relationship between structure and antituberculosis activity of a series of isoniazid derivatives. Chem Phys, 1996. **204**(2-3): p. 181-193.
64. Gesellschaft, F.B.A., *Derivative of Isonicotinic acid hydrazide*, in *State Patent Office London*. 1952: Great Britain. p. 1-4.
65. Hart, J.J.D., Rutherford, G., Anderson, F.E., Barkley, F.A., Mast, G.W., In vitro activity of N-isonicotinoyl-N'-(salicylidene)hydrazine (Salizid) against *Mycobacterium tuberculosis*. Antibiot Chemother, 1954. **4**: p. 803-808.
66. Mohamad, S., Ibrahim, P., Sadikun, A., Susceptibility of *Mycobacterium tuberculosis* to isoniazid derivative, 1-isonicotinyl -2- nonanoyl hydrazine: Investigation at cellular level. Tuberculosis, 2004. **84**: p. 56-62.
67. Maccari, R., Ottana, R., Vigorita, M.G., In vitro advanced antimycobacterial screening of isoniazid related hydrazones, hydrazides and cyanoboranes: Part14. Bioorg Med Chem Lett, 2005. **15**: p. 2509-2513.
68. Pandey, R., Khuller, G.K., Solid lipid particle based inhalable sustained drug delivery system against experimental tuberculosis. Tuberculosis, 2005. **85**: p. 227-234.
69. Ernst, J.D., Macrophage receptors for *Mycobacterium tuberculosis*. Infect Immun, 1998. **66**(4): p. 1277-1281.
70. Zimmerli, S., Edwards, S., Ernst, J.D., Selective receptor blockade during phagocytosis does not alter the survival and growth of *Mycobacterium tuberculosis* in human macrophages. Am J Respir Cell Mol Biol, 1996. **15**(6): p. 760-770.
71. Majumdar, S., Basu, S.K., Killing of intracellular *Mycobacterium tuberculosis* by receptor-mediated drug delivery. Antimicrob Agents Chemother, 1991. **35**(1): p. 135-140.
72. Yamaguchi, Y., Kunitomo, M., Haginaka, J., Assay methods of modified lipoproteins in plasma. J Chromatogr B Analyt Technol Biomed Life Sci, 2002. **781**(1-2): p. 313-330.
73. Baginski, M., Resat, H., Borowski, E., Comparative molecular dynamics simulations of amphotericin B-cholesterol/ergosterol membrane channels. Biochim Biophys Acta, 2002. **1567**(1-2): p. 63-78.
74. Hervé, M., Debouzy, J.C., Borowski, E., Cybulska, B., Gary-Bobo, C.M., The role of the carboxyl and amino groups of polyene macrolides in their interactions with sterols and their selective toxicity. A ^{31}P-NMR study. Biochim Biophys Acta, 1989. **980**(3): p. 261-272.
75. Ehrenfreund-Kleinman, T., Azzam, T., Falk, R., Polacheck, I., Golenser, J., Domb, A.J., Synthesis and characterization of novel water soluble amphotericin B-arabinogalactan conjugates. Biomaterials, 2002. **23**(5): p. 1327-1335.
76. Falk, R., Domb, A.J., Polacheck, I., A novel injectable water-soluble amphotericin B-arabinogalactan conjugate. Antimicrob Agents Chemother, 1999. **43**(8): p. 1975-1981.
77. Bekersky, I.I., Fielding, R.M., Buell, D., Lawrence, I. I., Lipid-based amphotericin B formulations: from animals to man. Pharm Sci Technol Today, 1999. **2**(6): p. 230-236.

78. Ghannoum, M.A., Rice, L.B., Antifungal agents: mode of action, mechanisms of resistance, and correlation of these mechanisms with bacterial resistance. Clin Microbiol Rev, 1999. **12**(4): p. 501-517.
79. Guardiola-Diaz, H.M., Foster, L.A., Mushrush, D., Vaz, A.D., Azole-antifungal binding to a novel cytochrome P450 from *Mycobacterium tuberculosis*: implications for treatment of tuberculosis. Biochem Pharmacol, 2001. **61**(12): p. 1463-1470.
80. Jackson, C.J., Lamb, D.C., Kelly, D.E., Kelly, S.L., Bactericidal and inhibitory effects of azole antifungal compounds on *Mycobacterium smegmatis*. FEMS Microbiol Lett, 2000. **192**(2): p. 159-162.
81. Hartsel, S., Bolard, J., Amphotericin B: new life for an old drug. Trends Pharmacol Sci, 1996. **17**(12): p. 445-449.
82. Vertut-Doi, A., Ohnishi, S.I., Bolard J., The endocytic process in CHO cells, a toxic pathway of the polyene antibiotic amphotericin B. Antimicrob Agents Chemother, 1994. **38**(10): p. 2373-2379.
83. Cheron, M., Petit, C., Bolard, J., Gaboriau, F., Heat-induced reformulation of amphotericin B-deoxycholate favours drug uptake by the macrophage-like cell line J774. J Antimicrob Chemother, 2003. **52**(6): p. 904-910.
84. Sau, K., Mambula, S.S., Latz, E., Henneke, P., Golenbock, D.T., Levitz, S.M., The antifungal drug amphotericin B promotes inflammatory cytokine release by a Toll-like receptor- and CD14-dependent mechanism. J Biol Chem, 2003. **278**(39): p. 37561-37568.
85. Aloia, R.C., Tian, H., Jensen, F.C., Lipid composition and fluidity of the human immunodeficiency virus envelope and host cell plasma membranes. Proc Natl Acad Sci U S A, 1993. **90**(11): p. 5181-5185.
86. Jones, J., Kosloff, B.R., Benveniste, E.N., Shaw, G.M., Kutsch, O., Amphotericin-B-mediated reactivation of latent HIV-1 infection. Virology, 2005. **331**(1): p. 106-116.
87. Clayette, P., Martin, M., Beringue, V., Dereuddre-Bosquet, N., Adjou, K.T., Seman, M., Dormont, D., Effects of MS-8209, an amphotericin B derivative, on tumor necrosis factor alpha synthesis and human immunodeficiency virus replication in macrophages. Antimicrob Agents Chemother, 2000. **44**(2): p. 405-407.
88. Putman, M., Van Veen, H.W., Konings, W.N., Molecular Properties of Bacterial Multidrug Transporters. Microbiol Mol Biol Rev, 2000. **64**(4): p. 672–693.
89. Payton, M., Auty, R., Delgoda, R., Everett, M., Sim, E., Cloning and characterization of Arylamine N-Acetyltransferase genes from *Mycobacterium smegmatis* and *Mycobacterium tuberculosis*: Increased expression results in isoniazid resistance. J Bacteriol, 1999. **181**(4): p. 1343-1347.
90. Rastogi, N., Goh, K.S., Horgen, L., Barrow W.W., , Synergistic activities of antituberculosis drugs with cerulenin and trans-cinnamic acid against *Mycobacterium tuberculosis*. FEMS Immunol Med Microbiol, 1998. **21**: p. 149-157.
91. Labana, S., Pandey, S., Sharma, S., Khuller G.K., Chemotherapeutic activity against murine tuberculosis of once weekly administered drugs (isoniazid and rifampicin) encapsulated in liposomes. Int J Antimicrob Agents, 2002. **20**: p. 301-304.

92. Brajtburg, J., Powderly, W.G., Kobayashi, G.S., Medoff, G., Amphotericin B: current understanding of mechanisms of action. Antimicrob Agents Chemother, 1990. **34**(2): p. 183-188.
93. Eldem, T., Arican-Cellat, N., Determination of Amphotericin B in human plasma using solid-phase extraction and high performance liquid chromatography. J Pharm Biomed Anal, 2001. **25**: p. 53-64.
94. Cleary, J., *Compositions comprising highly purified Amphotericin B*, W.I.P. Organization, Editor. 2004: USA.
95. Nicolaou, K.C., Daines, R.A., Ogawa, Y., Chakraborty, T.K., Total synthesis of Amphotericin B. The final stages. J Am Chem Soc, 1988. **110**: p. 4696-4705.
96. McMurray, J., *Organic Chemistry*. fifth ed, ed. J. Huber. 2000,Pacific grove, California, USA: Brooks/Cole.
97. Viguera, A., Villa, M., Goni, F.M., A water soluble polylysine-retinaldehyde Schiff base. J Biol Chem, 1990. **265**(5): p. 2527-2532.
98. Sridharan, V., Muthusubramanian, S., Sivasubramanian, S., A facile reduction procedure for N,N'bis[5-substituted salicylidene]-m/p-phenylenediamines with sodium borohydride - silica gel system. Synthetic Communications, 2004. **34**(6): p. 1087-1096.
99. Gribble, G.W., Sodium borohydride in carboxylic acid media: a phenomenal reduction system. Chem Soc Rev, 1998. **27**: p. 395-404.
100. Lu, Z., Bhongle, N., Su, X., Ribe, S., Senanayake, C.H., Novel diacid accelerated borane reducing agents for imines. Tetrahedron Lett, 2002. **43**: p. 8617-8620.
101. Sinha, A.K., Acharya, R., Joshi, B.P., A mild and convenient procedure for the conversion of toxic β-asarone into rare phenylpropanoids: 2,4,5, -trimethoxycinnamaldehyde and γ-asarone. J Nat Prod, 2002. **65**: p. 764-765.
102. Resat, H., Sungur, F.A., Baginski, M., Borowski, E., Aviyente, V., Conformational properties of Amphotericin B amide derivatives - impact on selective toxicity. J Comput Aided Mol Des, 2000. **14**: p. 698-703.
103. Paquet, M., Fournier, I., Barwicz, J., Tancrede, P., Auger, M., The effects of AmphotericinB on pure and ergosterol or cholesterol containing dipalmitoylphosphatidylcholine bilayers as viewed by ^{2}H NMR. Chem Phys Lipids, 2002. **119**: p. 1-11.
104. Matsuoka, S., Murata, M., Membrane permeabilizing activity of Amphotericin B is affected by chain length of phosphatidylcholine added as minor constituent. Biochim Biophys Acta, 2003. **1617**: p. 109-115.
105. Gabrielska, J., Gagos, M., Gubernator, J., Gruszecki, W.I., Binding of antibiotic Amphotericin B to lipid membranes: A ^{1}H NMR study. FEBS lett, 2006. **580**: p. 2677-2685.
106. Pfyffer, G.E., Bonato, D.A., Ebrahimzadeh, A., Gross, W., Hotaling, J., Kornblum, J., Laszlo, A., Roberts, G., Salfinger, M., Wittwer, F., Siddiq, S., Multicenter laboratory validation of susceptibility testing of *Mycobacterium tuberculosis* against classical second-line and new antimicrobial drugs by using the radiometric BACTEC 460 technique and the proportion method with solid media. J Clin Microbiol, 1999. **37**(10): p. 3179-3186.
107. Collins, L.A., Franzblau, S.G., Microplate alamar blue assay versus BACTEC 460 system for high-throughput screening of compounds against *Mycobacterium tuberculosis* and *Mycobacterium avium* Antimicrob Agents Chemother, 1997. **41**(5): p. 1004-1009.

108. White, E.L., Suling, W.J., Ross, L.J., Seitz, L.E., Reynolds, R.C., 2-Alkoxycarbonylaminopyridines: inhibitors of *Mycobacterium tuberculosis* Ftsz. J Antimicrob Chemother, 2002. **50**: p. 111-114.
109. Roberts, G.D., Goodman, N.L., Heifets, L., Larsh, H.W., Lindner, T.H., Kenneth McClathy, J., McGinnis, M.R., Siddiqi, S.H., Wright, P., Evaluation of the BACTEC radiometric method for recovery of mycobacteria and drug susceptibility testing of *Mycobacterium tuberculosis* from acid-fast smear positive specimens J Clin Microbiol, 1983. **18**(3): p. 689-696.
110. Montoro, E., Lemus, D., Echemendia, M., Martin, A., Portaels, F., Palomino, J.C., Comparative evaluation of the nitrite reduction assay, the MTT test, and the resazurin microtitre assay for drug susceptibility testing of clinical isolates of *Mycobacterium tuberculosis*. J Antimicrob Chemother, 2005. **55**: p. 500-505.
111. Goodrum, M.A., Siko, D.G.R., Niehues, T., Eichelbauer, D., Verschoor, J.A. , Mycolic acids from *Mycobacterium tuberculosis*: Purification by countercurrent distribution and T cell stimulation. Microbios, 2001. **106**: p. 55-67.
112. Al Dulayymi, J.R., Baird, M.S., Roberts, E., The synthesis of a single enantiomer of a major α-mycolic acid of *Mycobacterium tuberculosis*. Chem Commun, 2003: p. 228-229.
113. Villeneuve, M., Kawai, M., Kanashima, H., Watanabe, M., Minnikin, D.E., Nakahara, H., Temperature dependence of the Langmuir monolayer packing of mycolic acids from *Mycobacterium tuberculosis*. Biochim Biophys Acta, 2005. **1715**: p. 71-80.
114. Brajtburg, J., Bolard, J., Carrier effects on biological activity of amphotericin B. Clin Microbiol Rev, 1996. **9**(4): p. 512-531.
115. Barwicz, J.,Tancrede, P., The effect of aggregation state of amphotericin B on its interactions with cholesterol- or ergosterol-containing phosphotidylcholine monolayers Chem Phys Lipids, 1997. **85**: p. 145-155.
116. Hac-Wydro, K., Dynarowicz-Latka, P., Grzybowska, J., Borowski, E., How does N-acylation and esterification of amphotericin B molecule affect its interactions with cellular membrane components - the Langmuir monolayer study. Colloids and surfaces B: Biointerfaces, 2005. **46**: p. 7-19.
117. Sebatjane, S.I., *Anti-tuberculosis drug design based on a possible mimicry between host and pathogen lipids*, in *Faculty of Natural and Agricultural Sciences Department of Biochemistry*. 2003, University of Pretoria: Pretoria.
118. Dunne, D.W., Resnick, D., Greenberg, J.,Krieger, M., Joiner, K.A., The type I macrophage scavenger receptor binds to gram-positve bacteria and recognizes lipoteichoic acid. Proc Natl Acad Sci USA, 1994. **91**: p. 1863-1867.
119. Acton, S.L., Scherer,P.E., Lodish,H.F., Krieger,M., Expression cloning of SR-BI, a CD36 related class B scavenger receptor. J Biol Chem, 1994. **269**: p. 21003-21009.
120. Kondo, E., Kanai, K., An attempt to cultivate mycobacteria in simple synthetic liquid medium containing lecithin-cholesterol liposomes. Jpn J Med Sci Biol, 1976 (a). **29**(3): p. 109-121.
121. Pieters, J., Entry and survival of pathogenic mycobacteria in macrophages. Microbes Infect, 2001. **3**(3): p. 249-255.
122. de Chastellier, C., Lang, T., Thilo, L., Phagocytic processing of the macrophage endoparasite, *Mycobacterium avium*, in comparison to

phagosomes which contain *Bacillus subtilis* or latex beads. . Eur J Cell Biol, 1995. **68**: p. 167-182.

123. de Chastellier, C., Thilo, L., Phagosome maturation and fusion with lysosomes in relation to surface property and size of the phagocytic particle. Eur J Cell Biol, 1997. **74**: p. 49-62.

124. de Chastellier, C., Thilo, L., Cholesterol depletion in *Mycobacterium avium* - infected macrophages overcome the block in phagosome maturation and leads to the reversible sequestration of viable mycobacteria in phagolysosome derived autophagic vacuoles. Cell Microbiol, 2006. **8**(2): p. 242-256.

Appendixes

Appendix A

Operational method for preparative RP-HPLC on a C_{18} column

Detection wavelength: 210-600nm

Degas with He (g) : 20 ml/min. for all three lines

Solvent A: MeoH

Solvent B: MeOH: H2O (7:3)

Solvent C: MeOH: H2O (2:8)

Priming pump:

Pressure max. 4000 psi

	Time (min.)	Flow (ml/min.)	%A	%B	%C
1	0.01	3.00	100.0	0.0	0.0
2	5.00	3.00	100.0	0.0	0.0
3	10.00	3.00	0.0	0.0	100.0
4	25.00	3.00	0.0	0.0	100.0

Running samples:

Pressure max. 4300 psi

	Time (min)	Flow (ml/min.)	%A	%B	%C
1	0.01	3.00	0.0	0.0	100.0
2	2.00	3.00	0.0	0.0	100.0
3	5.00	3.00	0.0	100.0	0.0
4	30.00	3.00	0.0	100.0	0.0

5	31.00	3.00	100.0	0.0	0.0
6	36.00	3.00	100.0	0.0	0.0
7	41.00	3.00	0.0	0.0	100.0
8	51.00	3.00	0.0	0.0	100.0

Conditioning column after each set.

Pressure max 4000 psi

	Time (min.)	Flow (ml/min.)	%A	%B	%C
1	0.01	3.00	0.0	0.0	100.0
2	5.00	3.00	100.0	0.0	0.0
3	25.00	3.00	100.0	0.0	0.0
4	26.00	0.00	100.0	0.0	0.0

Degas action stopped

Appendix B

Data used for the determination of the biosensor results:

AmB or AmB DII onto immobilized cholesterol liposomes			
AmB experiment	Response (arc sec.)	AmB DII experiment	Response (arc sec.)
1	167.63	1	35.23
2	147.56	2	24.79
3	127.68	3	39.68
4	132.39	4	35.06
5	146.61	5	25.53
Average value	144.37	Average value	33.69
std. deviation	15.64	std. deviation	6.31

AmB or AmB DII onto immobilized MA liposomes			
AmB experiment	Response (arc sec.)	AmB DII experiment	Response (arc sec.)
1	193.07	1	58.04
2	181.06	2	61.68
3	177.77	3	33.62
4	147.72	4	37.18
5	169.22	5	27.61
Average value	173.77	Average value	43.63
std. deviation	16.89	std. deviation	15.26

AmB onto immobilized PC liposomes	
AmB experiment	Response (arc sec.)
1	30.23
2	-16.68
3	72.06
4	28.11
5	-20.75
Average value	18.59
std. deviation	38.33

AmB onto immobilized synthetic protected α-MA liposomes	
AmB experiment	Response (arc sec.)
1	18.52
2	10.89
3	20.42
4	34.25
5	15.91
Average value	19.99
std. deviation	7.81

Appendix C

Calculations and concentrations used for the BACTEC 460 experiments

	INH	AmB	CID-II reduced	INH-D	TPA	INH+ AmB	DMSO Control
MM (g/mol)	137.1	924.1	1159.35	253.2599	134.1		Prepared asif INH
Solubility							
MIC (µg/ml)	0.03						
Molar ratio:	1	1	1	1	1		
Final concentrations:							
Max IC (M) 10 x	2.19E-06	2.18818E-06	2.18818E-06	2.19E-06	2.19E-06	2.19E-06	
Med IC (M)	2.18818E-07	2.18818E-07	2.18818E-07	2.18818E-07	2.18818E-07	2.18818E-07	
Min IC (M) 1/10	2.18818E-08	2.18818E-08	2.18818E-08	2.18818E-08	2.18818E-08	2.18818E-08	
Therefore the final dilution range amounts to:							
	Type in mass below:	Type in mass below:	Type in mass below:				
Stock (mg)	1	1.5	1.6	1	2	Take 50ul INH stock + 50ul AmB stock	
DMSO µl	100.00	150.00	160.00	100.00	200.00		100
water µl	100.00	150.00	160.00	100.00	200.00		100
Stock	Stock INH	Stock AmphoB	Stock CIDII reduced				
Concentrations c = n/v n= m/Mw							
n (mol)	7.29395E-06	1.6232E-06	1.38008E-06	3.94851E-06	1.49142E-05		
c (mol/l)	0.03646973	0.00541067	0.004312761	0.019742565	0.037285608	0.0209402	
Stock dilutions							
100 x diltution	10ul sample + 990ul saline	10 x dilution: 100ul sample + 900ul saline	10 x dilution: 100ul sample + 900ul saline	10ul sample + 990ul saline	10ul sample + 990ul saline	10ul sample + 990ul saline	10ul sample + 990ul saline
c (mol/l)	0.000364697	0.000541067	0.000431276	0.000197426	0.000372856	0.000209402	
1000 x dilution	100ul of 100 x dil. + 900ul saline	100 x dilution: 100ul of 10 x dil. + 900ul saline	100 x dilution: 100ul of 10 x dil. + 900ul saline	100ul of 100 x dil. + 900ul saline	100ul of 100 x dil. + 900ul saline	100ul of 100 x dil. + 900ul saline	100ul of 100 x dil. + 900ul saline
c (mol/l)	3.64697E-05	5.41067E-05	4.31276E-05	1.97426E-05	3.72856E-05	2.09402E-05	
10 000 x dilution	100ul of 1000 dil. + 900ul saline	1000 x dilution: 100ul of 100 x dil. + 900ul saline	1000 x dilution: 100ul of 100 x dil. + 900ul saline	100ul of 1000 dil. + 900ul saline	100ul of 1000 dil. + 900ul saline	100ul of 1000 dil. + 900ul saline	100ul of 1000 dil. + 900ul saline
c (mol/l)	3.64697E-06	5.41067E-06	4.31276E-06	1.97426E-06	3.72856E-06	2.09402E-06	
C1V1 = C2V2	C2 = final conc. V2 = final vol 0.0042 L	C1 = dil of stock V1 = ? Of stock					
V1 (ul) of stock solution to be added							
Max IC (M) 10 x	use 100 dil. Stock	use 10 dil. Stock	use 10 dil. Stock	use 100 dil. Stock	use 100 dil. Stock	use 100 dil. Stock	
	25.2	16.98564551	21.30971554	46.55105383	24.64857768	43.88865435	
Med IC (M)	use 1000 dil stock	use 100 dil stock	use 100 dil stock	use 1000 dil stock	use 1000 dil stock	use 1000 dil stock	
	25.2	16.98564551	21.30971554	46.55105383	24.64857768	43.88865435	
Min IC (M) 1/10	use 10 000dil stock	use 1000 dil stock	use 1000 dil stock	use 10 000dil stock	use 10 000dil stock	use 10 000dil stock	
	25.2	16.98564551	21.30971554	46.55105383	24.64857768	43.88865435	
Add saline (ul) to final volume of 100ul							
Max IC (M) 10 x	74.8	83.01435449	78.69028446	53.44894617	75.35142232	56.11134565	
Med IC (M)	74.8	83.01435449	78.69028446	53.44894617	75.35142232	56.11134565	
Min IC (M) 1/10	74.8	83.01435449	78.69028446	53.44894617	75.35142232	56.11134565	
Stock dilutions in ul (10 times)							
Max IC (M) 10 x	use 100 dil. Stock	use 10 dil. Stock	use 10 dil. Stock	use 100 dil. Stock	use 100 dil. Stock	use 100 dil. Stock	use 100 dil. Stock
	252	169.8564551	213.0971554	465.5105383	246.4857768	438.8865435	252
Med IC (M)	use 1000 dil stock	use 100 dil stock	use 100 dil stock	use 1000 dil stock	use 1000 dil stock	use 1000 dil stock	use 1000 dil stock
	252	169.8564551	213.0971554	465.5105383	246.4857768	438.8865435	252
Min IC (M) 1/10	use 10 000dil stock	use 1000 dil stock	use 1000 dil stock	use 10 000dil stock	use 10 000dil stock	use 10 000dil stock	use 10 000dil stock
	252	169.8564551	213.0971554	465.5105383	246.4857768	438.8865435	252
Add saline (ul) to final volume of 1000ul							
Max IC (M) 10 x	748	830.1435449	786.9028446	534.4894617	753.5142232	561.1134565	748
Med IC (M)	748	830.1435449	786.9028446	534.4894617	753.5142232	561.1134565	748
Min IC (M) 1/10	748	830.1435449	786.9028446	534.4894617	753.5142232	561.1134565	748

Appendix D

Average Growth index values obtained for the BACTEC 460 experiments

	day1	day2	day3	day4	day5	day6	day7
INH Max IC	7	11	13	9	7	6	5
INH MED IC	7	13	114	110	113	126	145
INH MIN IC	7	13	183	229	312	425	449
AmB MAC IC	7	14	181	233	340	496	671
AmB MED IC	7	13	190	224	338	494	660
AmB MIN IC	7	13	167	215	296	432	577
TPA MAX IC	7	13	172	227	321	477	628
TPA MED IC	7	14	184	239	343	489	672
TPA MIN IC	8	13	181	240	334	485	654
INH-D MAX IC	7	14	168	208	271	377	470
INH-D MED IC	8	14	180	234	333	496	662
INH-D MIN IC	8	14	185	243	342	507	682
CIDII reduced Max IC	7	14	171	236	336	496	651
CIDII reduced Med IC	8	14	183	235	333	496	650
CIDII reduced Min IC	8	15	205	258	348	529	702
INH + AmB MAX IC	8	11	14	9	7	5	4
INH + AmB MED IC	7	16	170	196	247	336	444
INH + AmB MIN IC	8	15	206	273	390	582	752
Mtb.H37Rv + control	6	14	194	253	366	539	731
No bacteria - control	50	4	2	1	0	0	0

Appendix E

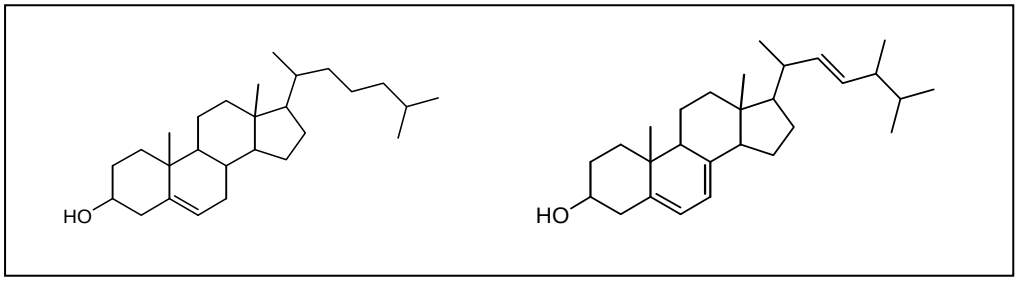

Fig. E.1General structure of cholesterol (left) and ergosterol (right)

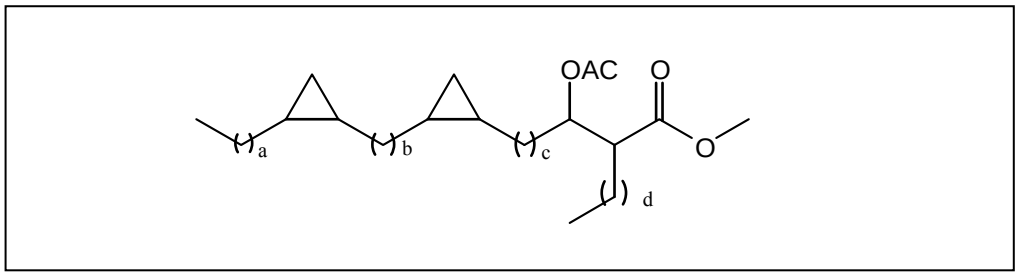

Fig. E.2 Structure of synthetic protected α-MA [112]

Appendix F

NMR data of synthesized compounds

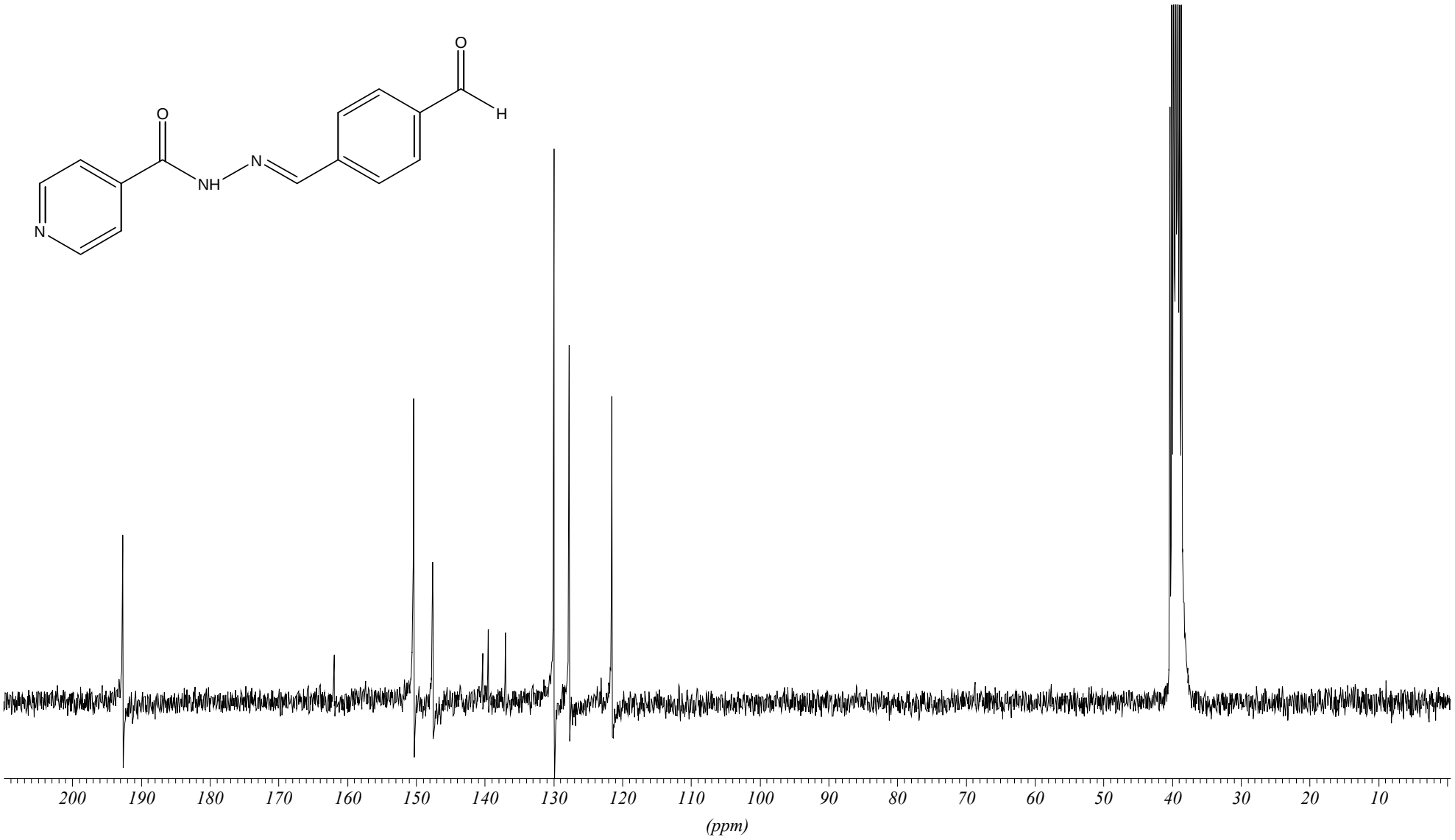

Fig. F.1. ^{13}C spectra of INH-TPA

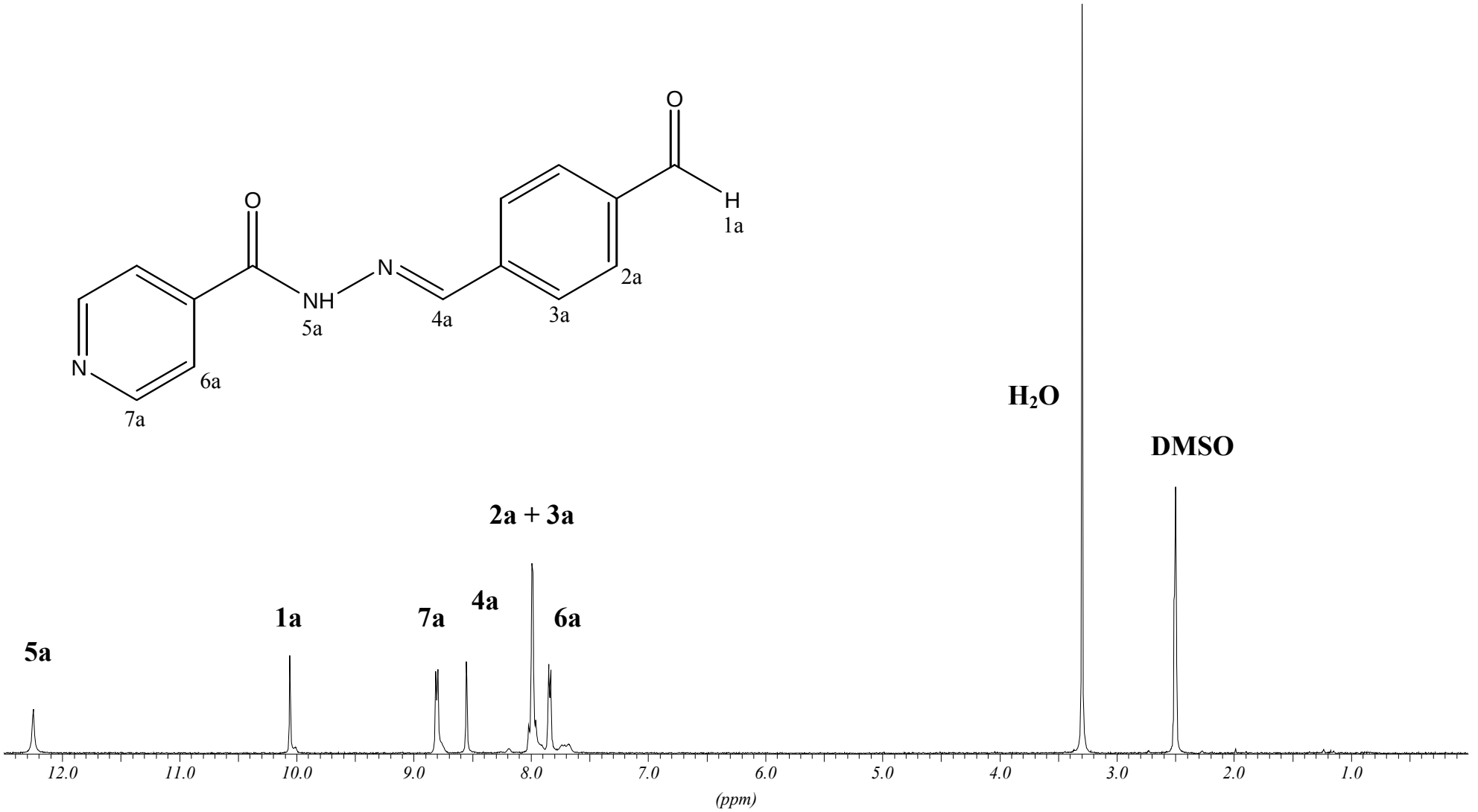

Fig. F.2. ^{1}H spectra of INH-TPA

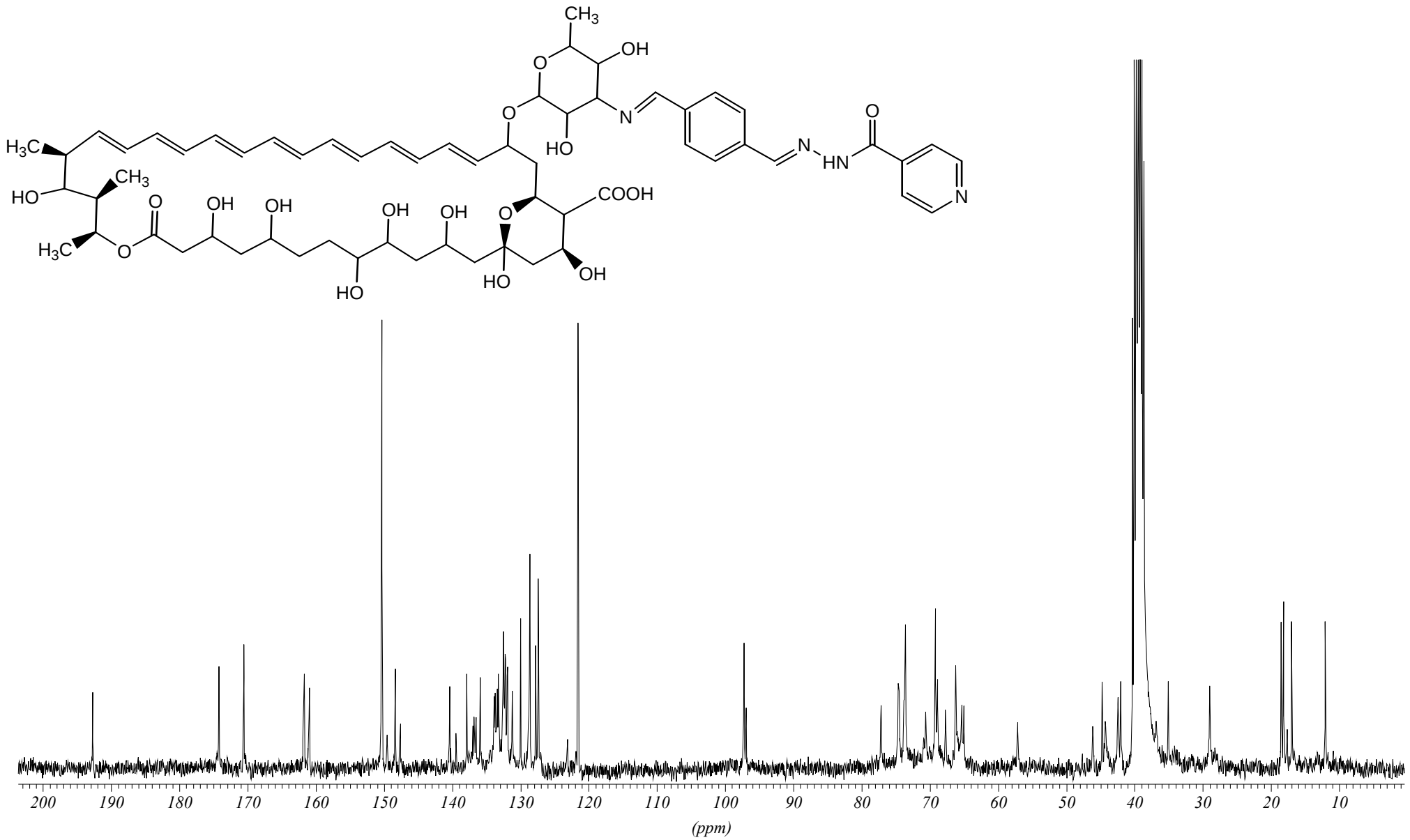

Fig. F.3. ^{13}C spectra of AmB derivative I

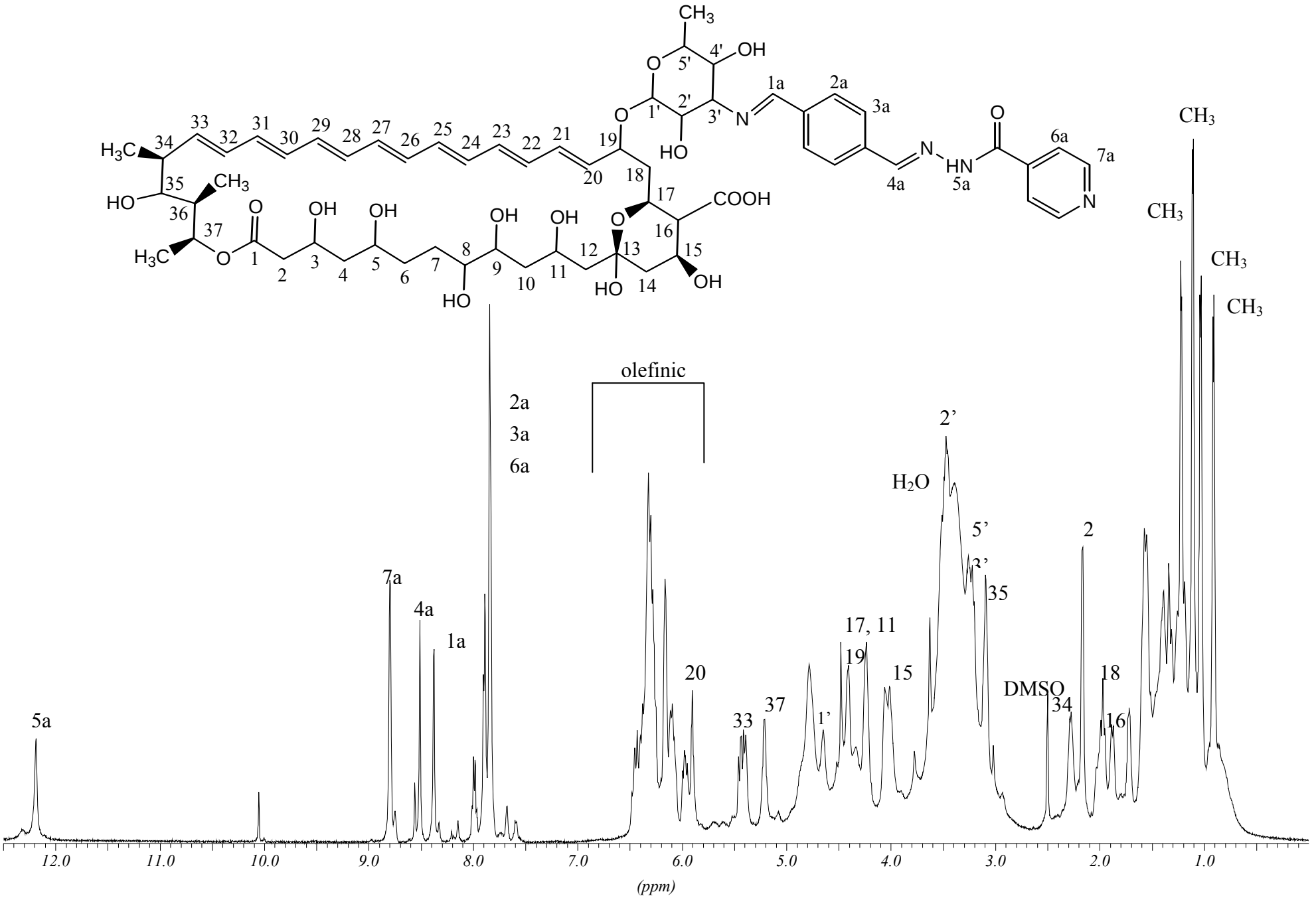

Fig. F.4 ^{1}H spectra of AmB derivative I

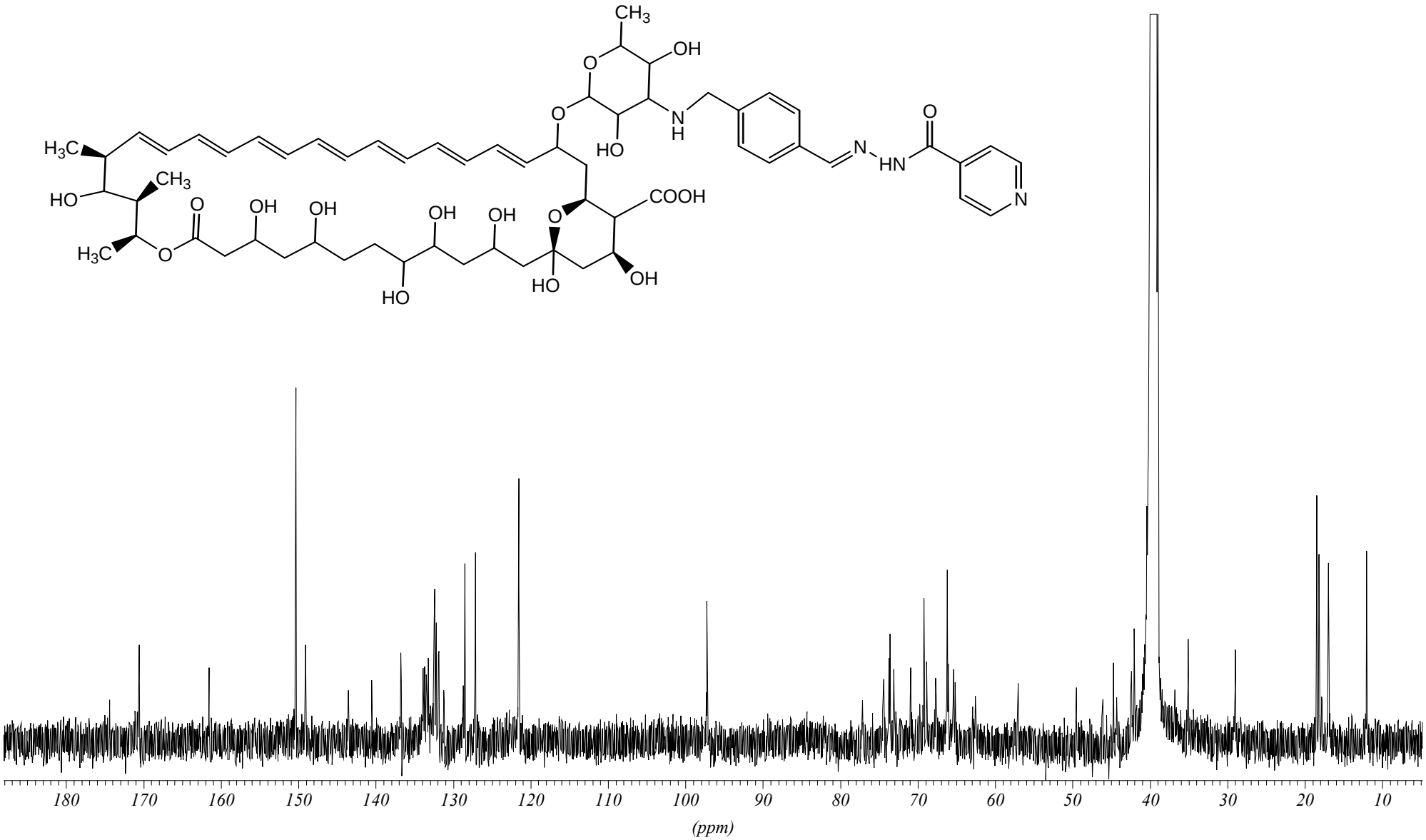

Fig. F.5. ^{13}C spectra of AmB derivative II

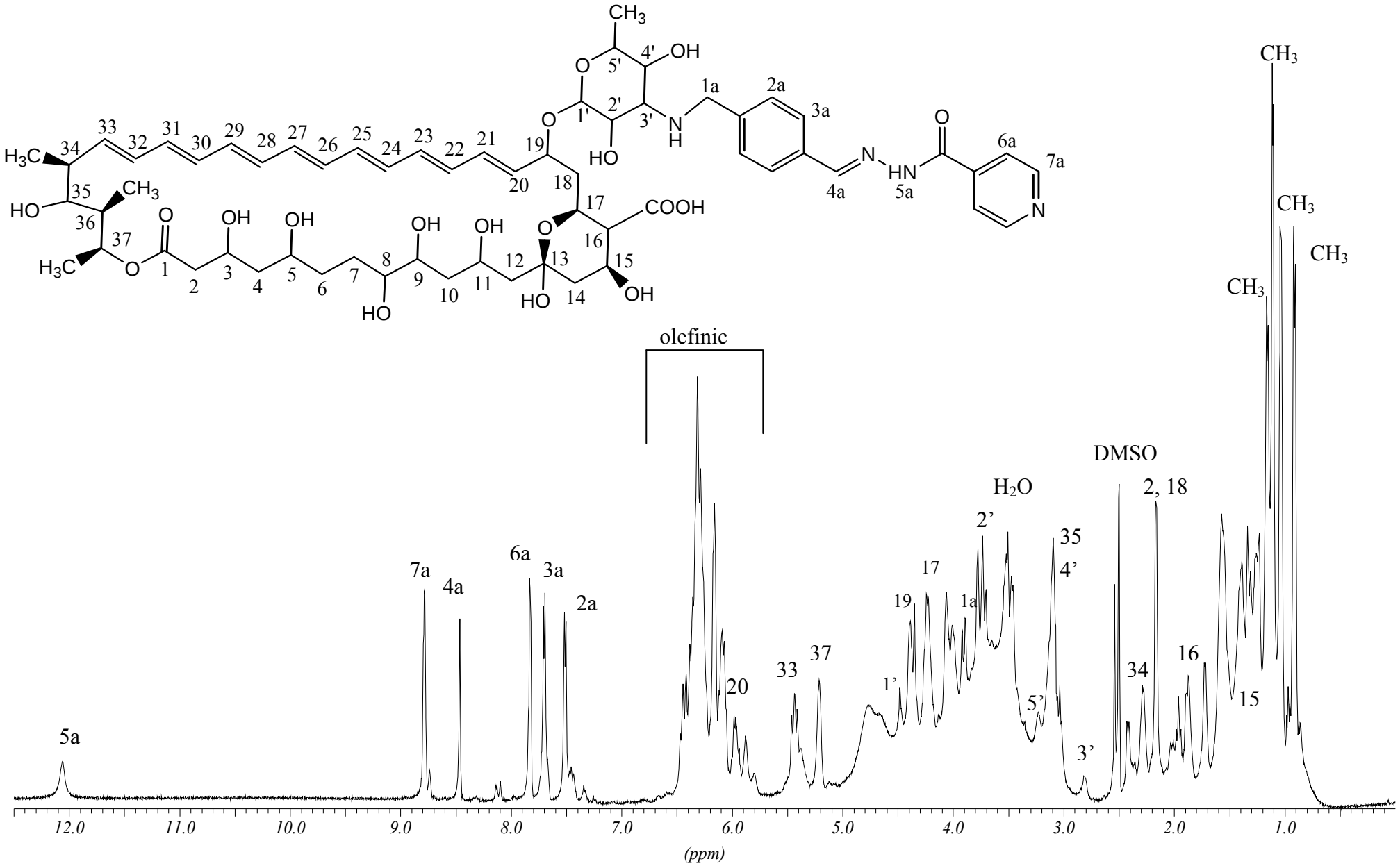

Fig. F.6 ^{1}H spectra of AmB derivative II